

University of Windsor

Scholarship at UWindor

Electronic Theses and Dissertations

Theses, Dissertations, and Major Papers

2018

Mercury and Polychlorinated Biphenyl Bioaccumulation Dynamics in Fish

Jiajia Li

University of Windsor

Follow this and additional works at: <https://scholar.uwindsor.ca/etd>

Recommended Citation

Li, Jiajia, "Mercury and Polychlorinated Biphenyl Bioaccumulation Dynamics in Fish" (2018). *Electronic Theses and Dissertations*. 7374.

<https://scholar.uwindsor.ca/etd/7374>

This online database contains the full-text of PhD dissertations and Masters' theses of University of Windsor students from 1954 forward. These documents are made available for personal study and research purposes only, in accordance with the Canadian Copyright Act and the Creative Commons license—CC BY-NC-ND (Attribution, Non-Commercial, No Derivative Works). Under this license, works must always be attributed to the copyright holder (original author), cannot be used for any commercial purposes, and may not be altered. Any other use would require the permission of the copyright holder. Students may inquire about withdrawing their dissertation and/or thesis from this database. For additional inquiries, please contact the repository administrator via email (scholarship@uwindsor.ca) or by telephone at 519-253-3000ext. 3208.

Mercury and Polychlorinated Biphenyl Bioaccumulation Dynamics in Fish

by

Jiajia Li

A Dissertation
Submitted to the Faculty of Graduate Studies
through the Great Lakes Institute for Environmental Research
in Partial Fulfillment of the Requirements for
the Degree of Doctor of Philosophy at the
University of Windsor

Windsor, Ontario, Canada

2018

© 2018 Jiajia Li

Mercury and Polychlorinated Biphenyl Bioaccumulation Dynamics in Fish

by

Jiajia Li

APPROVED BY:

C. Madenjian, External Examiner
Great Lakes Science Center, United States Government

X. Xu
Civil and Environmental Engineering

C. Weisener
Great Lakes Institute for Environmental Research

J. Gagnon
Great Lakes Institute for Environmental Research

D. Haffner, Co-Advisor
Great Lakes Institute for Environmental Research

K. Drouillard, Co-Advisor
Great Lakes Institute for Environmental Research

Feb 5, 2018

DECLARATION OF CO-AUTHORSHIP/ PREVIOUS PUBLICATION

I. Co-Authorship Declaration

I hereby declare this thesis incorporates material that is result of joint research, as follows:

I was the primary author and person responsible for the experimental implementation and majority of writing for each chapter included in this thesis. Chapter 2 was co-authored by Dr. Ken G. Drouillard, Dr. Brian Branfireun, and Dr. G. Douglas Haffner. Ken G. Drouillard and G. Douglas Haffner provided intellectual guidance, and editorial support and it is published in the journal, Environmental Science and Technology. Chapter 3 was co-authored by Dr. Dingyong Wang, Dr. Lei Zhang, Dr. Yun Li, Dr. Huatang Deng, Dr. G. Douglas Haffner, and Dr. Ken G. Drouillard. Lei Zhang, Yun Li, and Huatang Deng contributed to the research with sample collecting and processing. Dingyong Wang provided technical support for laboratory analysis. Ken G. Drouillard and G. Douglas Haffner provided intellectual guidance and editorial support and is being prepared for submission to the journal, Environmental Science and Technology. Chapter 4 was co-authored by Dr. Gordon Paterson, Dr. David M. Walters, Michael D. Burtnyk, Dr. G. Douglas Haffner, and Dr. Ken G. Drouillard. Gordon Paterson, David M. Walters, and Michael D. Burtnyk contributed to the research with sample collections and location identification. Ken G. Drouillard and G. Douglas Haffner provided intellectual guidance, and all of my co-authors provided editorial support. This manuscript was submitted to the journal, Environmental Toxicology and Chemistry.

I am aware of the University of Windsor Senate Policy on Authorship and I certify that I have properly acknowledged the contribution of other researchers to my thesis, and

have obtained written permission from each of the co-author(s) to include the above material(s) in my thesis.

I certify that, with the above qualification, this thesis, and the research to which it refers, is the product of my own work.

II. Declaration of Previous Publication

This thesis includes three original papers that have been previously published/will be submitted for publication in peer reviewed journals, as follows:

Thesis Chapter	Publication title/full citation	Publication status
Chapter 2	Li, J.; Drouillard, K. G.; Branfireun, B.; Haffner, G. D. Comparison of the toxicokinetics and bioaccumulation potential of mercury and polychlorinated biphenyls in Goldfish (<i>Carassius auratus</i>). Environ. Sci. Technol. 2015, 49, 11019-11027.	Published
Chapter 3	Li, J.; Wang, D.; Zhang, L.; Li, Y.; Deng, H.; Haffner, G. D.; Drouillard, K. G. Protein and lipid dynamics regulate bioaccumulation of PCBs and Hg in Bighead Carp (<i>Hypophthalmichthys nobilis</i>) and Silver Carp (<i>Hypophthalmichthys molitrix</i>) from the Three Gorges Reservoir, China	Paper in Preparation
Chapter 4	Li, J.; Paterson, G.; Walters, D. M.; Burtnyk, M. D.; Haffner, G. D.; Drouillard, K. G. Importance of growth rate on Hg and PCB bioaccumulation in fish	Submitted to <i>Environmental Toxicology and Chemistry</i>

I certify that I have obtained a written permission from the copyright owner(s) to include the above published material(s) in my thesis. I certify that the above material describes work completed during my registration as a graduate student at the University of Windsor.

III. General

I declare that, to the best of my knowledge, my thesis does not infringe upon anyone's copyright nor violate any proprietary rights and that any ideas, techniques, quotations, or any other material from the work of other people included in my thesis, published or otherwise, are fully acknowledged in accordance with the standard referencing practices. Furthermore, to the extent that I have included copyrighted material that surpasses the bounds of fair dealing within the meaning of the Canada Copyright Act, I certify that I have obtained a written permission from the copyright owner(s) to include such material(s) in my thesis.

I declare that this is a true copy of my thesis, including any final revisions, as approved by my thesis committee and the Graduate Studies office, and that this thesis has not been submitted for a higher degree to any other University or Institution.

ABSTRACT

Global contamination by mercury (Hg) and polychlorinated biphenyls (PCBs) coupled with high health risks to humans requires exposure models. The models must correctly predict Hg and PCB concentrations in fish, which in turn, requires accurate estimates of model parameters. This dissertation first quantified assimilation efficiencies (AE) and elimination coefficients (k_{tot}) of Hg and PCBs in Goldfish (*Carassius auratus*). Then, a non-steady state toxicokinetic model, combined with a Wisconsin bioenergetics model, was developed to simulate Hg and PCB bioaccumulation in Silver Carp (*Hypophthalmichthys molitrix*), Bighead Carp (*Hypophthalmichthys nobilis*), and Bluegill (*Lepomis macrochirus*) from multiple locations. Finally, a sensitivity analysis was performed for these three modeled species to evaluate the relative contribution of each parameter to the model outcomes.

The results indicated that dietary AEs were 98 ± 10 % and 40 ± 9 % for MeHg and PCBs, respectively, thus, Hg had a higher AE compared to PCBs. The k_{tot} of MeHg was $0.010 \pm 0.002 \text{ d}^{-1}$, which was equivalent to those measured for highly hydrophobic PCBs with $\log \text{KOW} = 7.2$. In addition, using the tissue specific growth rate, the non-steady state bioenergetics/kinetics model was generally able to simulate differences in the bioaccumulation trends of PCBs and Hg for the study species. The sensitivity analysis indicated that toxicokinetic parameters representing tissue growth rate are as influential as model parameters associated with ontogenetic diet shifts in terms of explaining age specific Hg and PCB bioaccumulation.

Overall, this dissertation was the first to directly compare chemical toxicokinetics between Hg and PCBs within the same organism, and to quantify the effect of tissue specific growth rate on bioaccumulation of these contaminants by fish using a non-steady state bioenergetics/ toxicokinetics model. It was concluded that Hg has a higher bioaccumulation potential than PCBs, and suggested tissue growth rates should be incorporated in future bioaccumulation models especially as they apply to modelling PCB dynamics in fish.

DEDICATION

*To my parents, Daishuang Li and Deqing Xue,
for making me believe.*

ACKNOWLEDGEMENTS

I would like to thank my supervisor Dr. G. Douglas Haffner for taking me on as a PhD student when I was looking for opportunities for studying abroad. I am deeply grateful to Dr. Haffner and my co-supervisor Dr. Ken G. Drouillard for their patient supervision, inspiring discussions, and warm encouragements.

I also would like to thank Dr. Xiaohong Xu, Dr. Chris Weisener, and Dr. Joel Gagnon for being my advisory committee members. I appreciate their valuable discussions and input to my research projects. I thank Dr. Charles P. Madenjian for being the external examiner for my defence.

I want to thank all members of the Haffner and Drouillard lab for their friendship and helping to shape some ideas on my projects. I also want to thank other fellow graduate students and staff at GLIER for their friendship and encouragements.

I thank my parents for their continued support all these years. They gave me the largest freedom and support to pursue my education in Canada, even during the most difficult times.

I thank my friends Qian Xu, Simo Kang, Yi Wang and Shifeng Yao for their companionship and continued encouragements, as well as their support with food and accommodations. I could not have gone this far without their love.

TABLE OF CONTENTS

DECLARATION OF CO-AUTHORSHIP/ PREVIOUS PUBLICATION	III
ABSTRACT.....	VI
DEDICATION.....	VIII
ACKNOWLEDGEMENTS.....	IX
LIST OF TABLES	XII
LIST OF FIGURES	XIV
CHAPTER 1 General Introduction.....	1
1.1 Global Contamination of Mercury (Hg) and Polychlorinated Biphenyls (PCBs)....	1
1.2 Bioaccumulation Kinetics of Hg and PCBs by Fish	2
1.3 Modeling Hg and PCB Bioaccumulation by Fish.....	4
1.4 Toxicokinetics Model and Parameters	5
1.5 Bioenergetics Model and Growth Rate	9
1.6 Study Objectives and Hypotheses.....	12
1.7 References	15
CHAPTER 2 Comparison of the Toxicokinetics and Bioaccumulation Potential of Mercury and Polychlorinated Biphenyls in Goldfish (<i>Carassius auratus</i>)	24
2.1 Introduction.....	24
2.2 Materials and Methods.....	27
2.3 Results	35
2.4 Discussion	40
2.5 References	45
CHAPTER 3 Protein and Lipid Dynamics Regulate Bioaccumulation of PCBs and Hg in Bighead Carp (<i>Hypophthalmichthys nobilis</i>) and Silver Carp (<i>Hypophthalmichthys molitrix</i>) From the Three Gorges Reservoir, China.....	54
3.1 Introduction.....	54
3.2 Methods	57
3.3 Results	66
3.4 Discussion	71
3.5 References	75
CHAPTER 4 Importance of Growth Rate on Hg and PCB Bioaccumulation in Fish.....	90

4.1 Introduction.....	90
4.2 Methods.....	93
4.3 Results.....	105
4.4 Discussion.....	112
4.5 References.....	116
CHAPTER 5 Sensitivity Analysis on a Non-steady State Bioenergetics/kinetic Model	128
5.1 Introduction.....	128
5.2 Methods.....	129
5.3 Results.....	136
5.4 Discussion.....	138
5.5 References.....	141
CHAPTER 6 General Discussion.....	151
6.1 Summary.....	151
6.2 Discussion.....	153
6.3 Future Studies.....	159
6.4 References.....	160
APPENDICES.....	164
Appendix A.....	164
VITA AUCTORIS.....	165

LIST OF TABLES

Chapter 2

Table 2.1 Mean (\pm SD) THg, MeHg, and PCB concentrations in control and dosed fish at the end (day 0 for elimination) of dosing, as well as in fish diet.....51

Chapter 3

Table 3.1 Bioenergetics and toxicokinetics parameters for Silver Carp and Bighead Carp.....82

Table 3.2 Summarized biological data, THg wet weight concentrations, MeHg wet weight concentrations, sumPCB (Σ PCB) wet weight concentrations, $\delta^{13}\text{C}$ and $\delta^{15}\text{N}$ signatures for Silver Carp and Bighead Carp.....84

Table 3.3 Measured total mass (Mean \pm SD), as well as lipid to whole body weight ratio (Mean \pm SD), and lean dry weight (LDW) to whole body weight ratio (Mean \pm SD) for Silver Carp and Bighead Carp under two growth scenarios.....85

Table 3.4 Linear regression between observed and simulated MeHg and PCB 180 concentrations for Silver Carp (SC) and Bighead Carp (BC).....86

Chapter 4

Table 4.1 Summarized biological data, total mercury (THg) concentrations, sum PCB (Σ PCB) concentrations, $\delta^{13}\text{C}$ and $\delta^{15}\text{N}$ signatures for Bluegill collected from five sampling locations across North America. Values represent mean \pm 1 standard error with data minima and maxima included in parentheses.....121

Table 4.2 Measured total mass (mean \pm SE), lipid to whole body weight ratio (mean \pm SE), and lean dry weight (LDW) to whole body weight ratio (mean \pm SE) for fish of each age class from each location.122

Table 4.3 Linear regression between predicted and observed total Hg and PCB 180 concentrations under two growth scenarios.....123

Table 4.4 The fraction of Hg and PCB retained for each age class under the model simulation.....124

Chapter 5

Table 5.1 Description for bioenergetics and toxicokinetics parameters.....145

Table 5.2 Mean and distribution of model inputs based on literature or assumptions...147

Table 5.3 Mean and standard deviation (SD) of model inputs based on observed field data.....149

Table 5.4 Sensitivity analysis on Hg lean dry weight concentration of an age 6 Bighead Carp, an age 4 Silver Carp, and an age 5 Bluegill. The parameters with the five greatest contributions to total variance are presented.....150

Table 5.5 Sensitivity analysis on PCB lipid-equivalent concentration of an age 6 Bighead Carp, an age 4 Silver Carp, and an age 5 Bluegill. The parameters with the 5 greatest contributions to total variance are presented.150

LIST OF FIGURES

Chapter 2

Figure 2.1 THg and MeHg elimination by fish from three treatments, squares represent low (■), circles represent medium (●), crosses represent high dosing treatment (×); THg was tested for fish at days 0, 7, 14, 21, 28, 42, 56, 72, and 84 (n=5, 5, 5, 5, 5, 5, 5, 5 and 5 for low dosed treatment, n=5, 5, 5, 5, 5, 4, 4, 4 and 5 for medium dosed treatment, and n=5, 5, 5, 5, 4, 4, 4, 5 and 5 for high dosed fish). MeHg was tested in fish on days 0, 28, 56, and 84 (n=2,4,5 and 5 for low dosed group, n=3, 5,4 and 4 for medium dosed group, and n=5, 4, 3 and 1 for high dosed treatment). Vertical bars represent standard error.....52

Figure 2.2 Elimination rate coefficients of PCB congeners from high dosed fish.....52

Figure 2.3 Assimilation efficiencies of THg, MeHg, and PCB 180; Grey bars for THg and MeHg represent the average AE value from each treatment sample. The grey bar for PCB 180 represents the mean AE value from the high dosed fish sample. Vertical bars represent standard error.....53

Figure 2.4 Biomagnification factors of PCB congeners in Goldfish. The solid line represents the curvilinear model, and the dashed line represents the linear model.....53

Chapter 3

Figure 3.1 Nitrogen (a) and carbon (b) stable isotopes versus body mass of fish; crosses (×) represent Silver Carp; triangles (▲) represent Bighead Carp.....87

Figure 3.2 Relationships between simulated and observed MeHg and PCB 180 concentrations under model assumptions of; (a) lipid growth rates proportional to whole body growth (Scenario 1); (b) population specific lipid growth rates (Scenario 2); (c) protein growth rates proportional to whole body growth (Scenario 1); and (d) population specific protein growth rates (Scenario 2). Solid circles (●) and open circles (○) represent PCB 180 in Silver Carp and Bighead Carp; and solid diamonds (◆) and open diamonds (◇) represent MeHg in Silver Carp and Bighead Carp, respectively; dashed lines represent the 1:1 regression fit.....88

Figure 3.3 PCB 180 lipid-equivalent concentration and MeHg lean dry weight concentration versus age of the fish; circles (●) represent measured chemical concentration of Silver Carp; crosses (×) represent measured concentration of Bighead Carp; dashed lines were the simulations of chemical bioaccumulation in Silver Carp; dotted lines modeled chemical bioaccumulation in Bighead Carp.....89

Chapter 4

Figure 4.1 Map of sampling location. Stars represent sampling sites.....125

Figure 4.2 Relationships between predicted and observed total Hg and PCB 180 concentrations across lake populations and age classes under model assumptions of; (a) lipid and protein growth rates proportional to whole body growth (Scenario 1) and; (b) population specific lipid and protein growth rates (Scenario 2). In both panels, solid (●) and open (○) circles represent Hg and PCB 180, respectively. Dashed lines represent the

1:1 regression fit. The outliers in (a) and (b) reflect PCB 180 concentrations of fish from the Detroit River.....125

Figure 4.3 Relationship between relative chemical level (chemical concentration in fish $[C_t]$ divided by chemical concentration in YOY $[C_{YOY}]$) and age for individual lake populations. Squares (■) represent THg and circles (●) represent PCB 180. Error bars used standard error; dashed lines (---) represent the modeled concentrations at activity levels = 1 (blue), 1.5 (black), and 2 (red), respectively.....126

Chapter 6

Figure 6.1 The mean protein growth rate ($k_{g,pro}$) to Hg elimination rate ($k_{tot,Hg}$) ratio (a) and the mean lipid growth rate ($k_{g,lip}$) to PCB elimination rate ($k_{tot,PCB}$) ratio (b) for each age class of Bighead Carp, Silver Carp as well as Bluegill from five locations. Circles (○) represent Bighead Carp, triangles (Δ) represent Silver Carp, and crosses (×) represent Bluegill.....163

CHAPTER 1

General Introduction

1.1 Global Contamination of Mercury (Hg) and Polychlorinated Biphenyls (PCBs)

Mercury (Hg) is a metal that is ubiquitously present in the environment. Although occurring naturally, Hg levels in the environment have increased significantly in the past century due to its wide applications in industry (Morel et al. 1998; Boening, 2000).

Methylmercury (MeHg) is one of the most toxic and common organic forms of Hg in aquatic ecosystems and can bioaccumulate through the aquatic food web (Harris et al. 2003). It has been concluded that more than 95% of the Hg present in aquatic species is in the form of MeHg (Bloom, 1992); thus, many fish bioaccumulation studies interchangeably use Hg and MeHg (Trudel and Rasmussen, 2006). A series of Hg poisoning incidents through fish consumption since the 1960s (Takizawa, 1979) has raised attention about the global environmental contamination by Hg.

Similarly, polychlorinated biphenyls (PCBs), which were synthesized and widely used in industry after world war II, have been recognized as globally dispersed persistent organic contaminants since 1966 (Mullin et al. 1984). There are 209 possible PCB congeners, each exhibiting different physicochemical properties resulting in different toxicity and environmental partitioning (Mackay, 1982). One of the major physical properties relating congener specific PCB fate and toxicity involves chemical hydrophobicity commonly referenced according to the *n*-octanol-water partition coefficient (K_{OW}), which exhibits log values in the range of 4.09 to 8.18 (Hawker and Connell, 1988). Most PCB congeners are considered highly hydrophobic; hence, these compounds are also readily bioaccumulated and biomagnified through the food web (Connelly and Pedersen, 1988;

Gobas et al. 1999). In addition, both Hg and PCBs can enter global atmospheric circulation and be redistributed anywhere on earth (Ullrich et al. 2001; Han et al. 2016). Elevated Hg and PCBs levels have been found in marine and freshwater systems, even in remote areas that are far from direct anthropogenic sources (Swain 1978; Hakanson et al. 1988; Bidleman et al. 1989; Rada et al. 1989; Lindqvist, 1991; Han et al. 2016).

The ability of Hg and PCBs to bioaccumulate in food webs has led to concerns about exposure of these contaminants to humans (Bargagli et al. 1998; Atwell et al. 1998; Campbell et al. 2005). Because the consumption of fish by humans represents the most important exposure route of these contaminants, bioaccumulation of Hg and PCBs by aquatic species has attracted a great deal of scholarly and environmental management focus (Myers et al. 2000; Stern et al, 2001; Trasande et al. 2005). Health advisories and regulatory fish consumption guidelines owing largely to PCBs and Hg have been issued in Canada, United States and many other countries (Oken et al. 2003; Mozaffarian and Rimm, 2006). The health risks coupled with the global contamination of aquatic ecosystems requires understanding of the mechanism of Hg and PCB bioaccumulation in fish.

1.2 Bioaccumulation Kinetics of Hg and PCBs by Fish

Bioaccumulation occurs when the chemical uptake rate in an organism exceeds its capacity for whole body elimination of the chemical (Thomann, 1981; Arnot and Gobas, 2003). There are many commonalities among the general bioaccumulation characteristics for Hg and PCBs (Li et al. 2015). For chemical uptake in aquatic species, the two main sources of intake consist of aqueous uptake via gills or skin and dietary uptake via the

gastrointestinal tract. It has been reported that food is the dominant pathway for MeHg (Hall et al. 1997) and highly hydrophobic PCBs ($\log K_{OW} > 5$) bioaccumulation in fish (Fisk et al. 1998). Highly hydrophobic PCBs are often the congeners of interest in bioaccumulation studies owing to their higher biomagnification potentials (Russell et al. 1995; Fisk et al. 1998). In contrast, chemical elimination pathways include (among others) loss across respiratory surfaces, loss via urine, feces, mucous, protein/lipid excretion (e.g. via reproductive output, sloughing of cells, scales or excretions), metabolic biotransformation and pseudo-elimination due to growth dilution (Sijm, 1992; Trudel and Rasmussen, 2001). Biotransformation of Hg and PCBs by fish usually is not considered because there is little evidence for biotransformation of MeHg by fish (Burrows and Krenkel, 1973) and biotransformation of PCB by fish is negligible relative to whole body elimination (Muir et al. 1988; Paterson et al. 2010). Among other elimination pathways, Paterson et al. (2010) found that loss through gills was the major elimination pathway for PCBs, while other studies suggest that feces play a more important role for the more hydrophobic chemicals (Gobas et al. 1988). However, less information is available about which of the above routes dominate Hg elimination by fish.

Despite the similarities in uptake and elimination processes between Hg and PCBs, these substances have different mechanisms of accumulation (Norstrom et al. 1976; Borgmann and Whittle, 1992; Mackay and Fraser, 2000; Dang and Wang, 2010). PCB transfer between aqueous and relevant biotic phases (lipid) is largely diffusion based and governed by gradients in chemical potential or fugacity between the organism and its environment (Connolly and Pedersen, 1988). This process is regulated by chemical-

physical properties (i.e. hydrophobicity) (Mackay, 1982); consequently, lipid content of the fish represents the primary storage compartment for PCBs (Drouillard et al. 2004). In contrast, Hg is strongly associated with sulfur-rich amino acids and distributes primarily to protein rich tissues (Stohs and Bagchi, 1995). As our understanding of the mechanism of PCB bioaccumulation by fish becomes more and more complete (Gobas et al. 1993; Gobas et al. 1999; Drouillard, 2008), there is still a lack of knowledge to clearly describe the mechanism of Hg uptake and elimination by fish.

1.3 Modeling Hg and PCB Bioaccumulation by Fish

In order to improve risk assessment and minimize exposure to consumers, numerous models have been developed to predict Hg and PCB bioaccumulation by fish (Trudel and Rasmussen, 2001&2006; Arnot and Gobas, 2004; Drouillard et al. 2009). Early studies first addressed bioaccumulation of hydrophobic chemicals from aqueous exposures (or bioconcentration) using simple equilibrium partitioning models (Neely et al. 1974), which assumed that thermodynamic gradients (or fugacity) drive chemical exchange between water and the animal until the fugacity is equal for all phases (Mackay, 1982). As the role of dietary uptake (or biomagnification) was recognized by many studies (Thomann and Connolly, 1984; Hall et al. 1997), bioaccumulation models which included both dietary and aqueous uptake were also developed using the thermodynamic-based approach (Clark et al. 1990). These models have primarily employed steady-state assumption, which defines the condition that total uptake of a pollutant equals to its total elimination by fish (Thomann, 1981; Connolly and Pedersen, 1988). The steady state models have the advantage of using relatively simple model inputs, which saves time and efforts for data collection.

However, field and laboratory studies have demonstrated that Hg and PCBs were unlikely to achieve steady state during the lifetime for many fresh water species (Paterson et al. 2007; Abma et al. 2015). For fish, growth and chemical elimination rates substantially decrease with size (Trudel and Rasmussen, 1997; Paterson et al. 2007; Dang and Wang, 2012), and older fish may also switch to more contaminated prey at higher trophic levels (Borgmann and Whittle, 1992; Dang and Wang, 2012). Relatively slow elimination coupled with increased uptake flux related to diet shifts to more contaminated prey items leads to increase of Hg and PCBs levels in fish at older ages and also changes in the bioaccumulation slope between age classes (Trudel and Rasmussen, 2006). Therefore, steady state might be a rare occurrence in nature, and non-steady state is a more realistic scenario for many species. Moreover, non-steady state bioaccumulation models have been shown to provide better predictions for risk assessment of long lived top predator fish which are the major focus for sport fish consumption advisories (McLeod et al. 2016).

1.4 Toxicokinetics Model and Parameters

As a result of the commonalities among the general bioaccumulation characteristics for Hg and PCBs, common bioaccumulation models were proposed by many studies (Norstrom et al. 1976; Borgmann and Whittle, 1992). Some of the most common models are toxicokinetic bioaccumulation models, which adopt mass balance principles and use rate coefficients derived from empirical data to describe pollutant uptake from water and food, whole body elimination, and growth dilution (Trudel and Rasmussen, 2001; McLeod et al. 2016). The model can be used for predicting daily changes of chemical concentration under non-steady state condition, and it is expressed by:

$$\frac{dC}{dt} = k_w \times C_w + AE \cdot Q_C \cdot C_d - (k_{tot} + k_g) \cdot C \quad (1.1)$$

where k_w is the chemical uptake rate via gill, C_w is the chemical concentration in water, AE is assimilation efficiency from food (unitless), Q_C is food consumption rate (g food g bw⁻¹ d⁻¹), C_d is chemical concentration in diet (ng g⁻¹), k_{tot} is the whole body elimination rate coefficient including all elimination routes (d⁻¹), k_g is the growth rate coefficient (g tissue g bw⁻¹ d⁻¹), and C is the chemical concentration in fish (ng g⁻¹).

Because dietary uptake is considered a major pathway for MeHg and hydrophobic PCBs (Hall et al. 1997; Madenjian et al. 1998), the dietary assimilation efficiency is a key toxicokinetic parameter that determines the chemical uptake rate of different chemicals (Trudel and Rasmussen, 2001; Madenjian et al. 2012). Assimilation efficiency is often assumed to be constant and independent of diet, although some studies have questioned this for PCBs (Liu et al. 2010). For example, although values of AE for PCBs are normally under 60%, high variation has been observed across diets and studies (Fisk et al. 1998; Buckman et al. 2004; Liu et al. 2010; Li et al. 2015). Furthermore, AEs of PCBs have been found to be a weak function of congener hydrophobicity (Gobas et al. 1988; Madenjian et al. 2012) and food quality (Dabrowska et al. 1999; Liu et al. 2010). For MeHg, previous studies have shown that AE varied from species to species and ranged from 65-99% (Wang and Wong, 2003; Trudel and Rasmussen, 2006; Pickhardt et al. 2006; Wang et al. 2010).

Food consumption rate, which is determined by an animal's metabolic rate and the energy density of ingested food (Trudel and Rasmussen, 2006), is an important physiological parameter that can significantly influence chemical bioaccumulation from the dietary

source. Wang and Wang (2012) observed that concentrations of MeHg in fish increased proportionally with consumption rate (Wang and Wang, 2012), while Borgmann and Whittle (1992) reported that a reduction in food ingestion rate caused a drop in PCB concentration of Lake Trout. However, the consumption rate might not always be positively related to the bioaccumulation rate, because consumption rate can also interact with other physiological parameters such as growth rate (Xu and Wang, 2002; Tsui and Wang, 2004). These complex relationships have rarely been considered in previous model studies (Wang and Wang, 2012).

The whole body elimination coefficient, which represents the sum of elimination coefficients across all chemical loss pathways, is also a key toxicokinetic parameter determining the extent of bioaccumulation of a given contaminant (Wallegghem et al. 2007). k_{tot} is usually described as a function of water temperature and body size for both Hg and PCBs (Trudel and Rasmussen, 1997; Paterson et al. 2007). Hg and PCB elimination by fish is assumed to be a first order process for most bioaccumulation models (Trudel and Rasmussen, 1997; Wang and Wong, 2003; VanWalleggham et al. 2007), which means elimination flux is concentration dependent while the elimination rate coefficient is concentration independent. Paterson et al. (2010) confirmed first order kinetics for PCB elimination by fish; however, the results of studies testing first order kinetics for Hg elimination are somewhat conflicting (Jarvenpaa et al. 1970; Burrows and Krenkel, 1973; Ruohtula and Miettinen, 1975; Trudel and Rasmussen, 1997). Thus there is still a need to verify first order or non-first order kinetics in order to quantify Hg bioaccumulation potentials in fish and adopt appropriate concentration dependent or independent bioaccumulation models.

Although growth rate receives less attention compared with other chemical elimination pathways (Eichinger et al. 2010; Wang and Wang, 2012), bioaccumulation in fish is also strongly influenced by growth dilution (Stafford and Haines, 2001). Previous studies found that rapid growth rate could significantly reduce chemical concentrations in fish by diluting the ingested chemicals (Stow and Carpenter 1994; Doyon et al. 1998; Essington and Houser 2003; Simoneau et al. 2005). However, other studies observed no effect of growth on chemical concentration, or a positive relationship between fish growth and chemical accumulation (Dutton, 1997; Karimi et al. 2007). The discrepancy among studies indicates that growth rate itself is not sufficient to explain patterns of contaminant accumulation in fish, and that factors affecting growth rate, such as water temperature, prey availability, prey quality, and fish activity level, need to be taken into consideration (Trudel and Rasmussen, 2006; Karimi et al. 2007). Moreover, as mentioned, a higher growth rate requires a higher food consumption rate, which in turn represents more chemical uptake from dietary source. Consequently, interpreting the effect of fish growth on contaminant bioaccumulation should also consider the relationship between growth and consumption rate.

Developing a common model to correctly predict Hg and PCB concentrations in fish requires accurate estimates of toxicokinetic parameters. Due to the differences in their environmental speciation, fate, and the physiological mechanisms regulating chemical assimilation and elimination pathways, as well as the differences in analytical procedure (Mason et al. 1994; Stohs and Bagchi, 1995; Gobas et al. 1999), no direct comparisons of toxicokinetics parameters have been made between Hg and PCBs within the same organism. Moreover, owing to the uncontrolled factors in different studies using different

experimental conditions, fish sizes, and fish diets, it is difficult to directly compare Hg and PCBs kinetic rate using current literature in a model fish species. In order to have a better understanding of how the magnitude of bioaccumulation potentials of Hg and PCBs differ, it is imperative to directly compare these key toxicokinetic parameters.

1.5 Bioenergetics Model and Growth Rate

Although early models assumed bioaccumulation process was mainly regulated by chemical-physical properties, it has been demonstrated that chemical toxicokinetics and bioaccumulation are significantly influenced by biological and ecological processes (Madenjian et al. 1994; Paterson et al. 2007; Daley et al, 2009; Dang and Wang, 2012). In Eq. 1.1, both dietary and aqueous uptake should be quantified according to species specific metabolic rate, growth, and environmental temperature. Moreover, once the Hg and PCB enters the fish body and is bound to protein and lipid, respectively, the elimination rate of these pollutants should be directly related to the turnover of the corresponding tissue components, which in turn also should be associated with metabolic rate, growth, and water temperature (Norstrom et al. 1976). Because the key parameters in the toxicokinetics model are all regulated by species specific physiological and environmental conditions, a bioenergetics model has been introduced to the field of bioaccumulation models for addressing fish metabolic and growth responses to varying environmental conditions (Madenjian et al. 1993; Stow et al. 1995).

The bioenergetics model was originally presented to study the energy flow between fish and its environment, and was described by Winberg (1956) as:

$$C = G + R + W \tag{1.2}$$

where C is consumption, G is growth, R metabolism, and W is wastes.

This model was further expanded by Hanson et al. (1997), and was used to estimate consumption or growth, respiration, egestion, and excretion for a wide range of species under various environmental conditions. The equation was expressed as follows:

$$C = G + R + A + S + F + U \quad (1.3)$$

where C is consumption, G is growth, R is respiration, A is active metabolism, S is specific dynamic action, F is fecal egestion, and E is excretion.

The application of the bioenergetics model in bioaccumulation studies has proven beneficial for generating accurate predictions, especially for fish experiencing complex field conditions (Drouillard et al. 2009). Norstrom et al. (1976) used a bioenergetics-based bioaccumulation model to successfully predict PCB and Hg concentration in Yellow Perch from Ottawa River. Madenjian et al. (1993) also found that variability in PCB concentration among Lake Trout from Lake Michigan could be explained by an individual-based bioenergetics model when variation in prey fish PCBs was included. Thus, introduction of bioenergetics models to toxicokinetics models have the advantage of being scalable to different species and different environmental conditions that organisms may experience in their natural habitat (Drouillard et al. 2009). In addition, combined bioenergetic-toxicokinetic models are capable of predicting chemical bioaccumulation under the non-steady state assumption, which is often the case for Hg and hydrophobic PCBs (Paterson et al. 2007; Abma et al. 2015; McLeod et al. 2016).

Both bioenergetics and toxicokinetics models are significantly influenced by growth rate. On the one hand, growth is a reflection of the difference between energy intake and expenditure, and is highly dependent on food consumption rate and animal activity levels (Wang and Wang, 2012). On the other hand, growth can significantly influence the chemical bioaccumulation patterns in fish by growth dilution (Eichinger et al. 2010) or bioamplification (Daley et al. 2014). Thus, understanding the effects of growth on bioaccumulation requires an understanding of the particular mechanism driving growth and the bioenergetics processes (Wang and Wang, 2012).

It is well known that lipid tissue is the main storage compartment for PCBs and dictates the maximum capacities for an individual to bioaccumulate PCBs (Mackay, 1982; Roesijadi, 1992). Thus, it is assumed that protein tissue can affect Hg bioaccumulation in a similar manner, because Hg is primarily associated with protein (Stohs and Bagchi, 1995). As such, growth may have different effects on Hg and PCB bioaccumulation when protein and lipid tissue exhibit differences in their respective growth rates. However, current bioaccumulation models only considered whole body growth rather than proximate growth of contaminant associated storage compartments, assuming that relevant tissue components growth is at the same rate as the whole body. However, body composition can change drastically for wild fish under complex field environments. For instance, Paterson et al. (2007) observed significant lipid loss in Yellow Perch during the winter period. Thus, application of specific growth rates of the associated tissue may be more ecologically realistic and can help us to further improve the accuracy of predictive models for Hg and PCB bioaccumulation, and further verification of this assumption on wild fish species still needs to be completed.

1.6 Study Objectives and Hypotheses

Global contamination of Hg and PCB in aquatic ecosystems coupled with the health risks associated with fish consumption requires a better understanding of the bioaccumulation mechanism of Hg and PCB, which can further assist with accurately predicting Hg and PCB concentration in fish. To develop a universal model for Hg and PCBs, it is imperative to quantify the differences in the magnitude of key toxicokinetic parameters between these chemicals. However, direct comparison of kinetic rate between Hg and PCBs is not possible using the current literature, owing to different studies using different experimental conditions. Moreover, due to Hg and PCBs being associated with different tissues in fish, it is still unclear if growth dilution has different effects on the bioaccumulation process of Hg and PCBs. To evaluate the effects of growth rate, a non-steady state model is necessary, which could allow changes in growth rate with time.

The aim of this study is to improve our understanding of the mechanisms of Hg and PCB dynamics in fish, and develop a universal bioaccumulation model that can be applied to these two contaminants. This dissertation involves a series of studies to measure the toxicokinetic parameters as described in Eq. 1.1, to apply non-steady state bioenergetics/toxicokinetic models on several wild fish species from various locations, to examine how specific tissue growth rates affect Hg and PCB accumulation in fish, and identify key parameters of the bioaccumulation model necessary for future focus using a sensitivity analysis. The objectives and hypotheses for each data chapter are as follows.

Chapter 2: Hg and PCB uptake as well as elimination coefficients were simultaneously quantified in Goldfish (*Carassius auratus*). The main objective of this chapter was to

directly compare bioaccumulation potential of Hg and PCB within the same organism.

The hypotheses tested in this chapter were:

- 1) To confirm that Hg elimination by fish is a first order process;
- 2) To quantitatively assess if Hg and PCB have different bioaccumulation potentials.

Chapter 3: Research is based on the development of a non-steady state bioenergetics/bioaccumulation model to simulate PCB and Hg bioaccumulation by Silver Carp (*Hypophthalmichthys molitrix*) and Bighead Carp (*Hypophthalmichthys nobilis*) from the Three Gorge Reservoir (TGR), China. Goodness of fit tests between model predictions and field collected data were generated using measured tissue growth rates and compared with the same model that only considered whole body growth rate. Two species of Asian carp were studied to determine if a non-steady state bioenergetics/toxicokinetic model could simulate Hg and PCB concentration in both species, and if the effect of growth rate was consistent in different species. The hypotheses tested in this chapter were:

- 1) A non-steady state, bioenergetic/toxicokinetic model can predict PCB and HG concentrations in two species of Asian Carp.
- 2) Models that apply tissue specific growth rate as opposed to consideration of only whole body growth rate provide a stronger explanation of bioaccumulation differences for Hg and PCBs bioaccumulation rates in Asian Carp.

Chapter 4: This chapter evaluated the effect of tissue specific growth on Hg and PCBs bioaccumulation by Bluegill (*Lepomis macrochirus*) collected from five different locations over a latitudinal gradient ranging from 34° to 46° north latitude. Latitudinal

gradient was adopted as a means of comparing different populations of Bluegill that differed in their growth rate. A non-steady state bioenergetics/toxicokinetic model was applied to simulate the Hg and PCB bioaccumulation in each population. Simulations using tissue specific growth rate were contrasted with simulations using whole body growth for their goodness of fit to field measured data. The hypotheses tested in this chapter were:

- 1) Bluegill populations from different latitudes exhibit differences in whole body growth and tissue specific growth.
- 2) A universal bioenergetic/kinetic bioaccumulation model incorporating tissue specific growth dilution as opposed to whole body growth can better account for deviations in bioaccumulation patterns of Hg and PCBs in Bluegill populations.

Chapter 5: This chapter evaluated the contribution of each model parameter to model output of the non-steady state bioenergetics/toxicokinetic model developed in Chapters 3 and 4. A sensitivity analysis (Monte Carlo analysis) was applied for the three model species (Bighead Carp, Silver Carp and Bluegill). Actual measured error generated from field observations was applied in the sensitivity analysis for growth rate, stable isotope signature, and chemical concentration in young of the year (YOY), while the rest of the toxicokinetic and bioenergetic parameters were assigned a uniform distribution with the same range of variability ($\pm 10\%$ of the value as upper and lower limits around the mean) in the sensitivity analysis. The main objective of this chapter was to identify common key factors that most influenced the output of the non-steady state bioenergetic/toxicokinetic bioaccumulation model. The hypothesis tested in this chapter was:

1) The parameters regulated by tissue specific growth rate, prey trophic position, and YOY chemical concentration, have comparable influence on the non-steady state bioenergetic/toxicokinetic model.

1.7 References

- Abma, R.; Paterson, G.; Mcleod, A.; Haffner, G. D. Cross-basin comparison of mercury bioaccumulation in Lake Huron lake trout emphasizes ecological characteristics. *Environ. Toxicol. Chem.* 2015, 34, 355-359.
- Arnot, J. A.; Gobas, F. A. P. C. A generic QSAR for assessing the bioaccumulation potential of organic chemicals in aquatic food webs. *QSAR Comb Sci.* 2003, 22:337-345.
- Arnot, J. A.; Gobas, F. A. P. C. A food web bioaccumulation model for organic chemicals in aquatic ecosystems. *Environ. Toxicol. Chem.* 2004, 23, 2343-2355.
- Atwell, L.; Hobson, K. A.; Welch, H. E. Biomagnification and bioaccumulation of mercury in an arctic marine food web: insights from stable nitrogen isotope analysis. *Can. J. Fish. Aquat. Sci.* 1998, 55, 1114-1121.
- Bargagli, R.; Monaci, F.; Sanchez-Hernandez, J. C.; Cateni, D. Biomagnification of mercury in an Antarctic marine coastal food web. *Mar. Ecol. Prog. Ser.* 1998, 169, 65-76.
- Bidleman, T. F.; Patton, G. W.; Walla, M. D.; Hargrave, B. T.; Vass, W. P.; Erickson, B.; Fowler, B.; Scott, V.; Gregor, D. J. Toxaphene and other organochlorines in the arctic ocean fauna: evidence for atmospheric delivery. *Arctic.* 1989, 42, 307-313.
- Bloom, N. S. On the chemical form of mercury in edible fish and marine invertebrate tissue. *Can. J. Fish Aquat. Sci.* 1992, 49, 1010-1017.
- Boening, D. W. Ecological effects, transport, and fate of mercury: a general review. *Chemosphere.* 2000, 40:1335-1351.

- Borgmann, U.; Whittle, B. M. Bioenergetics and PCB, DDE, and mercury dynamics in Lake Ontario lake trout (*Salvelinus namaycush*): a model based on surveillance data. *Can. J. Fish. Aquat. Sci.* 1992, 49, 1086-1896.
- Buckman, A. H.; Brown, S. B.; Hoekstra, P. F.; Solomon, K. R.; Fisk, A. T. Toxicokinetics of three polychlorinated biphenyl technical mixtures in rainbow trout (*Oncorhynchus mykiss*). *Environ. Toxicol. Chem.* 2004, 23, 1725-1736.
- Burrows, W. D.; Krenkel, P. A. Studies on uptake and loss of methylmercury-203 by bluegills. *Environ. Sci. Technol.* 1973, 7(13), 1127-1130.
- Campbell, L. M.; Norstrom, R. J.; Hobson, K. A.; Muir, D. C. G.; Backus, S.; Fisk, A. T. Mercury and other trace elements in a pelagic Arctic marine food web (Northwater Polynya, Baffin Bay). *Sci. Total. Environ.* 2005, 351, 247-263.
- Clark, K. E.; Gobas, F. A. P. C.; Mackay, D. Model of organic chemical uptake and clearance from fish from food and water. *Environ. Sci. Technol.* 1990, 24, 1203-1213.
- Connolly, J. P.; Pedersen, C. J. A thermodynamic-based evaluation of organic chemical accumulation in aquatic organisms. *Environ. Sci. Technol.* 1988, 22, 99-103.
- Dabrowska, H.; Fisher, S. W.; Dabrowski, K.; Staubus, A. E. Dietary uptake efficiency of 2,2',4,4',5,5'-hexachlorobiphenyl in yellow perch and rainbow trout: role of dietary and body lipids. *Environ. Toxicol. Chem.* 1999, 18, 938-945.
- Daley, J. M.; Leadley, T. A.; Drouillard, K. G. Evidence for bioamplification of nine polychlorinated biphenyl (PCB) congeners in yellow perch (*Perca flavescens*) eggs during incubation. *Chemosphere.* 2009, 75 (11), 1500-1505.
- Daley, J. M.; Paterson, G.; Drouillard, K. G. Bioamplification as a bioaccumulation mechanism for persistent organic pollutants (POPs) in wildlife. *Rev. Environ. Contam. Toxicol.* 2014, 227: 107-155.
- Dang, F.; Wang, W. X. Why mercury concentration increases with fish size? Biokinetic explanation. *Environ. Pollut.* 2012, 163, 192-198.

- Doyon, J. F.; Schetagne, R.; Verdon, R. Different mercury bioaccumulation rates between sympatric populations of dwarf and normal lake whitefish (*Coregonus clupeaformis*) in the La Grande complex watershed, James Bay, Quebec. *Biogeochemistry*. 1998, 40: 203-216.
- Drouillard, K. G. Ecotoxicology: Biomagnification. In Jørgensen, SE, BD Fath (Eds.), *Ecotoxicology*. Vol. 1 of *Encyclopedia of Ecology*, 5 vols. Oxford, Elsevier. 2008, 441-448.
- Drouillard, K. G.; Hagen, H.; Haffner, G. D. Evaluation of chloroform/methanol and dichloromethane/hexane extractable lipids as surrogate measures of sample partition capacity for organochlorines in fish tissues. *Chemosphere*. 2004, 55, 395-400.
- Drouillard, K. G.; Paterson, G.; Haffner, G. D. A combined food web toxicokinetic and species bioenergetic model for predicting seasonal PCB elimination by yellow perch (*Perca flavescens*). *Environ. Sci. Technol.* 2009, 43(8), 2858-2864.
- Dutton, M. D. Methyl mercury bioaccumulation: a study of factors influencing uptake and elimination in fish. Ph.D. dissertation, University of Waterloo, Waterloo, Ontario. 1997.
- Eichinger, M.; Loizeaua, V.; Roupsarda, F.; Le Guelleca, A. M.; Bacherb, C. Modelling growth and bioaccumulation of Polychlorinated biphenyls in common sole (*Solea solea*). *J. Sea Res.* 2010, 64 (3), 373-385.
- Essington, T. E.; Houser, J. N. The effect of whole-lake nutrient enrichment on mercury concentration in age-1 yellow perch. *Trans. Am. Fish. Soc.* 2003, 132: 57-68.
- Fisk, A. T.; Norstrom, R. J.; Cymbalisky, C. D.; Muir, D. C. G. Dietary accumulation and depuration of hydrophobic organochlorines: Bioaccumulation parameters and their relationship with the octanol/water partition coefficient. *Environ. Toxicol. Chem.* 1998, 17, 951-961.
- Giesy, J. P.; Kannan, K. Dioxin-like and non-dioxin-like toxic effects of polychlorinated biphenyls (PCBs): implications for risk assessment. *Crit. Rev. Toxicol.* 1998, 28(6), 511-569.

- Gobas, F. A. P. C.; Muir D. C. G.; Mackay, D. Dynamics of dietary bioaccumulation and fecal elimination of hydrophobic organic chemicals in fish. *Chemosphere*. 1988, 17, 943-962.
- Gobas, F. A. P. C.; Wilcockson, J. B.; Russell, R. W.; Haffner, G. D. Mechanism of biomagnification in fish under laboratory and field conditions. *Environ. Sci. Technol.* 1999, 33, 133-141.
- Gobas, F. A. P. C.; Wilcockson, J. B.; Russell, R. W.; Haffner, G. D. Mechanism of biomagnification in fish under laboratory and field conditions. *Environ. Sci. Technol.* 1999, 33, 133-141.
- Gobas, F. A. P. C.; McCorquodale, J. R.; Haffner, G. D. Intestinal absorption and biomagnification of organochlorines. *Environ. Toxicol. Chem.* 1993, 12, 567-576.
- Hakanson, L.; Nilsson, A.; Andersson, T. Mercury in fish in Swedish lakes. *Env. Poll.* 1988, 49, 145-162.
- Hall, B. D.; Bodaly, R. A.; Fudge, R. J. P.; Rudd, J. W. M.; Rosenberg, D. M. Food as the dominant pathway of methylmercury uptake by Fish. *Water, Air, and Soil Pollut.* 1997, 100, 13-24.
- Han, Y; Liu, W.; Hansen, H.; Chen, X.; Liao, X.; Li, H.; Wang, M.; Yan, N. Influence of long-range atmospheric transportation (LRAT) on mono-to octa-chlorinated PCDD/Fs levels and distributions in soil around Qinghai Lake, China. *Chemosphere*. 2016, 156, 143-149.
- Hanson, P. C.; Johnson, T. B.; Schindler, D. E.; Kitchell, J. F. *Fish Bioenergetics 3.0*. University of Wisconsin Sea Grant Institute; Madison; Wisconsin.
- Harris, H. H; Pickering, I. J.; George, G. N. The chemical form of mercury in fish. *Science*. 2003, 301(5637): 1203-1203.
- Hawker, D. W.; Connell, D. W. Octanol-water partition coefficients of polychlorinated biphenyl congeners. *Environ. Sci. Technol.* 1988, 22, 382-387.
- Jarvenpaa, T.J; Tillander, M.; Miettinen, J. K. Methylmercury: half-time of elimination in flounder pike and eel. *Suomen Kemistilehti* 1970, 43,439-442.

- Karimi, R.; Chen, C. Y.; Pickhardt, P. C.; Fisher, N. S.; Folt, C. L. Stoichiometric controls of mercury dilution by growth. *PNAS*. 2007, 104, 7477-7748.
- Karimi, R.; Chen, C. Y.; Pickhardt, P. C.; Fisher, N. S.; Folt, C. L.; Stoichiometric controls of mercury dilution by growth. *PNAS*. 2007, 104, 7477-7748.
- Li, J.; Drouillard, K. G.; Branfireun, B.; Haffner, G. D. Comparison of the toxicokinetics and bioaccumulation potential of mercury and polychlorinated biphenyls in goldfish (*Carassius auratus*). *Environ. Sci. Technol.* 2015, 49, 11019-11027.
- Lindqvist, O. (Ed.). Mercury in the Swedish environment: recent research on causes, consequences and corrective methods, *Water Air Soil Pollut.* 1991, 55(1-2).
- Liu, J.; Haffner, G. D.; Drouillard, K. G. The influence of diet on the assimilation efficiency of 47 polychlorinated biphenyl congeners in Japanese Koi (*Cyprinus carpio*). *Environ. Toxicol. Chem.* 2010, 29, 401-409.
- Mackay, D. Correlation of bioconcentration factors. *Environ. Sci. Technol.* 1982, 16, 274-278.
- Mackay, D.; Fraser, A. Bioaccumulation of persistent organic chemicals: mechanisms and models. *Environ. Pollut.* 2000, 110, 375-391.
- Madenjian, C. P.; Carpenter, S. R.; Eck, G. W.; Miller, M. A. Accumulation of PCBs by lake trout (*Salvelinus namaycush*): an individual-based model approach. *Can. J. Fish. Aquat. Sci.* 1993, 50:97-109.
- Madenjian, C. P.; Carpenter, S. R.; Rand, P. S. Why are the PCB concentrations of salmonine individuals from the same lake so highly variable. *Can. J. Fish. Aquat. Sci.* 1994, 51 (4), 800-807.
- Madenjian, C. P.; David, S. R.; Rediske, R. R.; O'Keefe, J. P. Net trophic transfer efficiencies of polychlorinated biphenyl congeners to lake trout (*Salvelinus namaycush*) from its prey. *Environ. Toxicol. Chem.* 2012, 31, 2821-2827.
- Mason, R. P.; Reinfelder, J. R.; Morel, F. M. M. Bioaccumulation of mercury and methylmercury. *Water, Air, and Soil Pollut.* 1995, 80, 915-921.

- McLeod, A. M.; Paterson, G.; Drouillard, K. G.; Haffner, G. D. Ecological implications of steady state and nonsteady state bioaccumulation models. *Environ. Sci. Technol.* 2016, 50, 11103-11111.
- Morel, F. M. M.; Kraepiel, A. M. L.; Amyot, M. The chemical cycle and bioaccumulation of mercury. *Annu. Rev. of Ecol. Syst.* 1998, 29: 543-566.
- Mozaffarian, D.; Rimm, E. B. Fish intake, contaminants, and human health - Evaluating the risks and the benefits. *JAMA.* 2006, 296, 1885-1899.
- Muir, D. C. G.; Norstrom, R. J.; Simon, M. Organochlorine contaminants in arctic marine food chains: accumulation of specific polychlorinated biphenyls and chlordane-related compounds. *Environ. Sci. Technol.* 1988, 22: 1071-79.
- Mullin, M. D.; Pochini, C. M.; McGrindle, S.; Romkes, M.; Safe, S. H.; Safe, L. M. High-resolution PCB analysis: synthesis and chromatographic properties of all 209 PCB congeners. *Environ. Sci. Technol.* 1984, 18, 468-476.
- Myers, G. J.; Davidson, P. W.; Cox, C.; Shamlaye, C.; Cernichiari, E.; Clarkson, T. W. Twenty-seven years studying the human neurotoxicity of methylmercury exposure. *Environ. Res.* 2000, 83, 275-285.
- Neely, W. B.; Branson, D. R.; Blau, G. E. Partition coefficients to measure bioconcentration potential of organic chemicals in fish. *Environ. Sci. Technol.* 1974, 8, 1113-1115.
- Norstrom, R. J.; McKinnon, A. E.; DeFreitas, A. S. W. Bioenergetics-based model for pollutant accumulation by fish simulation of PCB and methylmercury residue levels in Ottawa River yellow perch (*Perca flavescens*). *J. Fish. Res. Bd. Can.* 1976, 33, 248-267.
- Oken, E.; Kleinman, K. P.; Berland, W. E.; Sitnn, S. R.; Rich-Edwards, J. W.; Gillman, M. W. Decline in fish consumption among pregnant women after a national mercury advisory. *Obstet. Gynecol.* 2003, 102, 346-351.
- Paterson, G.; Drouillard, K. G.; Haffner, G. D. PCB elimination by yellow perch (*Perca flavescens*) during an annual temperature cycle. *Environ. Sci. Technol.* 2007, 41, 824-829.

- Paterson, G.; Drouillard, K. G.; Leadley, T. A.; Haffner, G. D. Long-term polychlorinated biphenyl elimination by three size classes of yellow perch (*Perca flavescens*). *Can. J. Fish. Aquat. Sci.* 2007, 64, 1222-1233.
- Paterson, G.; Liu, J. A.; Haffner, G. D. ; Drouillard, K. G. Contribution of fecal egestion to the whole body elimination of polychlorinated biphenyls by Japanese Koi (*Cyprinus carpio*). *Environ. Sci. Technol.* 2010, 44, 5769-5774.
- Pickhardt, P. C.; Stepanova, M.; Fisher, N. S. Contrasting uptake routes and tissue distribution of inorganic and methylmercury in mosquitofish (*Gambusia affinis*) and redear sunfish (*Lepomis microlophus*). *Environ. Toxicol. Chem.* 2006, 25(8), 2132-2142.
- Rada, R. G.; Wiener, J. G.; Winfrey, M. R.; Powell D. E. Recent increases in atmospheric deposition of mercury to north-central Wisconsin lakes inferred from sediment analyses. *Arch. Envir. Contam. Toxicol.* 1989, 18:175-181.
- Roesijadi; G. Metallothioneins in metal regulation and toxicity in aquatic animals. *Aquat. Toxicol.* 1992, 22(2), 81-114.
- Ruotula, M.; Miettinen, J. K. Retention and excretion of ²⁰³Hg-labelled methylmercury in rainbow trout. *OIKOS.* 1975, 26, 385-390.
- Russell, R. W.; Lazar, R.; Haffner, G. D. Biomagnification of organochlorines in Lake Erie white bass. *Environ. Toxicol. Chem.* 1995, 14 (4), 719-724.
- Sijm, D. T. H. M.; Seinen, W.; Opperhulzen, A. Life-cycle biomagnification study in fish. *Environ. Sci. Technol.* 1992, 26, 2162-2174.
- Simoneau, M.; Lucotte, M.; Garceau, S.; Lalibert é D. Fish growth rates modulates mercury concentration in walleye (*Sander vitreus*) from eastern Canadian lakes. *Environ. Res.* 2005, 98: 73-82.
- Stafford, C. P.; Haines, T. A. Mercury contamination and growth rate in two piscivore populations. *Environ. Toxicol. Chem.* 2001, 20(9): 2099-2101.
- Stern, A. H.; Burger, J. Mercury and methylmercury exposure in the New Jersey pregnant population. *Arch. Environ. Health.* 2001, 56, 4-10.

- Stohs, S. J.; Bagchi, D. Oxidative mechanisms in the toxicity of metal ions. *Free Rad. Biol. Med.* 1995, 18, 321-336.
- Stow, C. A.; Carpenter, S. R. PCB accumulation in Lake Michigan coho and chinook salmon: individual based models using allometric relationships. *Environ. Sci. Technol.* 1994, 28: 1543-1549.
- Stow, C. A.; Carpenter, S. R.; Madenjian, C. P.; Eby, L. A.; Jackson, L. J. Fisheries management to reduce contaminant consumption. *BioScience.* 1995, 45: 752-758
- Swain, W. R. Chlorinated organic residues in fish, water, and precipitation from the vicinity of Isle Royale, Lake Superior. *J. Great Lakes Res.* 1978, 4, 398-407.
- Takizawa, Y. Epidemiology of mercury poisoning in: the biogeochemistry of mercury in the environment. J.O. Nriagu, Ed. Elsevier/North-Holland Biomedical Press, Amsterdam. 1979, 325-366.
- Thomann, R. V. Equilibrium model of fate of micro-contaminants in diverse aquatic food chains. *Can. J. Fish. Aquat. Sci.* 1981, 38, 280-296.
- Thomann, R.V.; Connolly, J. P. Model of PCB in the Lake Michigan Lake trout food chain. *Environ. Sci. Technol.* 1984, 18, 650-671.
- Trasande, L.; Landrigan, P. J. Schechter C. Public health and economic consequences of methyl mercury toxicity to the developing brain. *Environ. Health Perspect.* 2005, 113, 590-596.
- Trudel, M.; Rasmussen, J. B. Bioenergetics and mercury dynamics in fish: a modelling perspective. *Can. J. Fish. Aquat. Sci.* 2006, 63, 1890-1902.
- Trudel, M.; Rasmussen, J. B. Modeling the elimination of mercury by fish. *Environ. Sci. Technol.* 1997, 31, 1716-1722.
- Trudel, M.; Rasmussen, J. B. Predicting mercury concentration in fish using mass balance models. *Ecol. Appl.* 2001, 11, 517-529.
- Tsui, M. K. T.; Wang, W. -X. Uptake and elimination routes of inorganic mercury and methylmercury in *Daphnia magna*. *Environ. Sci. Technol.* 2004, 38, 808-816.

- Ullrich S. M.; Tanton T.W.; Abdrashitova S. A. Mercury in the aquatic environment: a review of factors affecting methylation. *Crit. Rev. Environ. Sci. Technol.* 2001, 31(3), 241-293.
- Vanwallegem, J. L. A.; Blanchfield, P. J.; Hintelmann, H. Elimination of mercury by yellow perch in the wild. *Environ. Sci. Technol.* 2007, 41, 5895-5901.
- Wang, R.; Wang, W-X. Contrasting mercury accumulation patterns in tilapia (*Oreochromis niloticus*) and implication on somatic growth dilution. *Aquat. Toxicol.* 2012, 114-115, 23-30.
- Wang, R.; Wong, M. H.; Wang, W. X. Mercury exposure in the freshwater tilapia *Oreochromis niloticus*. *Environ. Pollut.* 2010, 158, 2694-2701.
- Wang, W.; Wong, R. S. K. Bioaccumulation kinetics and exposure pathways of inorganic mercury and methylmercury in a marine fish, the sweetlips (*Plectorhinchus gibbosus*). *Mar. Ecol. Prog. Ser.* 2003, 261, 257-268.
- Winberg, G. G. Rate of metabolism and food requirements of fishes. Fisheries Research Board of Canada Translation Series 194. Ottawa, ON. Canada. 1956.
- Xu, Y.; Wang, W -X. Exposure and potential food chain transfer factor of Cd, Se and Zn in marine fish *Lutjanus argentimaculatus*. *Mar. Ecol. Prog. Ser.* 238. 2002, 173-186.

CHAPTER 2

Comparison of the Toxicokinetics and Bioaccumulation Potential of Mercury and Polychlorinated Biphenyls in Goldfish (*Carassius auratus*)

Reprinted with permission from (Li, J.; Drouillard, K. G.; Branfireun, B.; Haffner, G. D. Comparison of the toxicokinetics and bioaccumulation potential of mercury and polychlorinated biphenyls in goldfish (*Carassius auratus*). Environ. Sci. Technol. 2015. 49, 11019-11027). Copyright (2015) American Chemical Society.

2.1 Introduction

Bioaccumulation of mercury (Hg) and polychlorinated biphenyls (PCBs) by fish is a global issue because the consumption of fish is the most important exposure route of these toxic pollutants to human populations (Myers et al. 2000; Stern et al. 2001). Within North America, Hg is the main driver of fish consumption advisories issued by regulatory agencies (Mozaffarian and Rimm, 2006), followed by organochlorine compounds such as PCBs and polychlorinated dibenzo-p-dioxins (Tilden et al. 1997). Environmental contamination by Hg and PCB is observed in both marine and freshwater systems (Muir et al. 1992; Scheider et al. 1998; Abma et al. 2015), including systems considered far removed from point sources (Bidleman et al. 1989; Lindqvist et al. 1991).

One of the major factors contributing to Hg and PCB fish consumption advisories is related to their ability to biomagnify (Atwell et al. 1998; Fisk et al. 2001). Although biomagnification is commonly defined as a food web process, the actual mechanism of biomagnification occurs at the scale of the individual (Madenjian and Carpenter, 1993). Net positive bioaccumulation occurs in individuals as a result of kinetic conditions where

the chemical uptake rates via food exceed whole body elimination rates (Thomann, 1981; Trudel and Rasmussen, 2001). Kinetic processes vary with trophic level as a result of the size of organisms and different assimilation efficiencies. Quantifying the factors regulating food web biomagnifications in aquatic ecosystems requires a thorough understanding of chemical toxicokinetics at the level of the individual.

Although similarities between Hg and PCB biomagnification patterns are widely reported in food webs, these substances have different mechanisms of accumulation (Borgmann and Whittle, 1992; Mackay and Fraser, 2000; Dang and Wang, 2010). The tissue-distributions and retention of PCBs and other organochlorines are regulated by different processes than those of Hg. Organochlorines undergo passive partitioning (i.e. diffusive flux) between aqueous and organic phases (primarily neutral lipid) within the organism and external to the animal as regulated by chemical-physical properties such as hydrophobicity (Mackay, 1982) and lipid content of the animal (Drouillard et al. 2004). Hg, however, exhibits strong associations with sulphur-rich proteins and is poorly associated with tissue lipids (Stohs and Bagchi, 1995). Although the mechanism of biomagnification of organochlorines has been largely resolved (Gobas et al. 1999; Drouillard, 2008), there are yet to be clear mechanisms describing how Hg is taken up from food, sequestered within tissues and eliminated by fish. Furthermore, no studies have co-examined chemical toxicokinetics for organochlorines and Hg within the same organism. It is important to understand how the magnitude of key toxicokinetic parameters differs in order to directly compare their bioaccumulation potentials.

For Hg and PCBs, dietary uptake is considered a major pathway for exposure in fish (Madenjian et al. 1998; Hall et al. 2012). The dietary assimilation efficiency (AE) is a

key toxicokinetic parameter that regulates the relative importance of dietary uptake (Trudel and Rasmussen, 2001; Madenjian et al. 2012). For Hg, the AE in fish differs markedly between inorganic Hg and methyl mercury (MeHg) ranging from 4-51% and 65-99% for inorganic and organic forms, respectively (Wang and Wong, 2003; Pickhardt et al. 2006). For PCBs, AE shows very high variation among studies and is weakly related to congener hydrophobicity (Madenjian et al. 2012) as well as diet composition (Dabrowska et al. 1999). As a result of the high variation in AEs reported by different studies using different experimental conditions, fish sizes and fish diets, it is very difficult to directly compare AEs for Hg and PCBs using the current literature.

The main toxicokinetic parameter specifying the time it takes for an organism to reach steady state is the whole body elimination coefficient (k_{tot}). The k_{tot} incorporates the sum of individual elimination coefficients across different chemical loss pathways that include (among others): elimination of chemical across respiratory surfaces, via urine, feces, mucous, protein/lipid excretion (e.g. via reproductive output, sloughing of cells, scales or excretions), metabolic biotransformation and pseudo-elimination as a function of growth dilution (Sijm et al. 1992; Trudel and Rasmussen, 2001). PCBs are lost predominantly through gills (Paterson et al. 2010) although modeling studies suggest that, for more hydrophobic chemicals, feces play an increasingly more important role (Gobas et al. 1988). For Hg, however, less information is available about which of the above routes dominate k_{tot} of fish. Most bioaccumulation models of PCBs and Hg in fish have assumed that chemical elimination occurs by first-order processes (Trudel and Rasmussen, 1997; Vanwalleggem et al. 2007), whereby elimination rate coefficients are independent of the chemical concentration in the organism. This assumption has been

tested and met for PCBs (Sijm et al. 1992; Parterson et al. 2010) but is conflicting for Hg (Ruohtula and Miettinen, 1975; Trudel and Rasmussen, 1997). Thus, there remains a need to verify the first order assumption of elimination kinetics of Hg.

The main objective of this study was to simultaneously determine AEs and k_{tot} for PCBs and Hg in order to directly quantify their bioaccumulation potentials in a model organism, the Goldfish (*Carassius auratus*). Furthermore, this study design resulted in differences in the initial Hg levels among treatments enabling testing of first order elimination kinetics.

2.2 Materials and Methods

2.2.1 Fish Husbandry and Dosing

A total of 332 Goldfish (*Carassius auratus*) ($2.32 \pm 0.68\text{g}$) were obtained from Leadley Environmental Inc., Essex, Ontario, Canada. Goldfish were selected as the study organism because they are hardy under experimental conditions, have flexible feeding habits and are commonly used as a fish species in toxicokinetic studies for different pollutants including PCBs and Hg (Hattula and Karlog, 1973; Sharpe et al. 1977). Goldfish are also a common invasive species in North American waters, including the Great Lakes. Although not commonly consumed as a food fish, Goldfish bear similarities in feeding ecology and habitat to common carp (*Cyprinus carpio*) which frequently achieve high levels of fish consumption restrictions due to their degree of contamination. Fish were maintained in holding tanks (400L capacity) at the University of Windsor's Great Lakes Institute for Environmental Research (GLIER) at a constant temperature $20.9 \pm 1.4\text{ }^{\circ}\text{C}$. The stock density was 5L water per fish. A recirculating water

system and filters were used to maintain water quality, and half of the water from the tank was replaced by fresh dechlorinated water every week. Water pH was 7.4 ± 0.1 and the dissolved oxygen level was $5.7 \pm 1.3 \text{ mg L}^{-1}$. Fecal matter at the bottom of the tank was removed every three days to minimize re-uptake of chemicals by fish. Fish were inspected daily and observed to be in good health, and mortality during the experiment was below 10%.

The study consisted of three experimental tanks and one internal control tank, all sharing the same water supply. During the dosing period, fish from three experimental tanks were fed with fish pellets of three contamination levels every day to maximize chemical uptake. During the elimination period, the fish were fed with commercial fish flakes (Cobalt Aquatics, South Carolina, USA) once every two days to minimize growth. Commercial fish flakes were also used to feed the control fish during the uptake portion of the study. Fish food was weighed before feeding, and excess food was removed three hours later from each tank. The total amount of food consumed was determined by subtracting the dry weight of unconsumed food from the pre-weighed amount (dry weight).

To circumvent experimental artifacts associated with the dosing method and establish a more natural exposure for each pollutant, the contaminated food fed to experimental fish was generated by incorporating fish meal derived from feral fish collected from contaminated systems. This approach ensured that fish were exposed to chemicals in a manner that replicates normal environmental exposures. Three dosing treatments using three contamination levels of fish food were generated to achieve low, medium, and high contamination levels in experimental fish. In order to obtain a significant difference in

tissue residues between the low Hg and high Hg treatment fish for the elimination studies, the dosing duration was adjusted such that low treatment fish had their contaminated diet discontinued after 15 days whereas high dose fish were fed for 42 days. Sample collection during the uptake phase of the study took place at days 0, 7, and 15 (n=3, 5 and 5) for low dosed treatment fish, at days 0, 7, 14, 21, and 28 (n=3, 5, 5, 5 and 5) for medium dosed treatment fish, and days 0, 7, 14, 21, and 42 (n=3, 5, 5, 5 and 5) for the high dosed group. During the elimination phase, fish were placed back onto the control diet and collected from each tank on days 0, 7, 14, 21, 28, 42, 56, 72, and 84 (n=5, 5, 5, 5, 5, 5, 5, 5 and 5 for the low dosed tank, n=5, 5, 5, 5, 5, 4, 4, 4 and 5 for the medium dosed tank, and n=5, 5, 5, 5, 4, 4, 4, 5 and 5 for the high dosed tank, respectively), with day 0 representing the final day of the uptake study for each respective dose treatment. Fish were immediately euthanized using a concentrated clove oil solution, and body length and weight were measured in the lab. The University of Windsor's Animal Care Committee Guidelines were strictly followed throughout the duration of the experiment. Following euthanasia and morphometric measurements, whole fish was homogenized into a fine paste after removing the gut content. Samples were then frozen until analysis of Hg and PCBs.

2.2.2 Chemical Analysis

Total Hg and PCB analyses were conducted at the GLIER analytical laboratory, University of Windsor, using accredited standard operating procedures (accredited through the Canadian Association for Laboratory Accreditation; CALA). Total Hg concentrations were measured using a Direct Mercury Analyzer, DMA-80 (Milestone Inc.). The DMA-80 was calibrated using a 10 point calibration curve from a certified

liquid Hg standard (High-Purity Standards, Charleston, USA). Approximately 0.15g whole fish homogenate was weighed on a clean nickel boat, and then placed on the auto sampler of the instrument. QA/QC procedures included incorporation of blanks (empty nickel boats), duplication of a random sample for every six samples analyzed and certified reference tissues (Dorm-3 and Dolt-4, National Research Council Canada; BT-Cnt2L and W-CntVG, in house standards) randomly placed into the auto sampler wells to represent 20% of samples being analyzed within a given batch. Moisture content of samples was determined by gravimetric means to establish dry weight Hg concentrations.

MeHg analysis was performed on a subset of samples at the Biotron's Analytical Services laboratory at the University of Western Ontario (ISO 17025). Concentrations were analyzed by the Tekran 2700 MeHg auto-analyzer using US EPA method 1630. Approximately 0.15g whole fish homogenate were weighed into a 60mL Savillex digestion vessel, with 10 mL of 5M nitric acid solution added. Samples were vortexed for 10 seconds at 3000 RPM and allowed to sit overnight, followed by digestion in an oven at 80 °C for eight hours. 10 mL of ultrapure deionized water was added to each vessel after the samples were completely cool and then vortexed for 10 seconds at 3000 RPM. Approximately 0.1g digestion product was transferred from the sample vessel to the instrument vial, and ultrapure deionized water was added until a final weight of 28.5-29.5g was achieved. 1mL of acetate buffer was added to adjust the pH to 4-4.5, followed by ethylation with 30µL 1% NaBEt₄. Sample vials were then rapidly shaken three times after capping and placed onto the instrument auto sampler. The instrument was calibrated using an 8 point calibration curve from 1 ppm MeHg stock solution (Brooks Rand). QA/QC procedures included measurement of replicates, method blanks and certified

reference samples (Human Hair IAEA-086, International Atomic Energy Agency; Tort-3, National Research Council Canada) analyzed for approximately every 10th samples.

Owing to limitations in sample availability, MeHg analysis was conducted on selected samples. During uptake, MeHg was measured in treatment fish at 0, 7, and 15 days of dosing for low treatment fish (n=1, 5 and 2), at 0, 14, 21, and 28 days of dosing for medium treatment fish (n=1, 5, 4, and 3), and at days 0, 7, 14, 21, and 42 of dosing for the high dosing group (n=1, 4, 4, 5, and 5). During the elimination phase, MeHg was tested in treatment fish on days 0 (n=2, 3, and 5 for low, medium, and high treatment, respectively), 28 (n=4, 5, and 4), 56 (n=5, 4, and 3), and 84 (n=5, 4, and 1) of elimination. For controls, MeHg was measured in one control fish (n=1) from each sampling date throughout both phases of the study (days 0, 7, 14, 21, 28, and 42 during uptake, days 0, 7, 14, 21, 28, 42, 56, 70, and 84 during elimination) to verify if there was a significant change in the MeHg:THg ratio. MeHg analysis was also performed on fish food from the low (n=3), medium (n=2) and high (n=3) dosing treatments.

PCB concentrations were measured using an Agilent 6890 Series Plus gas chromatograph (GC) with a ⁶³Ni-micro electron capture detector (ECD) and an Agilent 7683 auto sampler. The PCB extraction method is described in Daley et al. (Daley et al. 2009) and clean-up is described by Lazar et al. (Lazar et al. 1992). Approximately 0.5g whole fish homogenate was added to a glass mortar, and then ground with 15g of activated sodium sulfate by a glass pestle. The mixture was transferred into a micro extraction column containing 25mL of 1:1 v/v dichloromethane: hexane (DCM:HEX) and spiked with 35 ng PCB 34 as a recovery standard. After one hour extraction, the column was eluted, followed by a second elution with 15mL of DCM:HEX. 10% of the extract was removed

for determination of neutral lipids by gravimetric means (Drouillard et al. 2004). Clean-up of remaining extracts was performed by activated florisil (Lazar et al. 1992) and concentrated to a final volume of 1 mL for GC-ECD analysis. QA/QC procedures included monitoring internal standard (PCB34) recoveries, use of a method blank (sodium sulfate) and an in-house tissue reference sample (Detroit River carp) co-extracted for every batch of six samples analyzed. PCB 34 recoveries averaged $73 \pm 11\%$.

2.2.3 Data Analysis

In order to account for differences in tissue capacity, all Hg concentrations are expressed in units of $\mu\text{g g}^{-1}$ lean dry weight (excluding moisture and lipid content) (Dibble and Meyerson, 2012). All PCB concentrations are expressed in units of $\mu\text{g g}^{-1}$ lipid weight. PCB congeners included in the analysis consisted of only those congeners where detection occurred in more than 60% of the samples. Congener specific log K_{OW} values for PCBs were obtained from Hawker and Connell (Hawker and Connell, 1988).

All concentrations were corrected for control contamination prior to calculating toxicokinetic parameters. Control correction was performed by subtracting the mean contaminant concentration in control fish from the contaminant concentrations measured in each treatment fish at the equivalent sampling point. There were no significant changes in control fish (ANOVA, $p > 0.05$) in the MeHg:THg ratio during the experiment. Thus, MeHg concentrations in each control fish were estimated using the product of the mean MeHg:THg ratios in control fish and respective THg concentrations.

Growth correction for THg and MeHg concentration was based on lean dry body weight pool over time while growth correction for PCBs considered growth on the change of the

lipid pool in fish over time. Two different growth models (linear, logarithmic) were evaluated to explain growth during the uptake and elimination phases, and it was found that the fish growth over time in this study was best fitted to linear growth models. For linear growth, growth rate (g, d^{-1}) within a given treatment was calculated to be equal to the slope generated from a plot of W_t/W_0 versus time (days), where W_0 and W_t refer to the weight (lean dry body weight for Hg or whole body lipid weight for PCB) in the organism at day 0 and day of sampling.

$$C_{cg(t)} = C_{c(t)} \cdot (1 + g \cdot t) \quad (2.1)$$

where $C_{cg(t)}$ is the control and growth corrected concentration ($\mu g \cdot g^{-1}$ lean dry body weight for Hg or $\mu g \cdot g^{-1}$ lipid weight for PCBs) in the animal at time (t) in days, $C_{c(t)}$ is the control corrected concentration ($\mu g \cdot g^{-1}$ lean dry body weight for Hg or $\mu g \cdot g^{-1}$ lipid weight for PCBs), and g is the growth rate (d^{-1}). If growth for a given compartment was non-significant over the uptake or elimination phase of the study, no growth correction was performed.

Whole body chemical elimination rate coefficients (k_{tot}, d^{-1}) were calculated for total Hg, MeHg and PCB congeners and set equal to the slope generated from a plot of $\ln[C_{cg(t)}/C_{cg(0)}]$ with time, where $C_{cg(0)}$ is the control and growth corrected concentration ($\mu g \cdot g^{-1}$ lean dry body weight for Hg or $\mu g \cdot g^{-1}$ lipid weight for PCBs) in the animal at day 0 of elimination. The chemical half-life ($t_{1/2}, d$) in fish was calculated as

$$t_{1/2} = \frac{\ln(2)}{k_{tot}} \quad (2.2)$$

Dietary chemical AEs were calculated for each treatment fish sacrificed during the uptake phase according to:

$$AE = \frac{X_f + X_{ex}}{X_c} = \frac{C_{c(t)} \cdot W_t + [C_{c(t)} \cdot (1 - e^{-k_{tot} \cdot t}) \cdot W_t]}{I \cdot C_{diet} \cdot t} \quad (2.3)$$

where X_f refers to the total mass of chemical (μg) in the fish at sacrifice, X_{ex} represents mass of chemical (μg) lost by elimination during the uptake period and X_c is the total mass of chemical (μg) ingested over the uptake period. $C_{c(t)}$ is the control-corrected (no growth correction) concentration ($\mu\text{g} \cdot \text{g}^{-1}$ lean dry body weight for Hg or $\mu\text{g} \cdot \text{g}^{-1}$ lipid weight for PCBs) in the fish at sacrifice, W_t is the tissue weight (lean dry weight (g) for Hg or whole body lipid weight (g) for PCBs), $C_{c(t)}$ is the chemical concentration (no growth correction) in fish at sacrifice ($\mu\text{g} \cdot \text{g}^{-1}$ lean dry body weight for Hg or $\mu\text{g} \cdot \text{g}^{-1}$ lipid weight for PCBs), assuming all fish consumed food equally, the food ingestion rates (I) were measured as dry weight fish food consumed by each fish per day (g dry food d^{-1}), C_{diet} is the dry weight concentration of chemical in food ($\mu\text{g} \cdot \text{g}^{-1}$ dry wt) and t is time of the uptake period (days).

The biomagnification factor (BMF) was calculated as per (Fisk et al. 1998; Trudel and Rasmussen, 2006) according to:

$$BMF = \frac{I_b \cdot AE}{k_{tot}} \quad (2.4)$$

where I_b is the body weight adjusted food ingestion rate. For consistency with the literature, BMFs for Hg are reported in g dry food g^{-1} dry wt organism by using an I_b with units of g dry food g^{-1} dry wt organism d^{-1} . For PCBs, the BMF is most commonly

reported in units of g lipid wt food g^{-1} lipid wt organism (Fisk et al. 1998; Buckman et al. 2004) and is calculated using an I_b with units of g lipid food g^{-1} lipid organism d^{-1} . To facilitate comparisons of the magnitude of BMF between Hg and PCBs, BMFs of PCB congeners were also expressed in a common unit of dry food g^{-1} dry wt organism.

Analysis of variance (ANOVA) was used to test for differences in Hg or PCBs in different food samples (control and treatments), and differences in contaminant levels in fish at the end of the uptake period (control and treatments). Linear regression analysis was performed to compute growth rates, determine k_{tot} values and describe the relationship between BMF of PCB congeners and $\log K_{OW}$. ANOVA was used with linear regression to test whether slopes were significantly different from a value of zero. Analysis of Covariance (ANCOVA) was used with linear regression to test for significant differences in the slope of contaminant concentrations with time across dosing treatments. Furthermore, ANOVA and nonlinear regression were used to describe the relationship between BMFs and $\log K_{OW}$. Prior to using parametric tests, data were evaluated for normality and homogenous variance between treatments using the Kolmogorov-Smirnov and Levene's tests. A non-parametric Kruskal-Wallis test was used to evaluate the difference in ingestion rates among treatments when data failed normality assumptions even after a \ln transformation. All statistical analyses were conducted using IBM SPSS version 20 (IBM Corp., USA).

2.3 Results

The chemical concentrations in fish and their diet in both control and dosing groups are summarized in Table 2.1. By the end of the uptake phase, THg concentrations

(mean±SD) were 0.45 ± 0.12 , 1.35 ± 0.21 and $3.13 \pm 0.37 \mu\text{g g}^{-1}$ lean dry wt for low, medium and high dosed fish, which were significantly higher than the mean THg concentrations from their corresponding control fish (ANOVA, $p < 0.01$). MeHg concentrations (mean±SD) were 0.48 ± 0.05 , 1.30 ± 0.25 , and $3.58 \pm 0.47 \mu\text{g g}^{-1}$ lean dry wt for three dosing treatments, which were also significantly higher than the mean MeHg concentrations from their corresponding control fish (ANOVA, $p < 0.05$). Significant differences were confirmed among the three treatment groups in both THg and MeHg concentrations using ANOVA ($p < 0.01$). The mean MeHg:THg ratios were $96 \pm 16\%$, $84 \pm 2\%$, $90 \pm 16\%$, and $114 \pm 13\%$ for control, low, medium and high dosed fish, respectively. No significant differences were observed in MeHg:THg ratios among treatments (ANOVA, $p > 0.05$).

A total of 34 PCB congeners (17/18, 28/31, 33, 44, 49, 52, 70, 74, 87, 95, 99, 101, 110, 128, 151/82, 149, 118, 153, 105/132, 138, 158, 156/171, 170, 177, 180, 183, 187, 191, 194, 199, 195/208, 205, 206, and 209) were detected in the fish samples, with 8 congeners (17/18, 28/31, 33, 44, 52, 70, 74, and 205) being excluded because less than 60% of the samples were above the detection limit. Sum PCB concentrations (mean±SD) were 0.31 ± 0.13 , 0.83 ± 0.29 , and $4.66 \pm 0.53 \mu\text{g g}^{-1}$ lipid for the three dosing groups. Only the high dose group showed a significantly higher sum PCB level ($p < 0.01$; ANOVA) in tissue residues compared to the control. Thus toxicokinetic parameters generated for PCBs were measured only for the high dose group.

2.3.1 Chemical Elimination

During the elimination phase of the study, the body weight adjusted food ingestion rates (mean \pm SD) were 0.040 ± 0.007 , 0.040 ± 0.005 , 0.040 ± 0.007 , and 0.040 ± 0.006 g dry wt food g^{-1} dry wt fish d^{-1} for low, medium, high treatment, and control fish, respectively. No significant differences were found in feeding rates across the treatments (ANOVA, $p > 0.05$). No significant growth was observed in either lipid weight or lean dry weight during the elimination phase (ANOVA, $p > 0.05$). No significant growth was observed in either lipid weight or lean dry weight during the elimination phase (ANOVA, $p > 0.05$). Thus, growth correction was not required for the Hg nor PCB data in the elimination study.

Elimination rate coefficients were determined for all chemicals that revealed significant elimination during the study period. For THg and MeHg significant elimination (ANOVA, $p < 0.05$) was observed for each dosing treatment. The mean MeHg:THg ratios (mean \pm SD) during elimination were $86 \pm 10\%$, $104 \pm 13\%$, and $103 \pm 13\%$ for low, medium, and high dosed fish, respectively. Within each treatment, the MeHg: THg ratio did not change significantly throughout the elimination phase of the study (ANOVA, $p > 0.05$). For sum PCBs, the high dose treatment samples showed significant elimination (ANOVA, $p < 0.05$) over time. On a congener specific basis, 24 PCB congeners (87, 95, 99, 101, 110, 118, 128, 138, 105/132, 149, 151/82, 153, 158, 170, 156/171, 177, 180, 183, 187, 194, 199, 195/208, 206, and 209) were observed to demonstrate significant elimination during the elimination phase.

Figure 2.1 presents elimination rates of control corrected THg and MeHg concentrations in fish through time. The mean k_{tot} of THg were 0.012, 0.011 and 0.007 d^{-1} in low, medium and high dose groups (linear regression, $p < 0.01$). ANCOVA revealed no

significant difference in THg elimination rates across the three dosing groups ($p > 0.05$). For MeHg, k_{tot} in low, medium and high dose groups were 0.017, 0.010 and 0.011 d^{-1} (linear regression, $p < 0.05$). MeHg also showed no significant difference in elimination among the treatments (ANCOVA, $p > 0.05$). Given the lack of differences in k_{tot} between dosing groups, data were combined across doses to yield overall mean (\pm SD) k_{tot} values of $0.010 \pm 0.003 \text{ d}^{-1}$ and $0.010 \pm 0.005 \text{ d}^{-1}$ for THg and MeHg, respectively, corresponding to a half-life of 69 days.

The k_{tot} values for individual PCB congeners ranged from 0.007 to 0.022 d^{-1} . There was a strong negative relationship (linear regression, $p < 0.01$) between PCB k_{tot} values and congener $\log K_{\text{OW}}$ (Figure 2.2). Half-lives for PCBs ranged from 28 to 100 days across congeners and were positively associated (linear regression, $p < 0.01$) with chemical $\log K_{\text{OW}}$ according to the equation:

$$t_{1/2(\text{PCBs})} = 20.38 \pm 4.72 \cdot \log K_{\text{OW}} - 77.25 \pm 32.89; R^2 = 0.45 \quad (2.5)$$

Given the measured Hg half-life of 69 days in these same fish, Eq. 2.5 can be used to demonstrate that Hg is eliminated at the same rate as a PCB having a $\log K_{\text{OW}}$ value of 7.2 (e.g. PCB183).

2.3.2 Assimilation

Body weight adjusted food ingestion rates (mean \pm SD) during the uptake study were 0.060 ± 0.005 , 0.060 ± 0.004 , 0.060 ± 0.004 , and $0.070 \pm 0.01 \text{ g dry wt food g}^{-1} \text{ dry wt d}^{-1}$ fish for low, medium, high treatment, and control fish, respectively. No significant differences in feeding rates were measured among treatments (ANOVA, $p > 0.05$). There were

significant linear relationships between lean dry weight and days of dosing from high dosed fish, and between lipid weight and days of dosing for both medium and high dosed fish (linear regression, $p < 0.05$). Such relationships were also found to be significant when using the logarithmic growth model (linear regression, $p < 0.05$), but with a lower R value, indicating the linear model provided a better prediction of fish growth. Thus, growth correction was performed for Hg concentrations in high dosed fish and for PCB concentrations in medium and high dosed fish during the uptake portion of this study.

Chemical AEs were calculated for THg and MeHg from each treatment sample, as well as for each of 24 PCB congeners (87, 95, 99, 101, 110, 118, 128, 138, 105/132, 149, 151/82, 153, 158, 170, 156/171, 177, 180, 183, 187, 194, 199, 195/208, 206, and 209) from high dosed fish. The AE for PCB congeners ranged from 23% to 63%, however, no significant relationship was observed between AE and $\log K_{OW}$ (linear regression, $p > 0.05$). Because no significant difference was found in AE among congeners (ANOVA, $p > 0.05$), the AE of one of the most common PCB (PCB 180, $\log K_{OW} = 7.4$) was used for comparison with the AE of Hg. Figure 2.3 shows mean (\pm SD) AE values for THg and MeHg, and PCB 180, which were $75 \pm 12\%$, $98 \pm 10\%$, and $44 \pm 16\%$, respectively. The mean AE values for THg, MeHg, and PCBs differed significantly from each other (ANOVA, $p < 0.05$).

Biomagnification factors were calculated for MeHg and THg using mean AE, I and k_{tot} values derived from each treatment, and for PCB congeners using the PCB data from high dosed fish. The mean BMF values for MeHg and THg were 6.1 and 4.5 g dry wt food g^{-1} dry wt fish. The BMF value for PCB congeners ranged from 1.4 to 7.4 g lipid food g^{-1} lipid fish. Figure 2.4 showed BMF for PCB calculated on a dry weight food to

dry weight fish basis, and it ranged from 0.72 to 3.8 g dry wt food g⁻¹ dry wt fish. There was a significantly linear relationship ($BMF = 0.90 \log K_{OW} - 4.07$, $R^2 = 0.41$, $p < 0.01$) and curvilinear relationship ($BMF = -0.66 \log K_{OW}^2 + 10.20 \log K_{OW} - 36.59$, $R^2 = 0.52$, $p < 0.01$) observed between BMF and $\log K_{OW}$. The curvilinear model had a larger R value, and predicted the maximum BMF to be 2.8.

2.4 Discussion

This study is the first to simultaneously compare dietary assimilation efficiencies and elimination rate coefficients of Hg and PCB in a freshwater fish species. The results showed that mean dietary AEs for MeHg were higher than those observed for all PCB congeners. The AE was $98 \pm 12\%$ for MeHg, and $40 \pm 9\%$ for PCBs, which are both comparable to those reported in previous studies (Gobas et al. 1993; Trudel and Rasmussen, 2006). Leaner and Mason (2004) reported that MeHg dietary AEs ranged from 90% to 92% in sheepshead minnows (*Cyprinodon variegatus*), while Pickhardt et al. (2006) found AE values between 90% and 94% in mosquito fish (*Gambusia affinis*), and 85% to 91% in red ear sunfish (*Lepomis microlophus*). For PCBs, AE had varied from 23% to 101% (Madenjian et al. 1988; Gobas et al. 1988; Liu et al. 2010). Buckman et al. (2004) found that AE for 92 PCB congeners ranged from 40% to 50%, and Liu et al. (Liu et al. 2010) concluded that AE values for 47 PCBs were under 60% when using a similar fish diet (high-fat pellet), all of which are consistent with our values. There are many factors that regulate chemical AEs for Hg and PCBs in fish, such as composition of the dietary matrices, digestibility of the food, ingestion rates, fish physiology, and water chemistry and temperature (Arnot and Gobas, 2004; Wang and Wang, 2012).

The elimination rate coefficient for MeHg in our study falls within the lower end of the range of elimination rate coefficients measured for PCB congeners. Also, the half-life of Hg was equivalent to that estimated for highly chlorinated PCBs with $\log K_{OW} = 7.2$. Considering the elevated dietary AE of Hg coupled with it having an elimination rate coefficient equivalent to the most hydrophobic PCB congeners indicates that Hg has a higher bioaccumulation potential than most of the PCB congeners.

The k_{tot} for MeHg in our study is comparable with past laboratory studies on Goldfish (Sharpe et al. 1977). De Freitas and colleagues reported Hg elimination rate coefficients of 0.02 and 0.008 d^{-1} in Goldfish weighing 1 and 7.4g respectively, at 22 °C. Our k_{tot} was 0.01 d^{-1} for fish of 2.32 ± 0.68 g at 20.9 ± 1.4 °C falls within the above range (Sharpe et al. 1977). The consistency of k_{tot} across dosing treatments as determined in this study supports the conclusion that Hg elimination in fish is a first order process. The k_{tot} values for THg and MeHg were not significantly different from each other because MeHg was the dominant Hg species in the fish. Thus, the first order kinetics of Hg elimination observed from this study is driven by the elimination kinetics of MeHg. The data for inorganic Hg were insufficient to characterize its elimination kinetics.

The evidence supporting first order kinetics for Hg in the literature is conflicting. A negative relationship between the dosage level in fish and half-life of MeHg was reported by Ruohtula and Miettinen (1975) for rainbow trout (*Salmo gairdneri*). However, their fish were dosed with 3.0, 0.4 and 0.1 $\mu g g^{-1}$ MeHg, and only the fish of the highest dosage revealed a significantly faster excretion. The fish from the two lower dosage groups did not show significantly different elimination, suggesting their results were inconclusive. In contrast, Trudel and Rasmusen (1997) demonstrated no correlation between initial Hg

concentration and the Hg elimination rate coefficient based on 41 previous case studies, which supports our findings.

Several studies on Hg elimination in freshwater and marine fish species (Ruohtula and Miettinen, 1975; Wang and Wong, 2003) reported a pattern of biphasic elimination, where there was a rapid loss of chemical immediately after dosing, followed by a slower loss process. Biphasic elimination kinetics was not observed in our study, which might be a result of the differences in the dosing method between this study and the earlier cited studies. Lags associated with the inter-tissue transport kinetics post assimilation often result in higher blood concentrations of the chemical relative to other tissues following initial chemical exposure (Gobas et al. 1988). Given the role of blood as a central compartment and its stronger association with chemical elimination, an elevated blood concentration favors a higher initial elimination of chemicals (Barron et al. 1990). In this study, fish were exposed to a naturally contaminated diet for several weeks prior to initiation of elimination, whereas fish in other studies were typically given a single oral dose, an intra muscular injection or a short term (from several hours to days) aqueous exposure. The dosing methodology of our study is more representative of natural exposure and uptake dynamics given that the Hg was ingested in a form (i.e. protein-associated) more consistent with Hg exposures taking place in aquatic ecosystems.

PCB elimination has been consistently shown to follow first order kinetics (Sijm et al. 1992; Paterson et al. 2010). PCB elimination has been studied in a wide range of fish species, but few investigations are available for Goldfish. The k_{tot} value for PCBs ranged from 0.007 to 0.022 d^{-1} in our study, while Hattula and Carlog (1973) reported the half-life for the sum PCB at 21 d in Goldfish, which corresponds to an elimination rate of 0.03

d^{-1} . Even though a similar body size of 1.8g and water temperature 21-23 °C were used in their study, comparisons of k_{tot} could not be made for individual congeners due to analytical limitations. Paterson et al. (Paterson et al. 2007) found k_{tot} values ranging from 0.004 to 0.02 d^{-1} , using yellow perch (*Perca flavescens*) of 8.3 g under summer water temperature (23 °C). Van Geest et al. (2011) reported that PCB elimination rate coefficients ranged from 0.009 to 0.037 d^{-1} , using fathead minnows (*Pimephales promelas*) of less than 1g and at 23 °C. Our k_{tot} values were comparable with both studies on the scale of individual congeners.

PCBs elimination by aquatic species is mechanistically understood to result from diffusive fluxes across respiratory surfaces and through fecal egestion, driven by the chemical fugacity gradients between the animal and the elimination media (Gobas et al. 1993; Gobas et al. 1999; Paterson et al. 2010). The physiological mechanism of Hg elimination, however, remains largely unknown for fish. It might involve demethylation biotransformation reactions as described to occur in some species of birds and mammals with subsequent loss of inorganic Hg by kidneys (Vahter et al. 1995) or as a result of protein turnover during routine metabolism. Madenjian et al. (2014) suggested that sex-based differences in Hg elimination from fish might be hormonally controlled.

BMFs estimated for MeHg approached a value of 6.1g dry wt food g^{-1} dry wt fish in Goldfish, and ranged from 1.4 to 7.4 g lipid food g^{-1} lipid fish for PCB congeners. Previous studies reported BMFs for MeHg in fish ranging between 1 and 10g dry wt food g^{-1} dry wt fish based on laboratory and field data (Borgmann and Whittle, 1992; Wang and Wong, 2003), while estimates of BMFs reported for PCB congeners have ranged from 0.7 to 9.0g lipid food g^{-1} lipid fish, depending on chemical hydrophobicity

(Fisk et al. 1998; Buckman et al. 2004). Figure 2.4 summarizes PCB BMFs (g dry wt food g^{-1} dry wt fish) as a function of K_{OW} with both linear and curvilinear fits to the obtained data. The curvilinear fit implies a maximum PCB BMF of 2.8g dry wt food g^{-1} dry wt fish, much less than the observed value for Hg. The linear model would indicate that only PCBs having log K_{OW} values greater than 11 would exhibit a BMF that approaches Hg. Although AEs from the present work did not show significant K_{OW} dependence as has been observed elsewhere (Gobas et al. 1988; Buckman et al. 2004; Liu et al. 2010), k_{tot} was observed to exhibit a slope transition for congeners exceeding a log K_{OW} of 7.0, consistent with the curvilinear BMF- K_{OW} relationship most commonly reported in the literature. Overall, it is concluded that Hg has a 118% higher biomagnification factor leading to a higher bioaccumulation potential compared with the highest BMF modeled for PCB congeners based on the curvilinear BMF relationship. Even under a linear BMF model, Hg BMFs exceeded BMFs for the most common super hydrophobic PCBs, e.g. PCB 180. This implies Hg has a higher bioaccumulation and food web biomagnification potential compared to PCBs and is consistent with the observation that Hg more frequently contributes to fish consumption advisories in in-land lakes that are remote from point sources, whereas PCBs tend to dominate fish consumption advice in the Laurentian Great Lakes where industrial sources and legacy contamination of sediments remain acute. Further research to understand differences in PCB and Hg toxicokinetics in other fish species using simultaneous chemical exposures would be useful to verify if bioaccumulation potential is consistent among different species, and whether observed differences are maintained across different food webs, diet conditions and environmental conditions.

2.5 References

- Abma, R.; Paterson, G.; Mcleod, A.; Haffner, G. D. Cross-basin comparison of mercury bioaccumulation in Lake Huron laketrout emphasizes ecological characteristics. *Environ. Toxicol. Chem.* 2015, 34, 355-359.
- Arnot, J. A.; Gobas, F. A. P. C. A food web bioaccumulation model for organic chemicals in aquatic ecosystems. *Environ. Toxicol. Chem.* 2004, 23, 2343-2355.
- Atwell, L. Hobson, K. A.; Welch, H. E. Biomagnification and bioaccumulation of mercury in an arctic marine food web: insights from stable nitrogen isotope analysis. *Can. J. Fish. Aquat. Sci.* 1998, 55, 1114-1121.
- Barron, M.G.; Stehly, G.S.; Hayton, W. L. Pharmacokinetic modeling in aquatic animals. I. Models and concepts. *Aquat. Toxicol.* 1990, 17, 187-212.
- Bidleman, T. F.; Patton, G. W.; Walla, M. D.; Hargrave, B. T.; Vass, W. P.; Erickson, B.; Fowler, B.; Scott, V.; Gregor, D. J. Toxaphene and other organochlorines in the arctic ocean fauna: evidence for atmospheric delivery. *Arctic* 1989, 42, 307-313.
- Borgmann, U.; Whittle, B. M. Bioenergetics and PCB, DDE, and mercury dynamics in Lake Ontario lake trout (*Salvelinus namaycush*): a model based on surveillance data. *Can. J. Fish. Aquat. Sci.* 1992, 49, 1086-1896.
- Buckman, A. H.; Brown, S. B.; Hoekstra, P. F.; Solomon, K. R.; Fisk, A. T. Toxicokinetics of three polychlorinated biphenyl technical mixtures in rainbow trout (*Oncorhynchus mykiss*). *Environ. Toxicol. Chem.* 2004, 23, 1725-1736.
- Dabrowska, H.; Fisher, S. W.; Dabrowski, K.; Staubus, A. E. Dietary uptake efficiency of 2,2',4,4',5,5'-hexachlorobiphenyl in yellow perch and rainbow trout: role of dietary and body lipids. *Environ. Toxicol. Chem.* 1999, 18, 938-945.
- Daley, J. M.; Leadley, T. A.; Drouillard, K. G. Evidence for bioamplification of nine polychlorinated biphenyl (PCB) congeners in yellow perch eggs (*Percaflavescens*) during incubation. *Chemosphere* 2009, 75, 1500-1505.
- Dang, F.; Wang, W. X. Sub cellular controls of mercury trophic transfer to a marine fish. *Aquat. Toxicol.* 2010, 99, 500-506.

- Dibble, K. L.; Meyerson, L. A. Tidal flushing restores the physiological condition of fish residing in degraded salt marshes. *PLOS ONE* 2012, 7(9): e46161.
- Drouillard, K.G. Ecotoxicology: Biomagnification. In *Ecotoxicology*. Jørgensen, S. E., Fath, B. D., Eds.; Elsevier: Oxford 2008; pp 441-448.
- Drouillard, K.G.; Hagen, H.; Haffner, G.D. Evaluation of chloroform/methanol and dichloromethane/hexane extractable lipids as surrogate measures of sample partition capacity for organochlorines in fish tissues. *Chemosphere* 2004, 55, 395-400.
- Fisk, A. T.; Hobson, K. A.; Norstrom, R. J. Influence of chemical and biological factors on trophic transfer of persistent organic pollutants in the northwater polynya marine food web. *Environ. Sci. Technol.* 2001, 35, 732-738.
- Fisk, A. T.; Norstrom, R. J.; Cymbalisty, C. D.; Muir, D. C. G. Dietary accumulation and depuration of hydrophobic organochlorines: bioaccumulation parameters and their relationship with the octanol/water partition coefficient. *Environ. Toxicol. Chem.* 1998, 17, 951-961.
- Gobas, F. A. P. C.; Muir D. C. G.; Mackay, D. Dynamics of dietary bioaccumulation and fecal elimination of hydrophobic organic chemicals in fish. *Chemosphere* 1988, 17, 943-962.
- Gobas, F. A. P. C.; Wilcockson, J. B.; Russell, R. W.; Haffner, G. D. Mechanism of biomagnification in fish under laboratory and field conditions. *Environ. Sci. Technol.* 1999, 33, 133-141.
- Gobas, F. A. P. C; McCorquodale, J. R.; Haffner, G. D. Intestinal absorption and biomagnification of organochlorines. *Environ. Toxicol. Chem.* 1993, 12, 567-576.
- Hall, B. D.; Bodaly, R. A.; Fudge, R. J. P.; Rudd, J. W. M.; Rosenberg, D. M. Food as the dominant pathway of methylmercury uptake by fish. *Water, Air, and Soil Pollut.* 1997, 100, 13-24.
- Hattula, M. L.; Karlog, O. Absorption and elimination of polychlorinated biphenyls (PCB) in Goldfish. *ActaPharmacol. Toxicol.* 1973, 32, 237-245.

- Hawker, D. W.; Connell, D. W. Octanol-water partition coefficients of polychlorinated biphenyl congeners. *Environ. Sci. Technol.* 1988, 22, 382-387.
- Lazar, R.; Edwards, R. C.; Metcalfe, C. D.; Gobas, F. A. P. C.; Haffner, G. D. A simple, novel method for the quantitative analysis of coplanar (non-ortho-substituted) polychlorinated biphenyls in environmental samples. *Chemosphere* 1992, 25, 493-504.
- Leaner, J. J.; Mason, R. P. Methylmercury uptake and distribution kinetics in sheepshead minnows, *Cyprinodon variegatus*, after exposure to CH₃Hg-spiked food. *Environ. Toxicol. Chem.* 2004, 23(9), 2138-2146;.
- Lindqvist, O.; Johansson, K.; Aastrup, M.; Andersson, A.; Bringmark, L.; Hovsenius, G.; Hakanson, L.; Iverfeldt, A.; Meili, M.; Timm, B. Mercury in the Swedish Environment: recent research on causes, consequences and corrective methods. *Water Air Soil Pollut.* 1991, 55, xi-261.
- Liu, J.; Haffner, G. D.; Drouillard, K. G. The influence of diet on the assimilation efficiency of 47 polychlorinated biphenyl congeners in Japanese Koi (*Cyprinus carpio*). *Environ. Toxicol. Chem.* 2010, 29, 401-409.
- Mackay, D. Correlation of bioconcentration factors. *Environ. Sci. Technol.* 1982, 16, 274-278.
- Mackay, D.; Fraser, A. Bioaccumulation of persistent organic chemicals: mechanisms and models. *Environ. Pollut.* 2000, 110, 375-391.
- Madenjian, C. P.; Blanchfield, P. J.; Hrenchuk L. E.; Van Walleghem, J. L. Mercury elimination rates for adult northern pike *Esox lucius*: evidence for a sex effect. *Bull. Environ. Contam. Toxicol.* 2014, 93, 144-148.
- Madenjian, C. P.; Carpenter, S. R. Accumulation of PCBs by lake trout (*Salvelinus namaycush*): an individual-based model approach. *Can. J. Fish. Aquat. Sci.* 1993, 50, 97-109.
- Madenjian, C. P.; David, S. R.; Rediske, R. R.; O'Keefe, J. P. Net trophic transfer efficiencies of polychlorinated biphenyl congeners to lake trout

- (Salvelinus namaycush) from its prey. Environ. Toxicol. Chem. 2012, 31, 2821-2827.
- Madenjian, C. P.; Elliott, R. F.; Schmidt, L. J.; Desorcie, T. J.; Hesselberg, R. J.; Quintal, R. T.; Begnoche, L. J.; Bouchard, P. M.; Holey, M. E. Net trophic transfer efficiency of PCBs to Lake Michigan coho salmon from their prey. Environ. Sci. Technol. 1998, 32 (20), 3063-3067.
- Mozaffarian, D.; Rimm, E. B. Fish intake, contaminants, and human health - Evaluating the risks and the benefits. JAMA 2006, 296, 1885-1899.
- Muir, D. C. G.; Wagemann, R.; Hargrave, B. T.; Thomas, D. J.; Peakall, D. B.; Norstrom, R.J. Arctic marine ecosystem contamination. Sci. Total. Environ. 1992, 122, 75-134.
- Myers, G. J.; Davidson, P. W.; Cox, C.; Shamlaye, C.; Cernichiari, E.; Clarkson, T. W. Twenty-seven years studying the human neurotoxicity of methyl mercury exposure. Environ. Res. 2000, 83, 275-285.
- Paterson, G.; Drouillard, K. G.; Haffner, G. D. PCB elimination by yellow perch (*Perca flavescens*) during an annual temperature cycle. Environ. Sci. Technol. 2007, 41, 824-829.
- Paterson, G.; Liu, J.; Drouillard, K. G.; Haffner, G. D. Contribution of fecal egestion to the whole body elimination of polychlorinated biphenyls by Japanese koi (*Cyprinus carpio*). Environ. Sci. Technol. 2010, 44, 5769-5774.
- Pickhardt, P. C.; Stepanova, M.; Fisher, N. S. Contrasting uptake routes and tissue distribution of inorganic and methylmercury in mosquitofish (*Gambusia affinis*) and redear sunfish (*Lepomis microlophus*). Environ. Toxicol. Chem. 2006, 25(8), 2132-2142.
- Ruohola, M.; Miettinen, J. K. Retention and excretion of ²⁰³Hg-labelled methylmercury in rainbow trout. OIKOS 1975, 26, 385-390.
- Scheider, W. A.; Cox, C.; Hayton, A.; Hitchin, G. Current status and temporal trends in concentrations of persistent toxic substances in sport fish and juvenile forage fish in

- the Canadian waters of the Great Lakes. *Environ. Monit. Assess.* 1998, 53, 1, 57-76.
- Sharpe, M. A.; deFreitas, A. S. W.; McKinnon, A. E. The effect of body size on methylmercury clearance by Goldfish (*Carassius auratus*). *Environ. Biol. Fish.* 1977, 2, 177-183.
- Sijm, D. T. H. M.; Seinen, W.; Opperhulzen, A. Life-cycle biomagnification study in fish. *Environ. Sci. Technol.* 1992, 26, 2162-2174.
- Stern, A. H.; Burger, J. Mercury and methyl mercury exposure in the New Jersey pregnant population. *Arch. Environ. Health.* 2001, 56, 4-10.
- Stohs, S. J.; Bagchi, D. Oxidative mechanisms in the toxicity of metal ions. *Free Rad. Biol. Med.* 1995, 18, 321-336.
- Thomann, R.V. Equilibrium model of fate of micro-contaminants in diverse aquatic food chains. *Can. J. Fish. Aquat. Sci.* 1981, 38, 280-296.
- Tilden, J.; Hanrahan, L. P.; Anderson, H.; Palit, C.; Olson, J.; MacKenzie, W. Health advisories for consumers of Great Lakes sport fish: is the message being received? *Environ. Health Perspect.* 1997, 105, 1360-1365.
- Trudel, M.; Rasmussen, J. B. Bioenergetics and mercury dynamics in fish: a modelling perspective. *Can. J. Fish. Aquat. Sci.* 2006, 63, 1890-1902.
- Trudel, M.; Rasmussen, J. B. Predicting mercury concentration in fish using mass balance models. *Ecol. Appl.* 2001, 11, 517-529.
- Trudel, M.; Rasmussen, J.B. Modeling the elimination of mercury by fish. *Environ. Sci. Technol.* 1997, 31, 1716-1722.
- Vahter, M. E.; Motteet, N. K.; Friberg, L. T.; Lind, S. B.; Charleston, J. S.; Burbacher, T. M. Demethylation of methyl mercury in different brain sites of macaca fascicularis monkeys during long-term subclinical methyl mercury exposure. *Toxicol. Appl. Pharmacol.* 1995, 134, 273-284.

- Van Geest, J. L.; Mackay, D.; Poirier, D. G.; Sibley, P. K.; Solomon, K. R. Accumulation and depuration of polychlorinated biphenyls from field-collected sediment in three freshwater organisms. *Environ. Sci. Technol.* 2011, 45, 7011-7018.
- Vanwallegem, J. L. A.; Blanchfield, P.J.; Hintelmann, H. Elimination of mercury by yellow perch in the wild. *Environ. Sci. Technol.* 2007, 41, 5895-5901.
- Wang, R.; Wang, W. X. Contrasting mercury accumulation patterns in tilapia (*Oreochromis niloticus*) and implication on somatic growth dilution. *Aquat. Toxicol.* 2012, 114-115, 23-30.
- Wang, W.; Wong, R. S. K. Bioaccumulation kinetics and exposure pathways of inorganic mercury and methylmercury in a marine fish, the sweetlips (*Plectorhinchus gibbosus*). *Mar. Ecol. Prog. Ser.* 2003, 261, 257-268.

Table 2.1 Mean (\pm SD) THg, MeHg, and PCB concentrations in control and dosed fish at the end (day 0 for elimination) of dosing, as well as in fish diet.

		Fish diet			Fish homogenate (day 0)		
		THg ($\mu\text{g g}^{-1}$ lean dry wt)	MeHg ($\mu\text{g g}^{-1}$ lean dry wt)	Sum PCBs ($\mu\text{g g}^{-1}$ lipid)	THg ($\mu\text{g g}^{-1}$ lean dry wt)	MeHg ($\mu\text{g g}^{-1}$ lean dry wt)	Sum PCBs ($\mu\text{g g}^{-1}$ lipid)
Low	control	0.05 \pm 0.003	0.03 \pm 0.003	0.01	0.11 \pm 0.02	0.07 \pm 0.02	0.18 \pm 0.12
	dosed	0.63 \pm 0.03 † a	0.44 \pm 0.02 † a	0.42 \pm 0.02 † a	0.45 \pm 0.12 † a	0.48 \pm 0.05 † a	0.31 \pm 0.13 a
Medium	control	0.05 \pm 0.003	0.03 \pm 0.003	0.01	0.16 \pm 0.06	0.12 \pm 0.06	0.45 \pm 0.27
	dosed	1.11 \pm 0.06 † b	0.92 \pm 0.01 † b	0.80 \pm 0.04 † b	1.35 \pm 0.21 † b	1.30 \pm 0.25 † b	0.83 \pm 0.29 b
High	control	0.05 \pm 0.003	0.03 \pm 0.003	0.01	0.22 \pm 0.06	0.20 \pm 0.06	0.61 \pm 0.54
	dosed	1.91 \pm 0.16 † c	1.86 \pm 0.34 † c	2.68 \pm 0.29 † c	3.13 \pm 0.37 † c	3.58 \pm 0.47 † c	4.66 \pm 0.53 † c

Note: Different lowercase letters indicate significant differences ($p < 0.05$; ANOVA) in mean THg, MeHg, and sum PCB concentrations among low, medium and high dosing treatments. † Indicates significant difference ($p < 0.05$; ANOVA) between control and treatment fish for THg, MeHg or sum PCBs

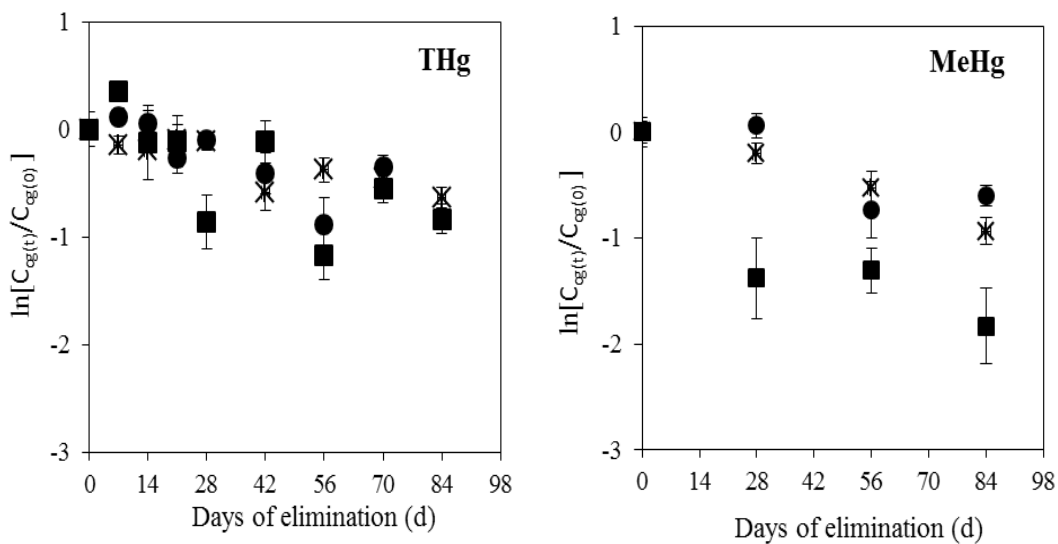


Figure 2.1 THg and MeHg elimination by fish from three treatments, squares represent low (■), circles represent medium (●), crosses represent high dosing treatment (×); THg was tested for fish at days 0, 7, 14, 21, 28, 42, 56, 72, and 84 (n=5, 5, 5, 5, 5, 5, 5, 5 and 5 for low dosed treatment, n=5, 5, 5, 5, 5, 4, 4, 4 and 5 for medium dosed treatment, and n=5, 5, 5, 5, 4, 4, 4, 5 and 5 for high dosed fish). MeHg was tested in fish on days 0, 28, 56, and 84 (n=2, 4, 5 and 5 for low dosed group, n=3, 5, 4 and 4 for medium dosed group, and n=5, 4, 3 and 1 for high dosed treatment). Vertical bars represent standard error.

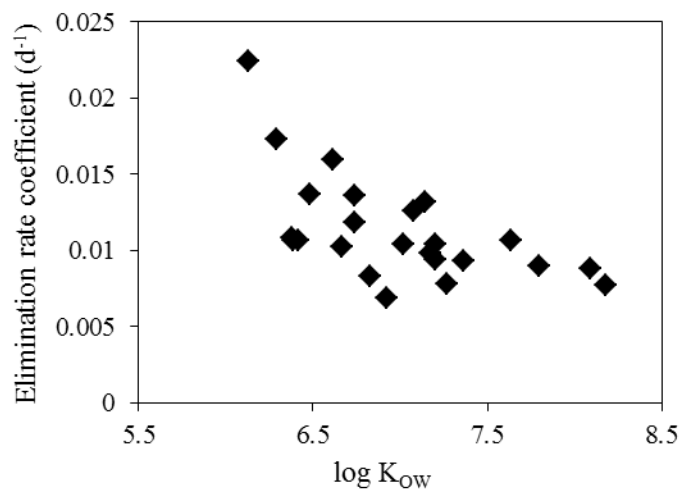


Figure 2.2 Elimination rate coefficients of PCB congeners from high dosed fish

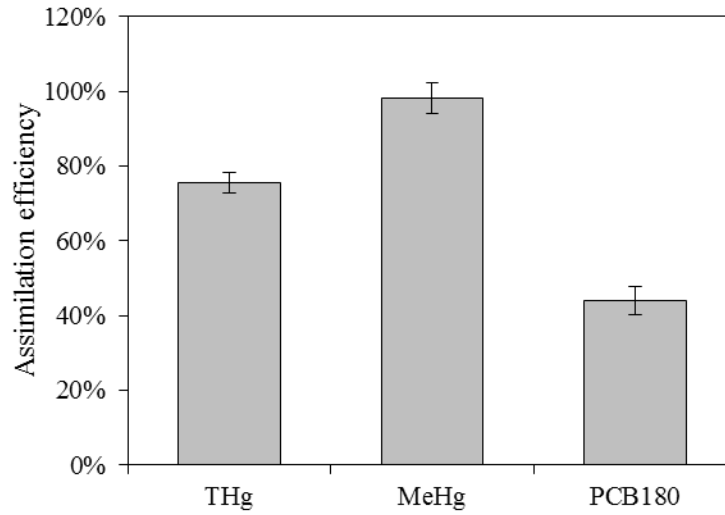


Figure 2.3 Assimilation efficiencies of THg, MeHg, and PCB 180; Grey bars for THg and MeHg represent the average AE value from each treatment sample. The grey bar for PCB 180 represents the mean AE value from the high dosed fish sample. Vertical bars represent standard error.

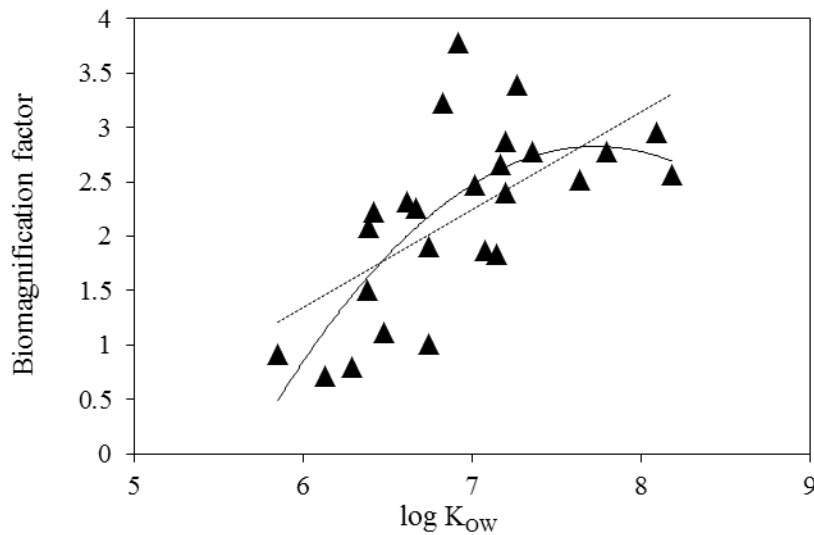


Figure 2.4 Biomagnification factors of PCB congeners in Goldfish. The solid line represents the curvilinear model, and dashed line represents the linear model.

CHAPTER 3

Protein and Lipid Dynamics Regulate Bioaccumulation of PCBs and Hg in Bighead Carp (*Hypophthalmichthys nobilis*) and Silver Carp (*Hypophthalmichthys molitrix*) From the Three Gorges Reservoir, China

3.1 Introduction

Mercury (Hg) and polychlorinated biphenyl (PCB) contamination in aquatic environments is a global problem (Borgmann and Whittle, 1992; Abma et al. 2015; Paterson et al. 2016) and these two contaminants are the main drivers of fish consumption advisories across North America (US Ministry of the Environment and Climate Change, 2015; EPA-FDA, 2017) and Asia (Ser and Watanabe, 2014). Bioaccumulation in fish is a complex process regulated by many biological and environmental processes that are often interactive and interdependent, making it difficult to resolve their relative contributions to bioaccumulation in feral organisms (McIntyre et al. 2007).

Bioaccumulation occurs when the chemical uptake rate exceeds the whole body elimination rate of a given contaminant (Thomann, 1981). Chemical uptake routes in aquatic species include aqueous uptake across the gill or skin and dietary uptake through the gastrointestinal tract, with the latter being the dominant pathway for methyl-mercury (MeHg) and hydrophobic PCBs ($\log K_{OW} > 5$) (Hall et al. 1997; Fisk et al. 1998; McLeod et al. 2015). MeHg usually accounts for more than 95% of total Hg in fish (Bloom, 1992). Highly hydrophobic PCBs ($\log K_{OW} > 6$) are often the congeners of interest in bioaccumulation studies as a result of their high biomagnification potentials (Russell et al. 1995; McLeod et al. 2015).

The uptake portion of the kinetic model can be readily parameterized for multiple fish species. Assimilation efficiency is often assumed to be constant and independent of diet, although some studies have questioned this for PCBs (Liu et al. 2010). Assimilation efficiencies of MeHg appear to be very consistent across different diets (Wang et al. 2003; Li et al. 2015). Values of AE are typically under 60% for PCBs (Fisk et al. 1998; Buckman et al. 2004; Liu et al. 2010; Li et al. 2015) and above 90% for MeHg (Leaner and Mason, 2004; Pickhardt et al. 2006; Li et al. 2015). Ingestion rate is influenced by water temperature and animal size as these govern fish metabolic rate, as well as the energy density of ingested food, and usually can be predicted by a bioenergetics model (Trudel and Rasmussen, 2006). Aside from some variation in AE in PCBs and potentially different concentration levels of Hg and PCBs in different prey items, the uptake portion of the kinetic model predicts similar uptake trajectories for both PCBs and Hg.

Whole body elimination of Hg and PCBs by fish is a first-order process under constant temperature conditions (Paterson et al. 2010; Li et al. 2015), but elimination rates are modified by the animal's metabolic rate and thus vary with water temperature and body size (Trudel and Rasmussen, 1997; Drouillard et al. 2009). Whole body elimination involves several different mechanisms that include loss from gills, loss to feces, excretion by kidneys (inorganic Hg) and various bodily secretions (e.g. potential loss of Hg in proteinaceous secretions such as mucous) (Gobas et al. 1988; Sijm, 1992; Trudel and Rasmussen, 2001; Paterson et al. 2010). Differences in the kinetic processes associated with k_{tot} for PCBs and Hg can result in different bioaccumulation trajectories between the two contaminants. Li et al. (2015) simultaneously quantified Hg and PCB elimination in goldfish, and observed k_{tot} of comparable magnitudes for highly hydrophobic PCBs

($K_{ow}>7$) and Hg. The commonalities among the general bioaccumulation characteristics for Hg and PCBs would suggest that the chemicals will have common bioaccumulation trajectories as observed in other studies (Borgmann and Whittle, 1992; Abma et al. 2015; Paterson et al. 2016).

Bioaccumulation in fish is also strongly influenced by growth dilution (Wang and Wang, 2012; Eichinger et al. 2010). Growth rate plays an important role when k_g approaches or exceeds k_{tot} and is commonly maximized in early life stages. Nevertheless, it may have very different effects on PCBs and Hg concentrations owing to differences in the tissue association of these two contaminants. PCBs are associated with neutral lipids and to a lesser extent with non-lipid hydrophobic organic matter in animal tissues (Mackay and Patersen, 1981; duBruyn and Gobas, 2007). In contrast, Hg has strong associations with sulfur-rich amino acids and distributes primarily to muscle and other protein rich tissues (Stohs and Bagchi, 1995). However, in many bioaccumulation studies, only whole body growth is considered rather than proximate growth of individual contaminant storage compartments. This assumes that relevant tissue components exhibit a constant and proportional rate of growth with the whole body of fish, which has already been refuted by previous studies (Dumas et al. 2007; Overturf et al. 2016). Lastly, growth is interactive with food consumption rates given that a high growth rate necessitates elevated food ingestion which also impacts chemical assimilation. Therefore, interpreting the effect of fish growth on contaminant bioaccumulation should consider differences in food intake between compared populations. The latter is best achieved by integrating bioenergetic models with empirically derived, or population specific, growth sub-models.

In order to investigate the effects of tissue growth on contaminant accumulation, a non-steady state bioaccumulation model was applied to simulate PCB and Hg bioaccumulation by Silver Carp (*Hypophthalmichthys molitrix*) and Bighead Carp (*Hypophthalmichthys nobilis*) from the Three Gorge Reservoir (TGR). To address the dependence of toxicokinetics parameters on metabolic rate and environmental condition, a water temperature sub-model, a growth sub-model, and a bioenergetics sub-model were incorporated to generate estimates for growth, food consumption, gill ventilation, fecal egestion, and chemical elimination. Simulations under two growth scenarios were contrasted for their goodness of fit to field measured data. Growth scenario 1 assumed lipid and lean dry protein growth was proportional to whole body growth. Scenario 2 applied population specific lipid and protein growth rates. The objectives of this study were to 1) determine if a common non-steady state bioaccumulation model could simulate age specific bioaccumulation of hydrophobic PCBs and Hg in Asian carp and 2) to test the hypothesis that using tissue specific growth rate can more accurately simulate bioaccumulation of Hg and PCBs compared to whole body growth rate.

3.2 Methods

3.2.1 Study System

Silver Carp and Bighead Carp were selected as model species because they are fast growing and stocked in the TGR as a fisheries resource (Hu, 2014; He et al. 2015). They are also invasive species of concern in North America because of their efficient filter feeding activities and very high growth rates (Nuevo et al. 2004; Williamson and Garvey, 2005; Hayer et al. 2014). In September 2013, 26 Silver Carp and 18 Bighead Carp were

collected from Daning River, Wushan, China (31.1 °N, 109.9 °E) by local fisherman. The Daning River is a large tributary of the Yangtze River, joining the Yangtze River at the western end of Wu Gorge and upstream of the Three Gorges Dam. It flows for 250 km, with an area of 3720 km². The annual average temperature of the tributary is approximately 18 °C.

Total length, fork length and body weight were measured for each fish and between 5 and 10 scales above the lateral line were removed for age determination. Fish were individually homogenized using a stainless steel meat grinder within 24 h of their collection. Samples were kept frozen until subsequent chemical analysis. Hg, PCBs, stable isotopes ($\delta^{15}\text{N}$, $\delta^{13}\text{C}$), moisture and lipid content were measured for each sample. Moisture was determined by gravimetric means after drying subsamples in an oven (110 °C) for 24 h.

Age determination followed the methods of Yin (1993), and Vilizzi and Walker (1999). Scales were cleaned and rinsed in distilled water, and then placed on glass slides for analysis. The annulus was identified under the microscope. Four to six scales per fish were examined to ensure age estimates for each sample were generated.

3.2.2 Chemical Analysis

Analysis for MeHg and total mercury (THg) was conducted at Southwest University, Chongqing, China. MeHg was measured by gas chromatography-cold vapor atomic fluorescence spectrometry (GC-CVAFS) as described in Yan et al (2005). MeHg concentration in the digested sample was determined by aqueous phase ethylation, Tenax trap collection, GC separation, and CVAFS. THg was measured using acid digestion

combined with CVAFS as described by Yan et al (2005). The THg concentration was determined by Tekran 2500. For quality control purposes, laboratory control samples (NRCC-TORT-2), method blanks, and matrix spike samples were also analyzed for every 10 samples.

The PCB extraction method is described in Lazar et al. (1992). Sample lipid contents were determined gravimetrically using 10% of the extract solvent. PCB concentrations were determined by GC-microECD (Agilent 6890 Series Plus gas chromatograph with a ^{63}Ni -micro electron capture detector) with an Agilent 7683 auto sampler using a $60\text{ m} \times 0.25\text{ mm} \times 0.10\text{ }\mu\text{m}$ DB-5 column. A method blank (sodium sulfate) and an in-house tissue reference sample (Detroit River carp) were co-extracted every six samples. PCB 34 recoveries averaged $74 \pm 13\%$ for this study. PCB concentrations in the reference tissue measured with each batch of samples were checked against the laboratory quality control charts and found to be in compliance with QA/QC protocols.

Stable isotopes were analyzed as in Paterson et al. (2006). Samples were analyzed using a ThermoFinnigan Delta^{Plus} mass spectrometer (ThermoFinnigan, San Jose, CA, USA) coupled with an elemental analyzer (Costech, Valencia, CA, USA) for determination of $\delta^{15}\text{N}$ and $\delta^{13}\text{C}$ values. Stable isotopes were expressed as ratios (R) of heavy to light nitrogen or carbon in the sample relative to that of a standard as follows: $\delta X = 1000 \cdot [R_{\text{sample}} / R_{\text{standard}} - 1]$ ($X = ^{15}\text{N}$ or ^{13}C and $R = ^{15}\text{N}:^{14}\text{N}$ or $^{13}\text{C}:^{12}\text{C}$). Precision was based on replicate analysis of NIST1577c (NIST standard bovine liver) and internal lab standard tilapia muscle (n=10 for all). The mean differences from the certified values were $\leq 0.14\text{‰}$ for $\delta^{15}\text{N}$ and $\leq 0.04\text{‰}$ for $\delta^{13}\text{C}$ for both standards.

3.2.3 Model Simulations

3.2.3.1 Water Temperature

A polynomial function was fitted to the 2011 water temperature profile of Daning River (Zhao et al. 2015), and then the function was used to simulate daily water temperature within a year and repeated across years. The function is as follows:

$$T_d = 0.00000001602 \cdot d^4 - 0.00001343 \cdot d^3 + 0.0033 \cdot d^2 - 0.1964 \cdot d + 15.209 \quad (3.1)$$

where T_d is the water temperature ($^{\circ}\text{C}$) for the day of year, d is the day of the year (Jan 1 to Dec 31 is day 1 to 365). The annual water temperature cycle was repeated every year to generate a six year repeating water temperature profile.

3.2.3.2 Growth Model

Two growth scenarios were established for each species in this study. Scenario 1 was based on the whole body growth measured for each population. The proportion of lean dry weight/protein (excluding moisture and lipid content (Li et al. 2015)) and lipid was assumed to be constant across all age classes and based on the measured mean lean dry protein ($\bar{X}_{P,B}$; unitless) and lipid fraction ($\bar{X}_{L,B}$; unitless) of each population. Assuming fish growth was dependent on water temperature (Berg and Bremset, 1998; Shoji et al, 2007); daily growth was scaled to each day according to the water temperature (Chezik et al. 2013). The daily growth increment of whole body ($\Delta W_{wb,d}$; g) was estimated as follows:

$$\Delta W_{wb,d} = \left(\bar{W}_{wb,y+1} - \bar{W}_{wb,y} \right) \cdot \left(\frac{T_d}{\sum_{d=1}^{365} T_d} \right) \quad (3.2)$$

where $\bar{W}_{wb,y}$ and $\bar{W}_{wb,y+1}$ are mean body weight (g) of fish for a given species in a given age class and the mean body weights (g) of fish from the same species in the next age class, and $\sum_{d=1}^{365} T_d$ is the sum of water temperatures over a year. Under scenario 1, the daily weight increments of lipid ($\Delta W_{lip,d}$; g) or lean dry protein ($\Delta W_{pro,d}$; g) growth were obtained by multiplying the $\Delta W_{wb,d}$ by $\bar{X}_{L,B}$ or $\bar{X}_{P,B}$.

Scenario 2 used the measured lipid, lean dry protein and whole body weight of each age class for each species. Daily growth increments of whole body, lipids ($\Delta W_{lip,d}$; g), and protein ($\Delta W_{pro,d}$; g) weight were generated according to the same procedure described in Eq. 3.2. For instance, the daily weight increment of lipids was given as:

$$\Delta W_{lip,d} = \left(\bar{W}_{lip,y+1} - \bar{W}_{lip,y} \right) \left(\frac{T_d}{\sum_{d=1}^{365} T_d} \right) \quad (3.3)$$

where $\bar{W}_{lip,y+1}$ and $\bar{W}_{lip,y}$ are the mean total lipid weights (g) of fish from a given population for the next age class and mean total lipid weight (g) of fish from the same lake for the current year class of simulation.

The daily growth rate of lipid weight ($k_{g,lip}$; g g d⁻¹) and lean dry protein ($k_{g,pro}$; g g d⁻¹) was also determined using the same procedure, according to:

$$k_{g,lip} = \frac{W_{lip,d+1} - W_{lip,d}}{t \cdot W_{lip,d}} \quad (3.4)$$

where $W_{lip,d}$ and $W_{lip,d+1}$ are mean lipid weight (g) of fish of a given species for a given day and the mean lipid weights (g) of fish from the same species for the next day.

3.2.3.3 Bioenergetic Model and Toxicokinetic Model

The Wisconsin fish bioenergetic model adapted for Silver Carp and Bighead Carp, according to Cooke and Hill (2010), was applied and modified as described for yellow perch by Drouillard et al. (2009). The main outputs of the bioenergetic sub-model were daily food consumption rates (Q_C ; g food g⁻¹ d⁻¹), gill ventilation volumes (Q_V ; mL g⁻¹ d⁻¹), and fecal production rates (Q_{EX} ; g feces g⁻¹ d⁻¹) and are predicted as follows:

$$Q_C = \frac{(G_L + G_P) + R \cdot D_{O_2} + SDA + U}{E_C \cdot ED_{food}} \quad (3.5)$$

$$Q_V = \frac{R \cdot D_{O_2} + SDA + U}{D_{O_2} \cdot C_{O_2} \cdot E_{O_2} \cdot W} \quad (3.6)$$

$$Q_{EX} = Q_C \cdot (1 - (X_{L,D} \cdot E_L + X_{P,D} \cdot E_P)) \quad (3.7)$$

All parameters in Eq. 3.5-3.7 are defined and summarized in Table 3.1. Specific rate of respiration (R ; g g⁻¹ d⁻¹) is calculated using Equation 1 of the Wisconsin bioenergetic model version 3.0 (Hanson et al. 1997), and described in Cooke and Hill (2010). R for Bighead Carp is:

$$R = 0.00528 \cdot W_{wb,d}^{-0.299} \cdot e^{0.048T_d} \quad (3.8)$$

R for Silver Carp is:

$$R = 0.00279 \cdot W_{wb,d}^{-0.239} \cdot e^{0.076T_d} \quad (3.9)$$

Specific dynamic action (SDA ; $\text{kJ g}^{-1} \text{d}^{-1}$) and energy excretion (U ; $\text{kJ g}^{-1} \text{d}^{-1}$) for both species are derived from R (Eq. 3.8-3.9) and daily growth increments generated by the tissue specific growth sub-model according to:

$$SDA = 0.1 \cdot (R \cdot D_{O_2} + |G_L| + |G_P|) \quad (3.10)$$

$$U = 0.031 \cdot T_d^{0.58} \cdot e^{-0.299} \cdot (R \cdot D_{O_2} + |G_L| + |G_P|) \quad (3.11)$$

Energy assimilation from food (E_C ; unitless), energy density of food (ED_{food} ; kJ g^{-1}) and oxygen concentration in water (C_{O_2} ; $\text{g O}_2 \text{ mL}^{-1}$) used to convert energy flows into material flows via Eqs. 3.12-3.14. These were taken from Drouillard et al. (2009) as follows.

$$E_C = \frac{ED_{lip} \cdot X_{L,D} \cdot E_L + ED_{pro} \cdot X_{P,D} \cdot E_P}{ED_{Food}} \quad (3.12)$$

$$ED_{Food} = ED_{lip} \cdot X_{L,D} + ED_{pro} \cdot X_{P,D} \quad (3.13)$$

$$C_{O_2} = \frac{14.45 - 0.413 \cdot T_d + 5.56 \times 10^{-3} \cdot T_d^2}{1000000} \quad (3.14)$$

Because virtually all (>95%) of the Hg that presents in fish is MeHg, and food is the dominant MeHg uptake route (Hall et al. 1997), the daily change in MeHg lean dry weight concentration in fish (C_P ; ng g^{-1}) is calculated as:

$$\frac{dC_P}{dt} = \frac{C_{d,Hg} \cdot Q_C \cdot W_{wb,d} \cdot AE_{Hg}}{W_{pro,d}} - \left(k_{tot,Hg} + \frac{\Delta W_{pro,d}}{W_{pro,d}} \right) \cdot C_P \quad (3.15)$$

MeHg concentration in food ($C_{d,Hg}$; ng g^{-1}) was considered constant for each species and initially calibrated to establish the best fit to field data. $k_{tot,Hg}$ ($\text{g g}^{-1} \text{d}^{-1}$) is scaled to the

routine metabolic rate based on empirical data (Trudel and Rasmussen, 1997), and it is estimated according to:

$$k_{tot,Hg} = ((G_L + G_P) + R \cdot D_{O_2} + SDA + U) \cdot 0.0659 \quad (3.16)$$

For PCBs, the daily change in PCB lipid equivalent concentration (C_L ; ng g⁻¹) is modeled by:

$$\frac{dC_L}{dt} = \frac{C_{d,PCB} \cdot Q_C \cdot W_{wb,d} \cdot AE_{PCB} + C_w \cdot W_{wb,d} \cdot Q_V \cdot E_w}{W_L} - (k_2 + k_{EX} + \frac{\Delta W_L}{W_L}) \cdot C_L \quad (3.17)$$

A similar procedure to $C_{d,Hg}$ is used to calibrate $C_{d,PCB}$ (ng g⁻¹). Since kinetics rates are usually related to body size, small fish with relatively high growth rate and elimination rate are more likely to achieve steady state (Mackay, 1982; Paterson et al. 2007). It is assumed that PCB concentration of the young-of-year fish (C_{YOY} , ng g⁻¹lipid) and PCB concentration of the water (C_w ; ng g⁻¹) is at thermodynamic equilibrium, and C_w is calculated as:

$$C_w = \frac{C_{YOY}}{K_{OW}} \quad (3.18)$$

The gill elimination rate constant (k_2 ; d⁻¹) is calculated as:

$$k_2 = \frac{E_w \cdot Q_V}{K_{BW}} \quad (3.19)$$

The algorithms for estimating chemical exchange efficiency across the gills (E_w ; unitless) and biota/water partition coefficient (K_{BW} ; unitless) are as follows:

$$E_w = (1.85 + \frac{155}{K_{OW}})^{-1} \quad (3.20)$$

$$K_{BW} = X_{L,B} \cdot K_{OW} + 0.05 \cdot X_{P,B} \cdot K_{OW} \quad (3.21)$$

Fecal elimination rate constants (k_{EX} ; d^{-1}) are estimated by:

$$k_{EX} = \frac{E_{EX} \cdot Q_{EX}}{K_{B,EX}} \quad (3.22)$$

The biota/feces partition coefficient ($K_{B,EX}$; unitless) is:

$$K_{B,EX} = \frac{X_{L,B} + 0.05 \cdot X_{P,B}}{X_{L,EX} + 0.05 \cdot X_{P,EX}} \quad (3.23)$$

3.2.4 Data Analysis

To compare residues in fish with fish consumption guidelines, THg, MeHg and sum PCB concentrations were reported on a wet body weight basis. Additionally, MeHg concentrations were expressed in units of $ng\ g^{-1}$ lean dry weight, and PCB concentrations were expressed in units of $ng\ g^{-1}$ lipid weight. Only PCBs congeners detected in more than 60% of the samples were included in the sum PCB analysis. PCB 180 was used as a representative congener for the model simulation because of its high hydrophobicity ($K_{OW}=7.36$; Hawker and Connell, 1988) and commonality in elimination rate coefficient compared to MeHg (Li et al. 2015).

Analysis of variance (ANOVA) was used to test for differences between Bighead and Silver Carp Hg concentration, PCB concentration, $\delta^{15}N$ and $\delta^{13}C$. ANOVA was also applied to test for differences in lipid and lean dry weight fractions among age classes of each population. Linear regression analysis was performed with ANOVA to test whether total wet weight, lean dry weight, lipid weight, ln-transformed weight (wet, lean dry, and

lipid weight), ln-transformed Hg and PCB concentrations and $\delta^{15}\text{N}$ and $\delta^{13}\text{C}$ ratios were significantly related to fish age. Linear regression was also performed with ANOVA between measured and predicted chemical concentrations for two growth scenarios. The significance level of the slope combined with the R square value of the linear regression were used as indicators to evaluate the performance of the model. Analysis of Covariance (ANCOVA) was used to test for significant differences between growth scenarios in the slopes of linear regression of measured against predicted chemical concentration. Prior to using parametric tests, data were evaluated for normality and homogenous variance between treatments using the Kolmogorov-Smirnov and Levene's tests. All statistical analyses were conducted using SPSS version 20 (IBM Corp., USA).

3.3 Results

3.3.1 Hg and PCB Concentrations in Asian Carp

The THg concentrations in Silver Carp ranged from 2.4 to 27.0 ng g⁻¹ wet wt and MeHg concentrations ranged from 1.2 to 15.4 ng g⁻¹ wet wt (Table 3.2). MeHg:THg ratios ranged from 15.1% to 99.6% with an average of 67.1% for Silver Carp. Sum PCB concentrations in this species ranged from 0.1 to 2.9 ng g⁻¹ wet wt. For Bighead Carp, the THg concentrations ranged from 9.2 to 53.5 ng g⁻¹ wet wt; MeHg concentrations ranged from 4.6 to 43.3 ng g⁻¹ wet wt. while MeHg:THg ratios ranged from 44.9% to 90.2% with an average of 73.4%. Sum PCB concentrations in Bighead Carp ranged from 0.1 to 4.7 ng g⁻¹ wet wt. The THg and MeHg wet weight concentration was linearly related to the body mass for both species (linear regression, $p < 0.05$). A weaker, but still significant linear relationship between sum PCB wet weight concentration and body mass was

observed for Silver Carp (linear regression, $p < 0.05$). However, there was no significant relationship between sum PCB wet weight concentration and body mass for Bighead Carp (linear regression, $p > 0.05$).

In Ontario, consumption advisories for sensitive populations (women of child-bearing age and children under 15 years old) come into effect when the THg concentration in fish exceeds 60 ng g^{-1} wet wt, or when the sum PCB concentration in fish exceeds 26 ng g^{-1} wet wt (Ministry of the Environment and Climate Change). No sample in our study approached or exceeded these threshold guidelines. Also, none of the fish sampled exceeded the Chinese government regulation for freshwater fish for THg (300 ng g^{-1} wet wt), nor for sum PCB (500 ng g^{-1} wet wt).

3.3.2 Whole Body and Proximate Tissue Growth in Asian carp

Table 3.3 presents the growth trajectories of fish in wet weight, as well as growth of lipid and lean dry weight. Significant linear and exponential relationships were observed between whole body weight and age for both carp populations. Scenario 1 adopted the mean lipid and lean dry weight to whole body weight ratio across all age classes for each species. The mean lipid weight fraction was $3.89 \pm 3.63\%$ and $4.02 \pm 5.05\%$, and the mean lean dry weight fraction was $18.03 \pm 1.98\%$ and $21.22 \pm 3.98\%$ for Silver Carp and Bighead Carp, respectively. Growth scenario 2 used the tissue to whole body ratios measured for each age class of each population. Significant differences in the lipid to whole body ratios among age classes were observed for Silver Carp (ANOVA, $p < 0.01$). There was no significant difference in the lean dry weight to whole body ratios among age classes for either species (ANOVA, $p > 0.01$).

The annual growth rate of lean dry weight was generally close to that of whole body weight for both species. However, the annual growth rate of the lipid weight was generally higher (80% ~209%) than the whole body growth rate for Bighead Carp. For Silver Carp, the lipid growth rate was similar (within 9%) to the whole body growth rate for 1-2 year old fish, and then it became much higher (190%~297%) than the whole body growth rate for 3-4 year old fish. Moreover, close examination of the Silver Carp growth data reveals an inflection in whole body and lean dry weight growth, shifting to slower growth between ages 2-3, while lipid growth shifted to higher growth after age 2. For Bighead Carp, it was observed that whole body weight, lean dry weight and lipid weight shifted to slower growth rate between ages 3-5.

3.3.3 Stable Isotopes and Feeding Ecology of Asian Carp

The $\delta^{15}\text{N}$ signatures ranged from 6.0 to 8.5‰ for Silver Carp, and from 8.7 to 11.9‰ for Bighead Carp (Table 3.2). The mean $\delta^{15}\text{N}$ value was significantly higher in Bighead Carp ($10.1 \pm 1.6\text{‰}$) compared with that of Silver Carp ($7.2 \pm 0.6\text{‰}$) (ANOVA, $p < 0.01$), indicating a full trophic position increase of Bighead Carp relative to Silver Carp. Figure 3.1a showed $\delta^{15}\text{N}$ significantly increased with the body mass for Silver Carp (linear regression, $p < 0.01$). However, there was no relationship between $\delta^{15}\text{N}$ and body mass for Bighead Carp (linear regression, $p > 0.05$).

The $\delta^{13}\text{C}$ signatures ranged from -24.7 to -19.3‰ for Silver Carp, and from -28.0 to -19.5‰ for Bighead Carp (Table 3.2). A significantly higher mean $\delta^{13}\text{C}$ value was found in Silver Carp ($-22.3 \pm 1.5\text{‰}$) compared with that of Bighead Carp ($-24.6 \pm 2.7\text{‰}$) ($p > 0.05$). As shown in Figure 3.1b, the $\delta^{13}\text{C}$ value of Bighead Carp was negatively

related to the body mass (linear regression, $p < 0.05$), implying fish changed habitats and potentially fed on a more pelagic energy source as they grew. No relationship was observed between $\delta^{13}\text{C}$ and age for Silver Carp (linear regression, $p > 0.05$).

3.3.4 Model Simulations versus Measured Chemical Concentrations

Figure 3.2 presents measured and simulated chemical concentrations under the two growth scenarios. To examine the goodness of fit of the model simulations under each growth scenario, linear regression was performed between the measured and modeled chemical concentrations. As shown in Figure 3.2, the model simulations under both growth scenarios showed similar results for MeHg concentrations. The linear regression equation between simulated and measured Hg concentration was $y = 0.4569x + 26.983$ ($R^2 = 0.35$, $p < 0.05$) for growth scenario 1, and $y = 0.5017x + 25.901$ ($R^2 = 0.40$, $p < 0.05$) for growth scenario 2. ANCOVA showed no significant difference between the slopes of the two linear regressions ($p > 0.05$). For PCB 180, the linear regression equations between simulated and measured concentration were $y = 0.1506x + 0.3246$ ($R^2 = 0.29$, $p > 0.05$) and $y = 0.373x + 0.2592$ ($R^2 = 0.53$, $p < 0.05$) for growth scenario 1 and 2, respectively.

ANCOVA revealed significant differences in slopes of the linear regression between the two growth scenarios ($p < 0.05$), indicating that simulation under growth scenario 2 showed a better fit to the measured PCB data compared with simulation under growth scenario 1. Table 3.4 summarizes linear regression of measured and simulated concentrations for each chemical from each species. For PCB 180, the simulations under growth scenario 2 showed evident improvements in the R square compared with growth scenario 1 for both species. For Hg, model fit was relatively higher for the species when combined but reduced to values of 5%-19% on an individual species fit basis (Table 3.4).

Although the Hg simulations under growth scenario 2 had slightly higher R square for both species, such improvement was less evident compared with PCB simulations.

Figure 3.3 presents trends in PCB 180 expressed on a lipid equivalent weight basis and MeHg expressed on a lean dry weight concentration basis with fish age. MeHg lean dry weight concentrations were significantly related to fish age for both species ($p < 0.01$ in both species using linear or exponential regression fits). Unlike MeHg, there were no significant relationships between PCB 180 lipid equivalent concentrations and fish age for either species. There was also no significant difference in PCB 180 lipid equivalent concentrations between the species due to high variability of the data (ANOVA, $p > 0.05$).

Figure 3.3 also summarizes simulations of PCB and MeHg bioaccumulation using the non-steady state bioenergetic/kinetic bioaccumulation model. For Silver Carp, a constant dietary concentration ($C_{d, PCB}$) of 0.006 ng g^{-1} wet weight provided the best model fit while the $C_{d, Hg}$ of 1.49 ng g^{-1} wet weight generated a best fit. The model accurately simulated an increase followed by a decrease with age in PCB 180 concentration. For MeHg, the model showed an initial increase with age followed by a plateau, whereas the field data of Silver Carp showed a constant increase with age from YOY-3 years and a sudden increase in mercury accumulation at age 4 not captured by the model. For Bighead Carp, the $C_{d, PCB}$ and $C_{d, Hg}$ was calibrated to 0.02 ng g^{-1} and 6.4 ng g^{-1} wet weight. The model correctly simulated a peak in PCB concentration at age 2, followed by a decrease. The Hg model demonstrated increases in MeHg concentration for 1-2 and 3-4 year old fish, and decreases for 2-3 and 4-6 year old fish, which was not observed in Bighead Carp. Under growth scenario 2, $k_{g, lip} / k_{tot, PCB}$ ranged from 0.45 to 8.10 for Silver Carp, and from 6.73 to 8.56 for Bighead Carp; $k_{g, pro} / k_{tot, Hg}$ ranged from 0.24 to 0.95 for

Silver Carp, and from 0.28 to 1.44 for Bighead Carp. In general, the model demonstrated better fit to field data for PCB accumulation compared with Hg for both species.

3.4 Discussion

In this study, a higher trophic level for Bighead Carp compared to Silver Carp was observed, which was consistent with previous studies (Rogowski et al. 2009). It has been reported that Bighead Carp have a gill raker spacing that filters larger zooplankton sized particles while Silver Carp more commonly consume smaller particles in the size range of phytoplankton (Jayasinghe et al. 2015). Even though a significant positive relationship was found between $\delta^{15}\text{N}$ and age for Silver Carp, the highest $\delta^{15}\text{N}$ value in Silver Carp was still lower than the lowest $\delta^{15}\text{N}$ value of Bighead Carp. Typically, chemical concentration was positively related to trophic level (Cabana and Rasmussen, 1994), indicating a potentially higher C_d for food consumed by Bighead Carp compared with Silver Carp for both Hg and PCBs. In addition, the $\delta^{13}\text{C}$ results indicated that Silver Carp were feeding mainly in littoral zones, while Bighead Carp shift from littoral to pelagic areas as they age (>3 year). Even though this diet shift of Bighead Carp was not reflected in $\delta^{15}\text{N}$, pelagic energy sources may contain different contamination signatures compared with that of the littoral energy source (Arcagni et al. 2013; Laitano et al. 2016). Overall, the stable isotope analysis revealed differences in the feeding ecology between the two study species consistent with what has been described in the literature (Chick and Pegg, 2001; Rogowski et al. 2009; Jayasinghe et al. 2015). Bighead Carp feed at higher trophic level compared to Silver Carp but also exploit different habitats over their lifespan. Silver Carp appear to exhibit a small ontogenetic diet shift in trophic position over their life, but for the most part exploit the same habitat.

Because Bighead Carp and Silver Carp are mainly feeding on zooplankton and phytoplankton, $C_{d,PCB}$ and $C_{d,Hg}$, which were derived from the model calibration, should reflect the PCB 180 and MeHg levels of the plankton from sampling area. Wei et al. (2016) reported that the THg concentration in seston (which contains plankton) from TGR area was 5 ng g^{-1} wet weight, which was comparable to the model calibrated $C_{d,Hg}$ values. However, no such information was available for PCBs. In addition, $C_{d,PCB}$ and $C_{d,Hg}$ for Bighead Carp were generally four times higher than that for Silver Carp, which agreed with the higher trophic level of the former species. Notably, given the fact that $\delta^{13}\text{C}$ data indicated a habitat shift for older Bighead Carp, there could also be a shift in $C_{d,PCB}$ or $C_{d,Hg}$ for older fish. Unfortunately, measurements of seston contaminant levels in the nearshore and offshore habitats of Bighead Carp were not available to compare with model inferred prey contaminant levels.

A combined toxicokinetic and bioenergetics model was used to simulate PCB and Hg bioaccumulation by Silver Carp and Bighead Carp. Simulations using whole body growth rate and a constant tissue to whole body weight ratio were compared with simulations using tissue specific growth rate for their goodness of fit to field data. It was found that the simulation using tissue specific growth rate demonstrated better fit to measured PCB concentrations for both species (24% improved R^2). However, simulations under both growth scenarios showed a similar degree of model fit to the measured Hg bioaccumulation curve. This could be a result of high variability in lipid growth (lipid to whole body weight ratio), and low variability in protein growth (protein to whole body weight ratio) of these fish. While previous model practice usually employed whole body growth rate to predict Hg and PCB bioaccumulation (Norstrom et al. 1976; Eichinger et

al. 2010), this study demonstrated that using tissue growth rate could improve the accuracy of model outcomes. Particularly, such improvement would be more evident when proximate tissue growth shows distinct differences compared to whole body growth between age classes as was the case for lipids in the study species. In general, a non-steady state bioenergetics/kinetics model using tissue growth rate was generally able to explain differences in the bioaccumulation patterns of PCB ($R^2=0.53$) and Hg ($R^2=0.40$) in two species of Asian carp as a function of fish age. The relatively poor performance of the model could be a result of changes in the feeding behavior and associated change in prey contamination with such diet and habitat shifts.

For simulations using the empirical tissue growth rate, a much higher $k_{g,lip}/k_{tot,PCB}$ compared to $k_{g,pro}/k_{tot,Hg}$ was observed, which was a result of a higher relative growth rate of the lipid compartment compared to lean dry weight. The magnitude of $k_{g,pro}$ tended to approach $k_{tot,Hg}$, whereas $k_{g,lip}$ tended to exceed $k_{tot,PCB}$. This indicated that growth dilution was the dominant process (pseudo elimination) regulating the bioaccumulation of PCBs while for Hg was deemed of approximate equal importance to whole body elimination. In addition, changes in Hg and PCB concentration trajectories were evident when there were changes in the protein and lipid growth rates supporting the conclusion that tissue growth rate had a major influence on Hg and PCB bioaccumulation in the study species.

Although tissue growth plays an important role in chemical bioaccumulation rate, the majority of bioaccumulation studies model fish growth according to whole animal body weight or total body length, rather than proximate tissue growth (Norstrom et al. 1976; Eichinger et al. 2010). Thus, it is often expected that both Hg and PCBs should respond in a similar manner to growth dilution (Norstrom et al. 1976). However, several studies

show that Hg almost universally increases in fish as a function of body size (Dang and Wang, 2012), whereas body size of the fish often is a poor predictor of PCBs concentrations (Dufour et al. 2001; Sakizadeh et al. 2011; Mcleod et al. 2014). This study observed a higher variation in lipid growth rate compared with lean dry protein growth rate when scaled to body weight, which implies that the generally much higher variation in lipid content of fish with age contributes to deviations from a conventional bioaccumulation curve expected for PCBs. In contrast, growth of lean dry protein is scaled more directly with whole body weight leading to more consistent bioaccumulation patterns of Hg across populations and species when scaled with body size.

Based on the results of this research, the discrepancy in contaminant bioaccumulation trends for Hg and PCBs at the population and food web scales can be related to both differences in feeding ecology, as well as the difference in the rate of growth of proximate tissues representative of the major storage compartments for each contaminant. Lipid composition and the lipid growth coefficient increased with fish age resulting in growth dilution of PCBs, whereas the impact of protein growth is less evident for Hg. It is suggested that consideration of age specific lipid and to a lesser extent protein growth can tease out cases where PCB and Hg bioaccumulation are likely to be similar or in other cases different from one another. Also, as PCB concentrations are commonly expressed on a lipid-equivalent basis in toxicokinetic models (Connelly and Pederson, 1988), we suggest that the expression of Hg on a lean dry weight basis more accurately reflect its chemical activity. In addition to proximate tissue growth differences, differences in prey concentrations were also important in explaining species differences

in contamination. Further verification of the model's input, as well as contamination level in ingested food items, is required to provide a more robust validation of the model.

3.5 References

- Abma, R.; Paterson, G.; Mcleod, A.; Haffner, G. D. Cross-basin comparison of mercury bioaccumulation in Lake Huron lake trout emphasizes ecological characteristics. *Environ. Toxicol. Chem.* 2015, 34, 355-359.
- Arcagni, M.; Campbell, L.; Arrib e, M. A.; Marvin-DiPasquale, M.; Rizzo, A.; Guevara, S. R. Differential mercury transfer in the aquatic food web of a double basined lake associated with selenium and habitat. *Sci. Total Environ.* 2013, 454-455,170-180.
- Arnot, J. A.; Gobas, F. A. P. C. A food web bioaccumulation model for organic chemicals in aquatic ecosystems. *Environ. Toxicol. Chem.* 2004, 23, 2343-2355.
- Bloom, N. S. On the chemical form of mercury in edible fish and marine invertebrate tissue. *Can. J. Fish Aquat. Sci.* 1992, 49, 1010-1017.
- Borgmann, U.; Whittle, B. M. Bioenergetics and PCB, DDE, and mercury dynamics in Lake Ontario lake trout (*Salvelinus namaycush*): a model based on surveillance data. *Can. J. Fish. Aquat. Sci.* 1992, 49, 1086-1896.
- Buckman, A. H.; Brown, S. B.; Hoekstra, P. F.; Solomon, K. R.; Fisk, A. T. Toxicokinetics of three polychlorinated biphenyl technical mixtures in rainbow trout (*Oncorhynchus mykiss*). *Environ. Toxicol. Chem.* 2004, 23, 1725-1736.
- Cabana, G.; Rasmussen, J. B. Modelling food chain structure and contaminant bioaccumulation using stable nitrogen isotopes. *Nature* 1994, 372, 255-257.
- Chezik, K. A.; Lester, N. P.; Venturelli, P. A. Fish growth and degree-days I: selecting a base temperature for a within-population study. *Can. J. Fish. Aquat. Sci.* 2014, 71, 47-55.
- Chick, J. H.; Pegg, M. A. Invasive Carp in the Mississippi River Basin. *Science* 2001, 292, 2251-2252.

- Connolly, J. P.; Pedersen, C. J. A Thermodynamic-based evaluation of organic chemical accumulation in aquatic organisms. *Environ. Sci. Technol.* 1988, 22, 99-103.
- Cooke, S. L.; Hill, W. R. Can filter-feeding Asian carp invade the Laurentian Great Lakes? A bioenergetic modelling exercise. *Freshwater Biology* 2010, 55, 2138-2152.
- Daley, J. M.; Leadley, T. A.; Pitcher, T. E.; Drouillard, K. G. Bioamplification and the selective depletion of persistent organic pollutants in Chinook salmon larvae. *Environ. Sci. Technol.* 2012, 46, 2420-2426.
- Dang, F.; Wang, W. X. Why mercury concentration increases with fish size? Biokinetic explanation. *Environ. Pollut.* 2012, 163, 192-198.
- deBruyn, A. M.; Gobas, F. A. The sorptive capacity of animal protein. *Environ. Toxicol. Chem.* 2007, 26 (9), 1803-1808.
- Drouillard, K. G.; Paterson, G.; Haffner, G. D. A combined food web toxicokinetic and species bioenergetic model for predicting seasonal PCB elimination by yellow perch (*Perca flavescens*). *Environ. Sci. Technol.* 2009, 43(8), 2858-2864.
- Dufour, E.; Gerdeaux, D.; Corvi, C.; Khim-Heang, S.; Mariotti, A. Assessment of the contaminant concentration variability among Lake Geneva arctic char using stable isotopic composition ($\delta N-15$ and $\delta C-13$). *Environ. Toxicol.* 2001, 16(2), 185-191.
- Dumas, C.F.M.; de Lange, J.; France, Bureau, D.P. Quantitative description of body composition and rates of nutrient deposition in rainbow trout (*Oncorhynchus mykiss*) *Aquaculture* 2007, 273, 165-181.
- Eichinger, M.; Loizeau, V.; Roupsarda, F.; Le Guellec, A. M.; Bacherb, C. Modelling growth and bioaccumulation of Polychlorinated biphenyls in common sole (*Solea solea*). *J. Sea Res.* 2010, 64 (3), 373-385.
- EPA-FDA. Eating fish: what pregnant women and parents should know. www.epa.gov/fishadvice. 2017.

- Fisk, A. T.; Norstrom, R. J.; Cymbalisty, C. D.; Muir, D. C. G. Dietary accumulation and depuration of hydrophobic organochlorines: Bioaccumulation parameters and their relationship with the octanol/water partition coefficient. *Environ. Toxicol. Chem.* 1998, 17, 951-961.
- Gobas, F. A. P. C.; Muir D. C. G.; Mackay, D. Dynamics of dietary bioaccumulation and fecal elimination of hydrophobic organic chemicals in fish. *Chemosphere* 1988, 17, 943-962.
- Hall, B. D.; Bodaly, R. A.; Fudge, R. J. P.; Rudd, J. W. M.; Rosenberg, D. M. Food as the dominant pathway of methylmercury uptake by fish. *Water, Air, and Soil Pollut.* 1997, 100, 13-24.
- Hanson, P. C.; Johnson, T. B.; Schindler, D. E.; Kitchell, J. F. *Fish Bioenergetics 3.0*. University of Wisconsin Sea Grant Institute, Madison, Wisconsin. 1997.
- Hasen, B. G.; Paya-Presez, A. B.; Rahman, M.; Larsen, B. R. QSARs for K_{OW} and K_{OC} of PCB congeners: a critical examination of data, assumptions, and statistical approaches. *Chemosphere* 1999, 39(13), 2209-2228.
- Hawker, D. W.; Connell, D. W. Octanol-water partition coefficients of polychlorinated biphenyl congeners. *Environ. Sci. Technol.* 1988, 22, 382-387.
- Hayer, C. A.; Breeggemann, J. J.; Klumb, R. A.; Graeb, B. D. S.; Bertrand, K. N. Population characteristics of bighead and Silver Carp on the northwestern front of their North American invasion. *Aquat. Invasions* 2014, 9 (3), 289-303.
- He, W.; Liang, L.; He, R.; Jiang, L.; Zheng, S.; Ye, S. The comprehensive evaluation of the benefits on the ecological fishery in the typical bays of the Three Gorges Reservoir-An example of the Ganjing River water ranch in Zhongxian county of Chongqing. *Acta Hydrobiol. Sin.* 2015, 39 (5), 930-939.
- Hu, Y. X. The physiological adaptation of stocking Silver Carp and Bighead Carp to water environmental change in the Three Gorges Reservoir water ranch. M.Sc. Dissertation, Southwest University, Chongqing, China, 2014.

- Jayasinghe, U. A. D.; Garc á-Berthou, E.; Li, Z.; Li, W.; Zhang, T.; Liu, J. Co-occurring bighead and Silver Carps show similar food preference but different isotopic niche overlap in different lakes. *Environ. Biol. Fish* 2015, 98, 1185-1199.
- Laitano, M. V.; Silva Barni, M. F.; Costa, P. G.; Cledon, M.; Fillmann, G.; Miglioranza, K. S. B.; Panarello, H. O. Different carbon sources affect PCB accumulation by marine bivalves. *Mar. Environ. Res.* 2016, 113, 62-69.
- Lazar, R.; Edwards, R. C.; Metcalfe, C. D.; Gobas, F. A. P. C.; Haffner, G. D. A simple, novel method for the quantitative analysis of coplanar (non-ortho-substituted) polychlorinated biphenyls in environmental samples. *Chemosphere* 1992, 25, 493-504.
- Leaner J. J.; Mason R. P. Methylmercury uptake and distribution kinetics in sheepshead minnows, *cyprinodont variegatus*, after exposure to CH₃Hg-spiked food. *Environ. Toxicol. Chem.* 2004, 23(9), 2138-2146.
- Li, J.; Drouillard, K. G.; Branfireun, B.; Haffner, G. D. Comparison of the toxicokinetics and bioaccumulation potential of mercury and polychlorinated biphenyls in goldfish (*Carassius auratus*). *Environ. Sci. Technol.* 2015, 49, 11019-11027.
- Liu, J.; Haffner, G. D.; Drouillard, K. G. The influence of diet on the assimilation efficiency of 47 polychlorinated biphenyl congeners in Japanese Koi (*Cyprinus carpio*). *Environ. Toxicol. Chem.* 2010, 29, 401-409.
- Mackay, D.; Paterson, S. Calculating fugacity. *Environ. Sci. Technol.* 1981, 15, 1006-1014.
- Mackay, D. Correlation of bioconcentration factors. *Environ. Sci. Technol.* 1982, 16, 274-278.
- McIntyre, J. K.; Beauchamp, D. A. Age and trophic position dominate bioaccumulation of mercury and organochlorines in the food web of Lake Washington. *Science of the Total Environment.* 2007, 372, 571-584.
- McKim, J. M.; Schmieder, P. K.; Veith, G. D. Absorption dynamics of organic chemical transport across trout gills as related to octanol-water partition coefficient. *Toxicol. Appl. Pharmacol.* 1985, 77, 1-10.

- McLeod, A. M.; Arnot, J. A.; Borga, K.; Selck, H.; Kashian, D. R.; Krause, A.; Paterson, G.; Haffner, G. D.; Drouillard, K. G. Quantifying uncertainty in the trophic magnification factor related to spatial movements of organisms in a food web. *Integr Environ Assess Manag.* 2015, 11(2), 306-318.
- McLeod, A. M.; Paterson, G.; Drouillard, K. G.; Haffner, G. D. Ecological factors contributing to variability of persistent organic pollutant bioaccumulation within forage fish communities of the Detroit River, Ontario, Canada. *Environ. Toxicol. Chem.* 2014, 33(8), 1825-1831.
- Ministry of the Environment and Climate Change. Guide to eating Ontario fish. Queen's Printer for Ontario. 2015.
- Norstrom, R. J.; McKinnon, A. E.; DeFreitas, A. S. W. Bioenergetics-based model for pollutant accumulation by fish simulation of PCB and methylmercury residue levels in Ottawa River yellow perch (*Perca flavescens*). *J. Fish. Res. Bd. Can.* 1976, 33, 248-267.
- Nuevo, M.; Sheehan, R. J.; Wills, P. S. Age and growth of the Bighead Carp *Hypophthalmichthys nobilis* (RICHARDSON 1845) in the middle Mississippi River. *Arch. Hydrobiol.* 2004, 160(2), 215-230.
- Overturf, K.; Barrows, F. T.; Hardy, R. W.; Brezas, A.; Dumas, A. Energy composition of diet affects muscle fiber recruitment, body composition, and growth trajectory in rainbow trout (*Oncorhynchus mykiss*). *Aquaculture* 2016, 457, 1-14.
- Paterson, G.; Drouillard, K. G.; Haffner, G. D. An evaluation of stable nitrogen isotopes and polychlorinated biphenyls as bioenergetic tracers in aquatic systems. *Can. J. Fish. Aquat. Sci.* 2006, 63, 628-641.
- Paterson, G.; Drouillard, K. G.; Leadley, T. A.; Haffner, G. D. Long-term polychlorinated biphenyl elimination by three size classes of yellow perch (*Perca flavescens*). *Can. J. Fish. Aquat. Sci.* 2007, 64, 1222-1233.
- Paterson, G.; Liu, J. A.; Haffner, G. D.; Drouillard, K. G. Contribution of fecal egestion to the whole body elimination of polychlorinated biphenyls by Japanese Koi (*Cyprinus carpio*). *Environ. Sci. Technol.* 2010, 44, 5769-5774.

- Paterson, G.; Ryder, M.; Drouillard, K. G.; Haffner, G. D. Contrasting PCB bioaccumulation patterns among lakes Huron lake trout reflect basin-specific ecology. *Environ. Toxicol. Chem.* 2016, 35, 65-73.
- Pickhardt, P. C.; Stepanova, M.; Fisher, N. S. Contrasting uptake routes and tissue distribution of inorganic and methylmercury in mosquitofish (*Gambusia affinis*) and redear sunfish (*Lepomis microlophus*). *Environ. Toxicol. Chem.* 2006, 25(8), 2132-2142.
- Rogowski, D. L.; Soucek, D. J.; Levengood, J. M.; Johnson, S. R.; Chick, J. H.; Dettmers J. M.; Pegg, M. A.; Epifanio, J. M. Contaminant concentrations in Asian carps, invasive species in the Mississippi and Illinois Rivers. *Environ. Monit. Assess.* 2009, 157, 211-222.
- Russell, R.W.; Lazar, R.; Haffner, G.D. Biomagnification of organochlorines in Lake Erie white bass. *Environ. Toxicol. Chem.* 1995, 14 (4), 719-724.
- Sakizadeh, M.; Sari, A.; Abdoli, A.; Bahramifar, N.; Hashemi, S. H. Determination of polychlorinated biphenyls and total mercury in two fish species (*Esox lucius* and *Carassius auratus*) in Anzali Wetland, Iran. *Environ. Monit. Assess.* 2012, 184(5), 3231-3237.
- Ser, P.H.; Waranabe, C. Fish advisories in the USA and Japan: risk communication and public awareness of a common idea with different backgrounds. *Asia Pac. J. Clin. Nutr.* 2012, 21 (4), 487-494.
- Sijm, D. T. H. M.; Seinen, W.; Opperhulzen, A. Life-cycle biomagnification study in fish. *Environ. Sci. Technol.* 1992, 26, 2162-2174.
- Stohs, S. J.; Bagchi, D. Oxidative mechanisms in the toxicity of metal ions. *Free Rad. Biol. Med.* 1995, 18, 321-336.
- Thomann, R.V. Equilibrium model of fate of microcontaminants in diverse aquatic food chains. *Can. J. Fish. Aquat. Sci.* 1981, 38, 280-296.
- Trudel, M.; Rasmussen, J. B. Modeling the elimination of mercury by fish. *Environ. Sci. Technol.* 1997, 31, 1716-1722.

- Trudel, M.; Rasmussen, J. B. Predicting mercury concentration in fish using mass balance models. *Ecol. Appl.* 2001, 11, 517-529.
- Vilizzi, L.; Walker, K. F. Age and growth of the common carp, *Cyprinus carpio*, in the River Murray, Australia: validation, consistency of age interpretation, and growth models. *Environ. Biol. Fishes.* 1998, 54 (1), 77-106.
- Wang, R.; Wang, W. X. Contrasting mercury accumulation patterns in tilapia (*Oreochromis niloticus*) and implication on somatic growth dilution. *Aquat. Toxicol.* 2012, 114-115, 23-30.
- Wang, W. *Fish aquaculture science*, China Agriculture Press: Beijing, 2000.
- Wang, W.; Wong, R. S. K. Bioaccumulation kinetics and exposure pathways of inorganic mercury and methylmercury in a marine fish, the sweetlips (*Plectorhinchus gibbosus*). *Mar. Ecol. Prog. Ser.* 2003, 261, 257-268.
- Wei, L.; Zhou, Q.; Xie, C.; Wang, J.; Li, J. Bioaccumulation and biomagnification of heavy metals in Three Gorges Reservoir and effect of biological Factors. *Environ. Sci.* 2016, 37(1), 325-334.
- Williamson, C. J.; Garvey, J. E. Growth, fecundity, and diets of newly established Silver Carp in the middle Mississippi River. *Trans. Am. Fish. Soc.* 2005, 134(6), 1423-1430.
- Yan, H.; Feng, X.; Liang, L.; Shang, L.; Jiang, H. Determination of methyl mercury in fish using GC-CVAFS. *Journal of Instrumental Analysis* 2005, 24 (6), 78-80.
- Yin, M. *Fish Ecology*, China Agriculture Press: Beijing, 1993.
- Zhao, X.; Feng, C.; Wu, M. Sophisticated 3D modeling for eutrophication in Daning River Three Gorges Reservoir area. *J. Yangtze River Sci. Res. Inst.* 2015, 32(06), 25-31.

Table 3.1 Bioenergetics and toxicokinetics parameters for Silver Carp and Bighead Carp.

Parameter	Description	Value/Equation
AE_{Hg}	Hg assimilation efficiency (unitless)	0.87 ^a
AE_{PCB}	PCB assimilation efficiency (unitless)	0.44 ^a
$C_{d,Hg}$	Hg concentration in fish diet ($ng\ g^{-1}$)	
$C_{d,PCB}$	PCB concentration in fish diet ($ng\ g^{-1}$)	
C_L	Lipid equivalent PCB concentration in the animal ($ng\ g^{-1}$)	Eq. 3.17
C_{O_2}	Concentration of oxygen dissolved in water ($g\ O_2\ mL^{-1}$)	Eq. 3.14
C_P	Hg lean dry weight concentration in the animal ($ng\ g^{-1}$)	Eq. 3.15
C_w	PCB concentration in water ($ng\ g^{-1}$)	Eq. 3.18
C_{YOY}	PCB lipid concentration in YOY fish ($ng\ g^{-1}$)	
D_{O_2}	Oxycalorific coefficient for converting O_2 respired to energy ($kJ\ g^{-1}O_2$)	14.3 ^b
E_C	Energy assimilation efficiency from food (unitless)	Eq. 3.12
ED_{Food}	Total energy density of food ($kJ\ g^{-1}$)	Eq. 3.13
ED_{lip}	Energy density of lipid ($kJ\ g^{-1}$)	39.3 ^c
ED_{pro}	Energy density of protein ($kJ\ g^{-1}$)	18.0 ^c
E_{EX}	PCB organism/fecal exchange efficiency (unitless)	44% ^a
E_L	Assimilation efficiencies of dietary lipid (unitless)	0.92 ^d
E_{O_2}	Oxygen extraction efficiency across the gills (unitless)	0.6 ^e
E_P	Assimilation efficiencies of dietary protein (unitless)	0.6 ^d
E_w	Chemical exchange efficiency across the gills (unitless)	Eq. 3.20
G_L	Growth of somatic lipid ($kJ\ g^{-1}\ d^{-1}$)	
G_P	Growth of somatic protein ($kJ\ g^{-1}\ d^{-1}$)	
k_2	Elimination rate constants for chemical depuration across the gills (d^{-1})	Eq. 3.19
$K_{B,EX}$	Biota/feces partition coefficient (unitless)	Eq. 3.23
K_{BW}	Biota/water partition coefficient (unitless)	Eq. 3.21
k_{EX}	Elimination rate constants for chemical depuration across feces (d^{-1})	Eq. 3.22
K_{OW}	Octanol/water partition coefficient of the chemical (unitless)	
$k_{tot,Hg}$	Whole body Hg elimination rate coefficient ($g\ g^{-1}\ d^{-1}$)	Eq. 3.17
Q_C	Consumption rate into a mass flow ($g\ food\ g^{-1}\ d^{-1}$)	Eq. 3.5
Q_{EX}	Fecal egestion rate ($g\ feces\ g^{-1}\ d^{-1}$)	Eq. 3.7

Q_V	Gill ventilation rate ($\text{mL g}^{-1} \text{d}^{-1}$)	Eq. 3.6
R	Specific rate of respiration ($\text{g g}^{-1} \text{d}^{-1}$)	Eq. 3.8, 3.9
SDA	Specific dynamic action ($\text{kJ g}^{-1} \text{d}^{-1}$)	Eq. 3.10
U	Energy lost to excretion ($\text{kJ g}^{-1} \text{d}^{-1}$)	Eq. 3.11
ΔW_L	Daily change of lipid equivalent weight (g)	
W_L	Lipid equivalent weight of the animal (g)	
$W_{wb,d}$	Fish body weight for a given day (g)	
$X_{L,B}$	Fraction of lipid in the animal (unitless)	
$X_{L,D}$	Mass fraction of lipid in the diet (unitless)	
$X_{L,EX}$	Fraction of lipid in the feces (unitless)	
$X_{P,B}$	Fraction of lean dry protein in the animal (unitless)	
$X_{P,D}$	Mass fraction of protein in the diet (unitless)	
$X_{P,EX}$	Fraction of lean dry protein in the feces (unitless)	

^aLi et al. 2015

^bNorstrom et al. 1976

^cDrouillard et al. 2009

^dArnot and Gobas, 2004

^eMcKim et al. 1985

^fCooke and Hill, 2010

Table 3.2 Summarized biological data, THg wet weight concentrations, MeHg wet weight concentrations, sum PCB (Σ PCB) wet weight concentrations, $\delta^{13}\text{C}$ and $\delta^{15}\text{N}$ signatures for Silver Carp and Bighead Carp.

Species (sample size)	Length (mm)	Mass (g)	THg (ng g ⁻¹)	MeHg (ng g ⁻¹)	Σ PCB (ng g ⁻¹)	$\delta^{15}\text{N}$ (‰)	$\delta^{13}\text{C}$ (‰)
	Mean \pm SD	Mean \pm SD	Mean \pm SD	Mean \pm SD	Mean \pm SD	Mean \pm SD	Mean \pm SD
	Min~Max	Min~Max	Min~Max	Min~Max	Min~Max	Min~Max	Min~Max
Silver Carp(26)	391.8 \pm 131.6 194.0~705.0	810.4 \pm 912.1 80~4300	8.0 \pm 5.4 2.4~27.0	5.2 \pm 3.5 1.2~15.4	1.3 \pm 0.7 0.09~2.9	10.1 \pm 1.6 8.7~11.9	-22.3 \pm 1.5 -24.7~ -19.3
Bighead Carp(18)	610.2 \pm 234.7 302.0~1083.0	3732.5 \pm 4157.3 244.6~15500	21.2 \pm 13.8 5.6~53.5	15.9 \pm 11.6 4.6~43.3	2.1 \pm 1.6 0.1~4.7	7.2 \pm 0.6 6.0~8.5	-24.6 \pm 2.7 -28.0~ -19.5

Table 3.3 Measured total mass (mean±SD), as well as lipid to whole body weight ratio (mean±SD), and lean dry weight (LDW) to whole body weight ratio (mean±SD) for Silver Carp and Bighead Carp under two growth scenarios

Species	Age (year)	Sample size (n)	Total weight (g)	Scenario 1		Scenario 2	
				LDW%	Lipid%	LDW%	Lipid%
Silver Carp	0	5	112.54±28.03			17.22±1.54	2.82±0.93
	1	8	289.94±84.43			16.80±1.93	2.66±1.36
	2	6	778.37±141.22	18.03±1.98	3.89±3.63	19.38±2.00	2.75±2.50
	3	6	1536.17±373.41			19.11±1.64	6.77±4.62
	4	1	4300.00			19.08	15.06
Bighead Carp	1	4	405.2±114.59			19.61±1.45	1.01±0.97
	2	4	810.075±141.42			20.16±1.57	1.58±0.90
	3	1	2419.60	21.22±3.98	4.02±5.05	21.63	2.42
	4	2	3202±1269.96			20.01±1.48	2.85±3.07
	5	4	4725±471.69			24.10±7.31	5.75±6.51
	6	2	9550±777.81			23.89±0.3	11.84±9.16

Table 3.4 Linear regression between observed and simulated MeHg and PCB 180 concentrations for Silver Carp (SC) and Bighead Carp (BC).

Species	Growth scenario	Chemical	β (slope)			α (intercept)		R square
			Value	SE	p	Value	SE	
SC	1	PCB	0.094	0.087	0.042	0.307	0.053	0.203
SC	2	PCB	0.506	0.121	0.000	0.185	0.027	0.522
BC	1	PCB	0.121	0.089	0.033	0.418	0.089	0.208
BC	2	PCB	0.309	0.097	0.000	0.350	0.048	0.492
SC	1	Hg	0.246	0.120	0.051	5.327	0.740	0.149
SC	2	Hg	0.290	0.121	0.025	5.178	0.751	0.192
BC	1	Hg	0.100	0.115	0.400	15.696	1.968	0.048
BC	2	Hg	0.164	0.125	0.211	14.963	2.145	0.102

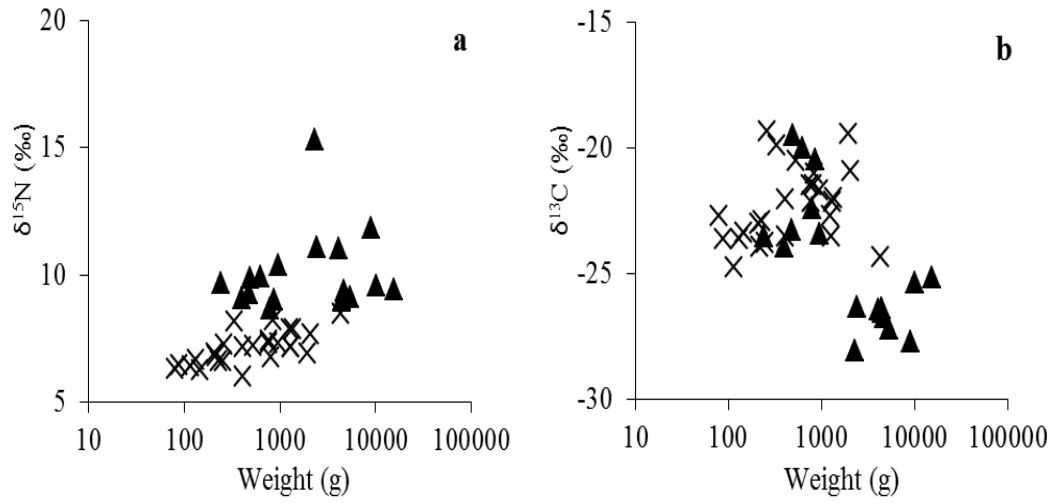


Figure 3.1 Nitrogen (a) and carbon (b) stable isotopes versus body mass of fish; crosses (×) represent Silver Carp; triangles (▲) represent Bighead Carp.

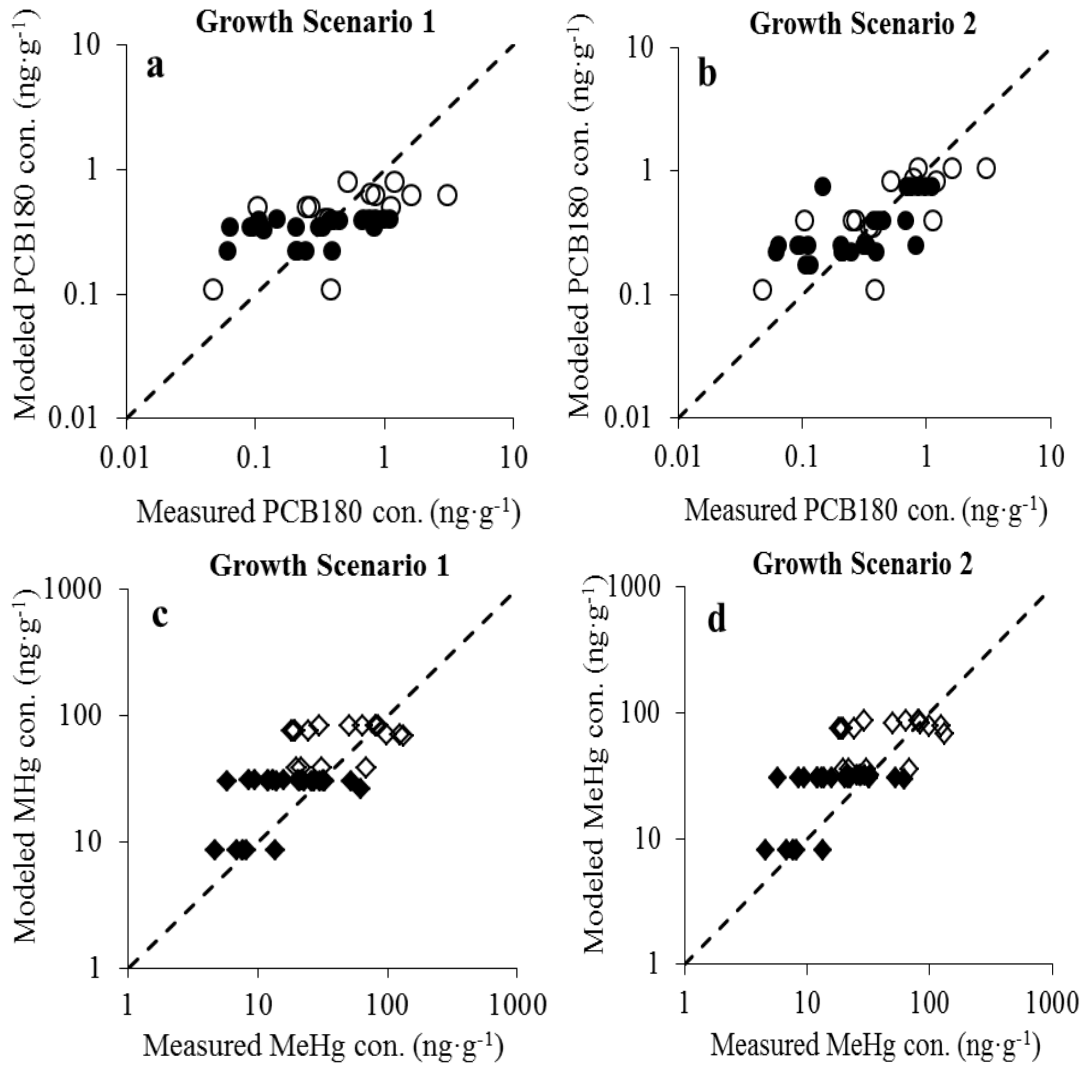


Figure 3.2 Relationships between simulated and observed MeHg and PCB 180 concentrations under model assumptions of; (a) lipid growth rates proportional to whole body growth (Scenario 1); (b) population specific lipid growth rates (Scenario 2); (c) protein growth rates proportional to whole body growth (Scenario 1); and (d) population specific protein growth rates (Scenario 2). Solid circles (●) and open circles (○) represent PCB 180 in Silver Carp and Bighead Carp; while solid diamonds (◆) and open diamonds (◇) represent MeHg in Silver Carp and Bighead Carp, respectively; dashed lines represents the 1:1 regression fit.

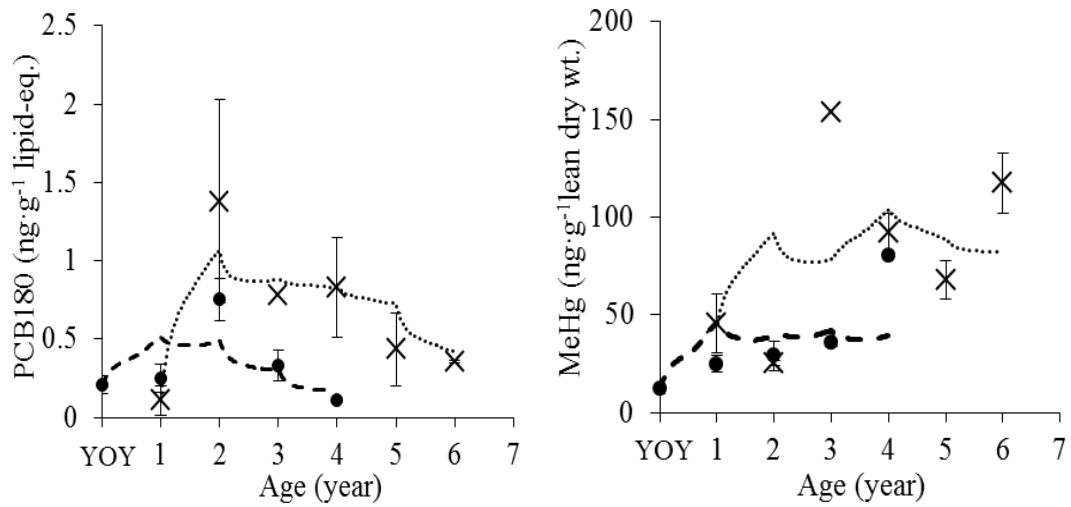


Figure 3.3 PCB 180 lipid-equivalent concentration and MeHg lean dry weight concentration versus age of the fish; circles (●) represent measured chemical concentration of Silver Carp; crosses (×) represent measured concentration of Bighead Carp; dashed lines were the simulations of chemical bioaccumulation in Silver Carp; dotted lines modeled chemical bioaccumulation in Bighead Carp.

CHAPTER 4

Importance of Growth Rate on Hg and PCB Bioaccumulation in Fish

4.1 Introduction

Mercury (Hg) and polychlorinated biphenyls (PCBs) are globally dispersed pollutants with high potential for bioaccumulation in aquatic species, food webs and ecosystems (McIntyre et al. 2007). Both of these chemicals present human health risks due to exposure through the consumption of contaminated fish and seafood (Watanabe et al. 2003). It is therefore imperative to accurately predict Hg and PCB bioaccumulation by fish in order to improve risk assessment predictions and develop appropriate mitigation solutions that help reduce the bioaccumulation of these toxic pollutants in biota and minimize exposure risks to higher level consumers.

Despite being the most frequent cause of fish consumption restrictions (US EPA 2010 & 2014; OMOE 2016), most research on Hg and PCBs typically only focus on one of these legacy pollutants. Direct comparisons of Hg and PCB bioaccumulation dynamics are rarely assumed due to the different instrumentation requirements for analysis, as well as differences in their environmental speciation, fate, and the physiological mechanisms regulating their assimilation, biotransformation and elimination pathways (Mason et al. 1995; Gobas et al. 1999). Yet, there are many commonalities among the general bioaccumulation characteristics for these two pollutants such that common predictive models for understanding their bioaccumulation by fish have been proposed (Li et al. 2015). Toxicokinetic bioaccumulation models adopt mass balance principles and use experimentally calibrated rate coefficients to describe pollutant uptake from water and food, whole body elimination, and growth dilution (Trudel and Rasmussen, 2001;

McLeod et al. 2016). However, toxicokinetic rate constants determined via controlled laboratory experiments are often specific to experimental conditions and the test species utilized, which can lead to inaccurate predictions when such coefficients are extrapolated to field conditions.

To better address species responses to field conditions, toxicokinetic models have been coupled with species specific bioenergetic sub-models that address animal metabolic rate and growth responses to varying environmental conditions. Such bioenergetics models were developed to predict food consumption, gill ventilation, fecal egestion, and growth rates over the range of environmental conditions that an individual or population may experience at daily, seasonal, and annual temporal scales (Kitchell and Stewart, 1977; Trudel and Rasmussen, 2006). Bioenergetic models have been calibrated for a wide variety of fish species thereby providing the capacity to predict changes in fish physiological processes across a wide range of temperature optima and allometric scaling coefficients (Madenjian et al. 2006; Holker and Haertel, 2004). Thus, coupled bioenergetic-toxicokinetic models have the advantage of being scalable to the different environmental conditions that fish populations are likely to experience over their natural habitat range with life history characteristics such as ontogenetic diet shifts being easily incorporated into model structure (Drouillard et al. 2009). Further, combined bioenergetic-toxicokinetic models provide the capacity to predict pollutant bioaccumulation under the assumption of non-steady state bioaccumulation, which is frequently the condition for highly persistent and hydrophobic pollutants such as PCBs (Paterson et al. 2007; McLeod et al. 2016) and Hg (Li et al. 2015).

Toxicokinetic models developed for predicting Hg and PCB bioaccumulation are generally sensitive to fish growth rates as tissue growth (dilution) and weight loss (bioamplification) represent key factors for understanding differences in pollutant bioaccumulation within and among fish populations (Simoneau et al. 2005; Paterson et al. 2007; Daley et al. 2014). However, many food web bioaccumulation models assume fish growth to be constant over an animal's life (Gobas 1995), yet fish growth in nature is both age and temperature dependent such that growth rates vary with season and age (Ricker 1979). Further, for Hg and PCBs, protein and lipid tissues, respectively, dictate the maximum capacities for an individual to bioaccumulate these pollutants (Mackay, 1982; Roesijadi, 1992). As such, differences in the rates of protein vs. lipid growth could have contrasting effects of growth dilution on Hg and PCB bioaccumulation potentially resulting in a decoupling of bioaccumulation trajectories between these pollutants.

In most bioaccumulation studies, growth is typically representative of whole body mass with individual tissue growth rates considered proportional to such somatic growth (Trudel and Ramussen, 2006; Drouillard et al. 2009). However, protein mass has a much stronger correlation to changes in whole body growth while the relationships between lipids and whole body mass are frequently weaker due to the supporting role of lipids as an energy reserve in many fish species (Overturf et al. 2016). Finally, growth itself has an energetic cost, requiring additional food consumption to generate new tissue above consumption required to satisfy routine metabolic rate. Therefore, growth dilution cannot be examined independently of chemical intake rates via food consumption. Bioenergetic models are thus necessary to tease out growth dilution effects while also considering associated changes in chemical intake rate.

The present study was developed to evaluate the effect of growth dilution on Hg and PCB bioaccumulation in different populations of Bluegill (*Lepomis macrochirus*) using a non-steady state bioenergetic/kinetic bioaccumulation model. Fish, aged 0 to 5 years, were collected from a set of five lakes over a latitudinal gradient ranging from 34 ° to 46 ° north latitude. This ensured that each population was subject to different thermal regimes known to impact annual fish growth. The bioenergetic/kinetic bioaccumulation model was used to simulate PCB and Hg accumulation with age in fish for each population using field measured growth rates and contrasted with empirical bioaccumulation trends. Two different simulations were contrasted for their predictive capability. Simulation 1, assumed lipid and lean dry protein growth was proportional to whole body growth to predict PCB and Hg bioaccumulation for each population. Simulation 2 applied population specific lipid and protein growth rates. Goodness of fit tests were used to discriminate between the simulations in order to test the hypothesis that a common bioenergetic/kinetic bioaccumulation model incorporating tissue specific growth dilution can better account for deviations in bioaccumulation patterns of Hg and PCBs in fish.

4.2 Methods

4.2.1 Sampling

Multiple sizes (0.1 to 130.9 g) of Bluegill were collected in October, 2006 from Apsey Lake (46.2268 °N, 81.7689 °W) (n=41), Sharbot Lake (44.7667 °N, 76.6833 °W) (n=47), the Detroit River (42.2167 °N, 83.1333 °W) (n=54), and Stonelick Lake (39.2203 °N, 84.0725 °W) (n=47). Bluegill were also sampled in June, 2006 from Lake Hartwell (34.4652 °N, 82.8455 °W) (n=62). Fish were stored at -30 °C prior to dissection.

Biological data, including wet weight, sex (if identifiable), total, fork, and standard lengths, were catalogued. Otoliths were removed to determine the age of each individual. Gut tracts were dissected from each fish, and stored in freezer prior to analysis. Each individual was then homogenized and analyzed for total Hg (THg), PCBs, carbon and nitrogen stable isotopes.

4.2.2 Chemical Analysis

THg and PCBs were measured at the Great Lake Institute for Environmental Research, University of Windsor. Standard operating procedures, which were accredited through the Canadian Association for Laboratory Analysis (CALA), were followed throughout the lab analysis.

THg concentrations were determined using a Direct Mercury Analyzer (DMA-80, Milestone Inc.). A 10 point calibration curve, using a certified standard (High-Purity Standards, Charleston, USA), was used for calibrating the instrument. Approximately 0.20 g fish homogenate was weighed on a clean nickel boat, and then placed on an auto-sampler. Method blanks, certified reference tissues (Dorm-3 and Dolt-4, National Research Council Canada), and in house standards (BT-Cnt2L and W-CntVG) were also analyzed for every 30 samples as quality assurance. Sample moisture contents were determined gravimetrically.

PCB concentrations were determined using an Agilent 6890 Series Plus gas chromatograph (GC) equipped with a ^{63}Ni -micro electron capture detector and an Agilent 7683 auto sampler, and a $60\text{ m} \times 0.25\text{ mm} \times 0.10\text{ }\mu\text{m}$ DB-5 capillary column. The PCB analysis method is described in Li et al. (2015). A small aliquot of whole fish

homogenate (approximately 0.5 g) was weighed, and added to a glass mortar with 15 g of activated Na₂SO₄. After being ground with a glass pestle, the mixture was packed into a micro extraction column with 25 mL of 1:1 mixture of dichloromethane:hexane (DCM:HEX) extraction solvent. Each column was spiked with 35 ng PCB 34 as a recovery standard. The column was eluted after one hour, followed by adding another 15 mL of DCM:HEX. Sample lipid contents were determined gravimetrically using 10% of the extraction volume. Clean-up of sample was completed by activated Florisil, followed by concentration to a volume of 1 mL for GC-ECD analysis. Internal standard (PCB34), a method blank (sodium sulfate) and an in-house tissue reference sample (Detroit River carp [*Cyprinus carpio*]) were also co-analyzed for every six samples as quality assurance. The PCB concentration of each sample was corrected by its corresponding method blank. The mean relative percent difference from the in-house tissue reference sample was 16±9%, and PCB 34 recoveries averaged 73±15%.

The stable isotopes analysis method was described in Burtnyk et al. (2009).

Approximately 1 g of whole fish homogenate was freeze-dried for 48 h, then ground into a fine powder with a glass mortar and pestle. Lipids were removed by 2:1 v/v chloroform:methanol. Then, the sample was allowed to dry in the fume hood with the caps removed for 24-48 hrs. Approximately 2 mg of the dried and lipid extracted material was weighed and put into a tin capsule. An elemental analyzer (Costech, Valencia, CA, USA) as well as a ThermoFinnigan Delta^{Plus} mass spectrometer (ThermoFinnigan, San Jose, CA, USA) were used for determination of δ¹⁵N and δ¹³C values. Ratios (R) of heavy to light nitrogen or carbon in the sample relative to that of the standard material was calculated as follows: δ¹⁵N or ¹³C = 1000 * [R_{sample} / R_{standard} - 1] (R = ¹⁵N:¹⁴N or

$^{13}\text{C}:^{12}\text{C}$). An internal lab standard of tilapia muscle and also NIST1577c (standard bovine liver) reference material were also analyzed for every 10 samples. The mean differences from the certified values were ≤ 0.14 ‰ and ≤ 0.04 ‰ for $\delta^{15}\text{N}$ and $\delta^{13}\text{C}$, respectively. Based on previous studies, changes in nitrogen stable isotope signatures were used as indicators of changes in the diets of fish populations with age (Post, 2002), and changes in carbon stable isotopes were used as indicators of habitat changes (Escobar-Briones et al. 1998).

4.2.3 Age Determination

The procedures for age determination are described in Burtnyk et al. (2009). The sagittal otoliths were removed from individual fish, then cleaned by forceps and distilled water. The otoliths were polished from both anterior and posterior directions toward the core using coarse (120 grit, 115 mm) and fine (3 mm) sandpaper (Ali Industries Incorporated, Fairborn, Ohio) until the annuli were readable under microscope. Fish age was determined by counting the annuli on the otolith of each fish. All otoliths were evaluated double blind by three individuals to avoid bias. Literature-based length at age ranges for Bluegill (Scott and Crossman, 1973) was also used for age estimation when there were discrepancies among the readers. For fish where no annulus could be identified from the otolith, age was defined as young of the year (YOY).

4.2.4 Model Simulations

4.2.4.1 Water Temperature

An annual water temperature cycle was estimated for each of the five lakes based on local air temperature, due to the unavailability of *in situ* field data. Daily air temperatures from November 2015 to October 2016 in the closest city for each lake were obtained from on-line weather reports. Because the littoral zone responds faster to air temperature changes than the whole lake, and Bluegill are mainly present in this area (McCobie, 1959; Wilson et al. 1996), average air temperature over 10 days was used as a proxy of littoral water temperature with some modification. The maximum and the minimum water temperature were each set to 28 °C and 1 °C, respectively. A polynomial function was fitted to the 10 d averaged temperature pattern for the 2015-2016 annual cycle for each lake, and then the function was used to predict daily water temperature within a year. The daily water temperature curve was repeated for five years to generate a five year littoral water temperature profile for each lake. The sampling date of each lake was set to day 0 for the corresponding lake simulations.

4.2.4.2 Growth Model

Two growth scenarios were established for fish from each location. Scenario 1 was based on the whole body growth measured in each population. The proportion of lean dry protein (excluding moisture and lipid content (Li et al. 2015)) and lipid was assumed to be constant and scaled to measured changes in whole body weight observed for each population and year class. Fish growth is dependent on water temperature (Berg and Bremset, 1998), and therefore daily growth was apportioned such that the highest daily growth was achieved during the summer periods of warmest water temperatures and slowest during the winters (Chezik et al. 2013). The whole body daily growth increment ($\Delta W_{wb,d}$; g) was calculated for each age class and population, such that:

$$\Delta W_{wb,d} = \left(\bar{W}_{wb,y+1} - \bar{W}_{wb,y} \right) \cdot \left(\frac{T_d}{\sum_{d=1}^{365} T_d} \right) \quad (4.1)$$

where $\bar{W}_{wb,y+1}$ and $\bar{W}_{wb,y}$ are the mean body weights (g) of fish from a given population for the next age class and mean body weight (g) of fish from the same lake for the current age class being simulated, T_d is the water temperature ($^{\circ}\text{C}$) for the day of year of the simulation derived from the water temperature submodel and $\sum_{d=1}^{365} T_d$ is the cumulative degree days over a model year for a given lake. For each population, the mean % lipid and % lean dry protein across fish samples from a given population were computed and applied to the daily whole body weight increment determined from Eq. 4.1 to compute the daily change in lipid and protein pool weights.

Scenario 2 allowed lipid and protein composition to vary according to measured changes in proximate tissue composition between year classes in each population. Whole body weight growth changes were measured according to the same procedure described in Eq. 4.1. Daily growth increments of lipids ($\Delta W_{lip,d}$) and protein ($\Delta W_{pro,d}$) were generated in an analogous fashion to whole body weight increments. Thus for lipids, the daily weight increment was given as:

$$\Delta W_{lip,d} = \left(\bar{W}_{lip,y+1} - \bar{W}_{lip,y} \right) \cdot \left(\frac{T_d}{\sum_{d=1}^{365} T_d} \right) \quad (4.2)$$

where $\bar{W}_{lip,y+1}$ and $\bar{W}_{lip,y}$ are the mean total lipid weights (g) of fish from a given population for the next age class and mean total lipid weight (g) of fish from the same lake for the current year class of simulation. An identical procedure was used to estimate daily weight increments ($\Delta W_{pro,d}$) of lean dry protein.

The daily growth rate of lean dry protein ($k_{g,pro}$) and lipid weight ($k_{g,lip}$) was also determined using the same procedure, according to:

$$k_{g,lip} = \frac{W_{lip,d+1} - W_{lip,d}}{t \cdot W_{lip,d}} \quad (4.3)$$

4.2.4.3 Bioenergetic Model

The Wisconsin bioenergetic model for Bluegill was applied to predict daily food consumption rates, gill ventilation volumes, and fecal production rates for each day of the simulation. The model was similar to that described by Drouillard et al. (2009), with a few changes in the algorithm based on the Bluegill physiological parameters. Food consumption rates (C ; $\text{kJ g}^{-1} \text{d}^{-1}$) were calculated according to:

$$C = \frac{(G_L + G_P) + R \cdot D_{O_2} + SDA + U}{E_C} \quad (4.4)$$

where G_L is growth of somatic lipid ($\text{kJ g}^{-1} \text{d}^{-1}$), G_P is growth of somatic protein ($\text{kJ g}^{-1} \text{d}^{-1}$; measured as lean dry weight), R is specific rate of respiration ($\text{g g}^{-1} \text{d}^{-1}$), D_{O_2} is the oxy-calorific coefficient for converting oxygen respired to energy of fish ($14.30 \text{ kJ g}^{-1} \text{O}_2$; Norstrom et al. 1976), SDA is the specific dynamic action ($\text{kJ g}^{-1} \text{d}^{-1}$), U is energy lost to excretion ($\text{kJ g}^{-1} \text{d}^{-1}$), and E_C is the energy assimilation efficiency from food (unitless).

G_L and G_P were calculated based on the aforementioned growth models by multiplying the energy value of the corresponding tissue with the daily weight increment estimated for each tissue type. Lipid carries an energetic value of 39.3 kJ g⁻¹ and protein carries an energetic value of 18.0 kJ g⁻¹ (Drouillard et al 2009).

R is calculated using Equation 2 of the Wisconsin bioenergetic model version 3 (Hanson et al. 1997) described for Bluegill and is summarized as follows:

$$R = 0.0154 \cdot W_{wb,d}^{-0.2} \cdot \left[\left(\frac{36 - T_d}{9} \right)^{2.04} e^{\left\langle 2.04 \left(1 - \left(\frac{36 - T_d}{9} \right) \right) \right\rangle} \right] \cdot A \quad (4.5)$$

where $W_{wb,d}$ is fish body weight for a given day (g), A is activity multiplier (unitless), which is usually between 1 to 2 ($A=1, 1.5,$ and 2 were each applied in this study to simulate 3 activity levels). SDA and U were estimated from the following equations:

$$SDA = 0.172 \cdot (R \cdot D_{O_2} + |G_L| + |G_P|) \quad (4.6)$$

$$U = 0.0253 \cdot T_d^{0.58} \cdot e^{-0.299} \cdot (R \cdot D_{O_2} + |G_L| + |G_P|) \quad (4.7)$$

E_C was estimated for the diet according to Arnot and Gobas (2004):

$$E_C = \frac{39.3 \cdot X_{L,D} \cdot E_L + 18.0 \cdot X_{P,D} \cdot E_P}{ED_{Food}} \quad (4.8)$$

where $X_{L,D}$ and $X_{P,D}$ refer to the mass fraction of lipid and protein in the diet (unitless, assumed to be equal to the YOY composition), E_L and E_P are assimilation efficiencies of dietary lipid and protein (unitless, $E_L=0.92$ and $E_P=0.60$ were applied according to Arnot and Gobas, 2004), the coefficients 39.3 and 18.0 are the energy density (kJ g⁻¹) of lipid and protein, and ED_{Food} is the total energy density (kJ g⁻¹) of food, which is calculated as:

$$ED_{Food} = 39.3 \cdot X_{L,D} + 18.0 \cdot X_{P,D} \quad (4.9)$$

The consumption rate from Eq 4.4 is converted into a mass flow (Q_C ; g food $g^{-1} d^{-1}$) by considering the energy density (ED_{Food} ; kJ g^{-1}) of consumed food;

$$Q_C = \frac{C}{ED_{Food}} \quad (4.10)$$

The fecal egestion rate (Q_{EX} ; g feces $g^{-1} d^{-1}$) and gill ventilation rate (Q_V ; mL $g^{-1} d^{-1}$) are required as inputs to the toxicokinetic submodel for PCB simulation. Q_{EX} and Q_V are calculated as:

$$Q_{EX} = Q_C \cdot (1 - (X_{L,D} \cdot E_L + X_{P,D} \cdot E_P)) \quad (4.11)$$

$$Q_V = \frac{R \cdot D_{O_2} + SDA + U}{D_{O_2} \cdot C_{O_2} \cdot E_{O_2} \cdot W_{wb,d}} \quad (4.12)$$

where C_{O_2} is the concentration of oxygen dissolved in water (g O_2 mL $^{-1}$) and E_{O_2} is the oxygen extraction efficiency (0.60 unitless; McKim et al. 1985) across the gills. Oxygen concentrations were assumed to be saturated and estimated by:

$$C_{O_2} = \frac{14.45 - 0.413 \cdot T_d + 5.56 \times 10^{-3} \cdot T_d^2}{1000000} \quad (4.13)$$

4.2.4.4 Toxicokinetic Model

Because Hg uptake from water only represents 0.1% of the Hg accumulated in fish, aqueous uptake is considered negligible (Hall et al. 1997). The daily change in Hg concentration was modeled by:

$$\frac{dC_P}{dt} = \frac{C_{d,Hg} \cdot Q_C \cdot W_{wb,d} \cdot AE_{Hg}}{W_{pro,d}} - (k_{tot} + \frac{\Delta W_{pro,d}}{W_{pro,d}}) \cdot C_P \quad (4.14)$$

where C_P is the Hg lean dry weight concentration (ng g^{-1}) in the animal, $C_{d,Hg}$ is the Hg concentration in fish diet (ng g^{-1}), AE_{Hg} is the Hg assimilation efficiency (unitless), and k_{tot} is the whole body Hg elimination rate coefficient ($\text{g g}^{-1} \text{d}^{-1}$).

The AE_{Hg} was set equal to 90% (Leaner and Mason, 2004, Li et al. 2015). $C_{d,Hg}$ of each site was estimated using Hg concentration of YOY from the corresponding site divided by a biomagnification factor (BMF). A calibrated BMF for each location was estimated using Hg concentration of YOY divided by the model best fit $C_{d,Hg}$, which was obtained by fitting $C_{d,Hg}$ into the bioaccumulation model to achieve the best fit to field data.

Calibrated BMFs from each lake were combined to generate a mean Bluegill BMF. The mean inter-lake BMF was then used for each lake to estimate lake specific $C_{d,Hg}$ values as the model input. k_{tot} for multiple species were taken from previous lab studies (Trudel and Rasmussen, 1997), and the routine metabolic rate for each species was estimated by the Wisconsin bioenergetic model. The ratios of the k_{tot} to the metabolic rate were calculated for each species, and the mean ratio of k_{tot} to the metabolic rate combining with the routine metabolic generated in this study was used to estimate the k_{tot} for Bluegill. The estimated conversion factor for Bluegill was treated as:

$$k_{tot} = ((G_L + G_P) + R \cdot D_{O_2} + SDA + U) \cdot 0.0659 \quad (4.15)$$

For PCB, according to the uptake and elimination mechanisms, the daily change in PCB concentration is:

$$\frac{dC_L}{dt} = \frac{C_{d,PCB} \cdot Q_C \cdot W_{wb,d} \cdot AE_{PCB} + C_w \cdot W_{wb,d} \cdot Q_V \cdot E_w}{W_L} - (k_2 + k_{EX} + \frac{\Delta W_L}{W_L}) \cdot C_L \quad (4.16)$$

where C_L is the lipid equivalent PCB concentration (ng g^{-1} lipid) in the animal, $C_{d,PCB}$ is the PCB concentration in fish diet (ng g^{-1}), Q_C is the consumption rate ($\text{g food g}^{-1} \text{d}^{-1}$) from Eq. 4.12, AE_{PCB} is the PCB assimilation efficiency (unitless), ΔW_L is the daily change of lipid equivalent weight (g), W_L is the lipid equivalent weight of the animal (g), C_w is the PCB concentration in water (ng g^{-1}), Q_V is the gill ventilation rate ($\text{m g}^{-1} \text{d}^{-1}$) from Eq. 4.14, E_w is the chemical exchange efficiency across the gills (unitless), and k_2 and k_{EX} refer to mass elimination rate constants (d^{-1}) for chemical depuration across the gills and feces.

The AE_{PCB} was set equal to 60% (Liu et al. 2010). $C_{d,PCB}$ of each location was calibrated using PCB concentration of YOY from the corresponding site divided by a BMF. The BMF was obtained by the same procedure as for Hg. Since kinetics rates are usually related to the body size, small fish with relatively high growth rate and elimination rate are more likely to achieve steady state (Mackay, 1982; Paterson et al. 2007). Under the assumption that PCB lipid concentration in YOY fish ($C_{YOY,PCB}$) is at thermodynamic equilibrium with water PCB concentration, C_w is calculated according to:

$$C_w = \frac{C_{YOY}}{K_{OW}} \quad (4.17)$$

where K_{OW} is octanol/water partition coefficient of the chemical (unitless). The gill elimination rate constant is calculated as:

$$k_2 = \frac{E_w \cdot Q_V}{K_{BW}} \quad (4.18)$$

where K_{BW} is the biota/water partition coefficient (unitless), which is estimated as:

$$K_{BW} = X_{L,B} \cdot K_{OW} + 0.05 \cdot X_{P,B} \cdot K_{OW} \quad (4.19)$$

where $X_{L,B}$ and $X_{P,B}$ is the fraction of lipid and lean dry protein in the animal (unitless). The lean dry protein partitioning capacity was 5% of the lipid partitioning capacity according to Debruyne et al. (2007). The recommended algorithm for estimating E_w is given as:

$$E_w = \left(1.85 + \frac{155}{K_{OW}}\right)^{-1} \quad (4.20)$$

Fecal elimination rate constants (k_{EX}) were estimated by:

$$k_{EX} = \frac{E_{EX} \cdot Q_{EX}}{K_{B,EX}} \quad (4.21)$$

where E_{EX} is the PCB organism/fecal exchange efficiency (assumed to be equal to AE_{PCB}), Q_{EX} is derived from Eq. 4.13, and $K_{B,EX}$ is the biota/feces partition coefficient (unitless).

$$K_{B,EX} = \frac{X_{L,B} + 0.05 \cdot X_{P,B}}{X_{L,EX} + 0.05 \cdot X_{P,EX}} \quad (4.22)$$

where $X_{L,EX}$ and $X_{P,EX}$ is the fraction of lipid and lean dry protein in the feces (unitless).

4.2.5 Data Analysis

PCB concentrations are expressed on a lipid-equivalent weight basis. PCB congeners included in the analysis consisted of only those congeners where detection occurred in more than 60% of the samples collected from all lakes. THg concentrations were expressed in units of ng g^{-1} lean dry weight. Because most of the THg (>95%) in fish is

MeHg (Bloom 1992), this study assumed that THg concentration equals MeHg concentration.

Analysis of variance (ANOVA) was used to test for differences among sampling sites in Hg concentration and PCB concentration. Linear regression analysis was performed with ANOVA to test whether total wet weight, lean dry weight, lipid weight, THg concentration, PCB concentration, and carbon and nitrogen stable isotope values were significantly related to fish age. Linear regression was also performed with ANOVA between measured and predicted chemical concentrations. T-tests were used to test if the constant was significantly different from 0, and if slope was significantly different from 1. The significance level of the slope combined with the R square value of the linear regression were used as indicators for evaluating the performance of the model simulations. Prior to using parametric tests, normality and homogenous variance were tested by Kolmogorov-Smirnov and Levene's tests. Data that failed the normality test were \log_{10} transformed. All statistical analyses were performed using IBM SPSS version 20 (IBM Corp., USA).

4.3 Results

4.3.1 Hg and PCB Concentrations in Bluegill

As shown in Table 4.1, the total length of Bluegill from five waterbodies ranged from 2.6 to 18.3 cm with an average of 8.3 cm across populations and age classes. Significantly higher mean total length was found in Bluegill from the most southern lake, Lake Hartwell, compared with fish from northern lakes including Apsey Lake and Sharbot Lake (ANOVA, $p < 0.05$). The Bluegill body weights from five waterbodies ranged from

0.2 to 130.9 g with an average of 14.2 g across populations and age classes. The mean body weights of Bluegill from the Detroit River and Lake Hartwell were significantly higher compared with those from Apsey Lake and Sharbot Lake (ANOVA, $p < 0.05$). These results indicate that Bluegill from southern waterbodies tended to have larger body sizes than those from northern waterbodies.

The THg lean dry weight concentration was positively related to age for fish from Apsey Lake, Sharbot Lake, Stonelick Lake, and Lake Hartwell (linear regression, $p < 0.05$), but no significant relationship between THg lean dry concentration and age was found for fish from Detroit River. For PCBs, there were positive relationships between the sum PCB lipid-equivalent concentration and age for fish from Detroit River and Lake Hartwell (linear regression, $p < 0.05$), but no significant relationship between sum PCB lipid-equivalent concentration and age for fish from Apsey Lake, Sharbot Lake, and Stonelick Lake. Our results showed changes in both chemical concentration and mass with time, indicating that chemical accumulation in these fish did not achieve steady state across the age groups sampled.

4.3.2 Whole Body and Proximate Tissue Growth

Table 4.2 summarizes the total wet weight growth with age, as well as changes in lipid fraction and lean dry weight fraction for two growth scenarios. For fish from all locations, the whole body weights were linearly related to age (linear regression, $p < 0.05$). The annual growth rates of fish wet weight were higher in early life stages, and then shifted to a slower growth as fish aged. Table 4.2 also illustrated the average tissue composition of Bluegill from each lake for two growth scenarios. Scenario 1 assumed the tissue growth

was constantly proportional to whole body growth at all ages. The mean lipid percentages were $3.28 \pm 0.19\%$, $3.95 \pm 0.75\%$, $3.72 \pm 0.22\%$, $3.40 \pm 0.15\%$, and $1.78 \pm 0.14\%$, and the lean dry weight percentages were $22.51 \pm 0.33\%$, $22.30 \pm 0.22\%$, $23.81 \pm 0.30\%$, $22.92 \pm 0.24\%$ and $22.47 \pm 0.21\%$ for fish across ages classes from Apsey Lake, Sharbot Lake, Detroit River, Stonelick Lake and Lake Hartwell, respectively.

For scenario 2, the tissue to whole body ratios were measured for each age class of each population. There were significant differences in lipid to whole body ratios among age classes for fish from Apsey Lake, Detroit River, and Stonelick Lake (ANOVA, $P < 0.05$). For Apsey Lake and Detroit River, the lipid proportion was significantly higher for 0-1 year old fish compared with that of 5 year old fish; for fish from Stonelick Lake, significantly higher lipid fractions were found in 3-4 year old fish compared with 5 year olds. There were no significant differences in lean dry weight fractions between ages for fish from four of the five lake populations except for the Detroit River. In the case of the Detroit River, the lean dry weight proportion was significantly higher for 1-2 year old fish compared with 5 year old fish.

4.3.3 Carbon and Nitrogen Stable Isotope Signature

$\delta^{15}\text{N}$ and $\delta^{13}\text{C}$ signatures of fish populations from the five lakes are presented in Table 4.1. The mean (\pm SD) $\delta^{13}\text{C}$ values were $-20.34 \pm 1.08\text{‰}$, $-28.08 \pm 1.43\text{‰}$, $-15.96 \pm 3.04\text{‰}$, $-25.80 \pm 0.71\text{‰}$, and $-25.94 \pm 1.50\text{‰}$ for Apsey Lake, Sharbot Lake, Detroit River, Stonelick Lake, and Lake Hartwell, respectively. No significant relationships were found between $\delta^{13}\text{C}$ signature and age of fish from four of the five lakes except for the Detroit

River (linear regression, $p > 0.05$) where a significantly negative relationship between $\delta^{13}\text{C}$ and age was observed, implying habitat shift for these fish.

The mean (\pm SD) $\delta^{15}\text{N}$ values were $8.36 \pm 0.51\text{‰}$, $9.34 \pm 0.46\text{‰}$, $10.73 \pm 0.91\text{‰}$, $11.81 \pm 0.57\text{‰}$, and $10.61 \pm 1.20\text{‰}$ for Apsey Lake, Sharbot Lake, Detroit River, Stonelick Lake, and Lake Hartwell, respectively. For Sharbot Lake, no significant relationship was observed between $\delta^{15}\text{N}$ signature and age (linear regression, $p > 0.05$). For fish from Apsey Lake, Detroit River, and Stonelick Lake, the $\delta^{15}\text{N}$ values were positively related to age (linear regression, $p < 0.05$). However, a negative relationship was observed between the $\delta^{15}\text{N}$ values and age for fish from Lake Hartwell (linear regression, $p < 0.05$). The $\delta^{13}\text{C}$ signatures suggested that there might be a habitat shift for fish from Detroit River as they age, and the $\delta^{15}\text{N}$ signature suggested that there was slight trophic level shift for fish from Apsey Lake, Detroit River, Stonelick Lake, and Lake Hartwell. Overall the isotope data provides support for ontogenetic diet shifts by the different fish populations, which could translate into differences in prey composition and contamination as a function of fish age.

4.3.4 Model Simulations

THg and PCB concentrations were simulated using each of the two growth scenarios and toxicokinetic parameters developed from previous studies. For PCB simulations, PCB 180 was used as a representative congener as a result of its high hydrophobicity and commonality in elimination rate coefficient compared to THg (Li et al. 2015). To examine the goodness of fit of each growth scenario model, linear regression was performed between the measured chemical concentrations and modeled chemical

concentrations (only A=1.5 was considered). The chemical concentrations were log 10 transformed to conform to normal distribution.

Figure 4.2 presents linear regressions between measured and predicted Hg and PCB 180 concentrations at each location. The linear regression equation was $y=0.9916x-0.0315$ ($R^2=0.88$, $p<0.05$) for growth scenario 1, and $y=0.988x-0.0197$ ($R^2=0.89$, $p<0.05$) for growth scenario 2. The constant in both regressions was not significantly different from 0 (t-test, $p>0.05$), and the slope was not significantly different from 1 (t-test, $p>0.05$), which indicated a relatively high predictive ability of the model under both growth scenarios. However, there were some outliers in Figure 4.2, which belonged to Detroit River (PCBs) and Lake Harwell (both contaminants), indicating the model generated relatively poor predictions for these locations ($p>0.05$, ANOVA).

Table 4.3 summarizes linear regression equations of measured and predicted concentrations for each chemical from each location. For Hg, the two growth scenarios provided similar results for all locations except for the Detroit River. Growth scenario 2 provided a better prediction compared with growth scenario 1 for the latter population. For PCB 180, both growth scenarios showed relatively poor predictive power ($p>0.05$, ANOVA) for Sharbot Lake, Detroit River, and Lake Hartwell. However, growth scenario 2 improved the model predictions, or R square value, compared with growth scenario 1 for Apsey Lake and Stonelick Lake ($p<0.05$, ANOVA). Thus, growth scenario 2 provided relatively better prediction in some lake systems.

Figure 4.3 summarizes modeled THg and PCB bioaccumulation trajectories and data fit using growth scenario 2. To better demonstrate the bioaccumulation trend of each

population regardless of their baseline chemical levels, the chemical concentration of each fish was divided by the mean chemical concentration of YOY fish (C_0) from its own sampling site.

Under the simulations for Hg, $C_{0,Hg}$ was 25.12, 47.68, 103.18, 29.36, and 19.98 ng g⁻¹ wet weight for Apsey Lake, Sharbot Lake, Detroit River, Stonelick Lake and Lake Hartwell, respectively. Based on the best fit $C_{d,Hg}$ of each sampling site, the mean BMF ($C_{0,Hg}/C_{d,Hg}$) across all locations was 1.79. Therefore, $C_{d,Hg}$ was estimated as 14.06, 26.69, 57.75, 16.44 and 11.18 ng g⁻¹ wet weight for Apsey Lake, Sharbot Lake, Detroit River, Stonelick Lake, and Lake Hartwell, respectively. Using three activity levels (Figure 4.3), the model was generally able to bracket field-collected Hg data for fish from Apsey Lake, Sharbot Lake, and Detroit River, but not for Stonelick Lake and Lake Hartwell. For Stonelick Lake, the model overestimated the Hg concentration for 2 year old fish, and underestimated the Hg concentration for 3-5 year old fish. For Lake Hartwell, the model underestimates Hg concentration for all age class.

In general, the fraction of assimilated Hg retained by fish decreased with age across all locations (Table 4.4). The cumulative (lifetime) proportion of dietary Hg that was retained by a 5 year old fish was 20.91%, 23.45%, 26.42%, 19.84%, and 14.99% for Apsey Lake, Sharbot Lake, Detroit River, Stonelick Lake, and Lake Hartwell, respectively. The ratios of $k_{g,pro}/k_{tot}$ ranged from 0.02 to 0.79 for Apsey Lake, from 0.04 to 1.06 for Sharbot Lake, from 0.06 to 0.88 for Detroit River, from 0.06 to 0.80 for Stonelick Lake, and from 0.11 to 0.45 for Lake Hartwell. This indicated that growth dilution in many cases approached, and in some cases exceeded, the magnitude of k_{tot}

implying the growth dilution is important for regulating Hg bioaccumulation compared with other elimination routes.

Under the PCB simulation, the $C_{0,PCB}$ values were 0.10, 0.18, 0.54, 0.27, and 28.39 ng g⁻¹ wet weight, and $C_{d,PCB}$ values were estimated as 0.06, 0.10, 0.30, 0.15, and 15.89 ng g⁻¹ wet weight for Apsey Lake, Sharbot Lake, Detroit River, Stonelick Lake, and Lake Hartwell, respectively. The PCB simulations were generally well fitted to the field collected data for all sampling locations except for fish from the Detroit River and Lake Hartwell. For the Detroit River, the model predicted a slow increase while the field data showed a faster bioaccumulation rate. For Lake Hartwell, the model overestimated the PCB 180 concentration for all age classes.

Similar to Hg, the fraction of assimilated PCB 180 retained by fish decreased with age across all locations (Table 4.4). The lifetime cumulative fraction of assimilated PCB 180 retained by a 5 year old fish was 21.39%, 33.63%, 32.73%, 23.09%, and 14.96% for Apsey Lake, Sharbot Lake, Detroit River, Stonelick Lake, and Lake Hartwell, respectively. The cumulative percentage of assimilated PCB 180 retained by fish was generally higher than that of Hg for all location except for Lake Hartwell. The ratio of $k_{g,lip} / k_{tot}$ ranged from -0.10 to 1.28 for Apsey Lake, from 0.09 to 2.08 for Sharbot Lake, from 0.05 to 1.36 for the Detroit River, from -0.34 to 1.46 for Stonelick Lake, and from 0.01 to 0.37 for Lake Hartwell. In general, growth dilution plays a major role in regulating PCB bioaccumulation rates as $k_{g,lip}$ became a dominant elimination pathway (pseudo-elimination) during the growing seasons ($k_{g,lip} / k_{tot} > 1$). However, growth played a less important role in PCB bioaccumulation compared with other PCB elimination

pathways for fish from Lake Hartwell which had the lowest lipid content of all fish populations examined.

4.4 Discussion

This study simulated PCB and Hg concentrations in Bluegill using a combined toxicokinetic and bioenergetics model. The simulations were performed under two growth scenarios. Growth scenario 1 required measurements for total growth rate, and growth scenario 2 required measurements for tissue specific growth rate. The results showed that growth scenario 2 provided improved predictions for Hg in fish from Detroit River (44% improved R^2 ; Table 4.3), as well as for PCBs in fish from Stonelick Lake (45% improved R^2). However, the two growth scenarios were nearly identical in their predictive power for Hg and PCB for most other locations. This could be a result of high variance in protein growth (protein to whole body weight ratio) of fish from the Detroit River and in lipid growth (lipid to whole body weight ratio) of fish from Stonelick Lake and Apsey Lakes. The tissue composition from other locations did not exhibit large differences between age classes, which minimized model predicted differences between the two growth scenarios. This study demonstrated that using lipid and lean dry protein growth rate could improve the accuracy of model outcomes, while previous studies usually adopt whole body growth rate in Hg and PCB bioaccumulation models (Trudel and Rasmussen, 2006; Drouillard et al. 2009). However, improvement of growth scenario 2 over scenario 1 will only be apparent in populations where proximate tissue growth shows distinct differences compared to whole body growth between age classes. Extending validation data sets to older age classes where growth performance is expected

to slow even more or to lake populations experiencing resource shortage stress would be useful for further discriminating against the two growth scenarios.

In this study, the k_g / k_{tot} ratio was generally higher for PCB simulations in comparison with Hg simulations. This indicated that growth dilution was a more important process for PCB accumulation compared with Hg accumulation. In addition, $k_{g,lip}$ exhibited much higher variation compared with $k_{g,pro}$ among populations and age classes. Among the age classes of each lake, coefficients of variation for lean dry weight to whole body weight ratios were 0.09, 0.07, 0.09, 0.07, and 0.07, while coefficients of variation for lipid weight to whole body weight ratios were 0.38, 0.19, 0.43, 0.31 and 0.61 for Apsey Lake, Sharbot Lake, Detroit River, Stonelick Lake, and Lake Hartwell, respectively. Moreover, higher variabilities in PCB 180 concentration were observed in comparison with Hg concentration. Among the age classes, the coefficients of variation for Hg concentration were 0.40, 0.21, 0.22, 0.55, and 0.52, whereas the coefficients of variation for PCB concentration were 0.66, 1.21, 1.38, 0.77, and 0.47 for Apsey Lake, Sharbot Lake, Detroit River, Stonelick Lake, and Lake Hartwell, respectively. Because lipid and lean dry protein represent the storage compartments for PCB and Hg respectively, our results suggested that high variabilities in PCB concentrations were partially a result of the highly variable lipid growth rates compared to protein.

Typically, lean dry protein represents a larger fraction of the total body weight of fish, whereas lipid represents a much smaller fraction of body weight and is expected to undergo wider fluctuations across ages and on a seasonal basis compared to protein (Paterson et al. 2007). Therefore, PCB concentrations in fish are expected to fluctuate much more compared with Hg concentrations in general. In this study, the goodness of fit

tests for Hg were much closer to a 1:1 line compared with that of PCBs (Figure 4.2), which indicated that the model outcome for Hg was more accurate compared with PCB 180. This also could be attributed to higher variability in individual lipid growth within and among age classes of fish.

For the present simulations, it was assumed that the fish diet was constant across age classes in each lake and could be estimated from YOY fish concentrations reflective of baseline inputs to each lake. Thus, model simulations accounted for body size and temperature related changes in both feeding rate and age class specific growth/proximate composition but had not considered variability in prey contamination or diet shifts with age. Overall, accounting for population specific growth and applying a constant diet concentration explained more than 80% of the variation ($R^2=0.89$) in chemical bioaccumulation for different age classes of Bluegill and lakes (Figure 4.2) and a mean explained variation of 83% for Hg and 78% for PCBs, respectively. The Bluegill was selected as a model fish species in the present research because of their strong littoral affiliation and dependence on littoral benthic invertebrates as diet items for most of their lives. This is consistent with past literature. Burtnyk et al. (2009) found no significant differences in either carbon or nitrogen stable isotope signatures between age classes (2-5) of Bluegill from Sharbot Lake. Paterson et al. (2006) observed no major shifts in diet for Bluegill from Detroit River. However, the isotope data from the present study did provide evidence for a habitat shift in fish populations from Detroit River, and diet shifts for fish from Apsey Lake, Detroit River, Stonelick Lake, and Lake Hartwell.

The above changes in diet could lead to changes in prey contamination levels with age, leading to relatively poor predictive power of the model in some of the lake systems

tested. Indeed, the model generated the poorest predictions for Lake Hartwell (both contaminants) and the Detroit River (PCBs) suggesting that diet shifts and associated prey contamination changes may have been as, or more, important to observed bioaccumulation rates than fish growth for these locations. In the case of PCB 180 in the Detroit River, the model fit could be improved by applying an increasing diet concentration with age rather than the constant diet concentration used in the model simulations. In the case of Lake Hartwell, the nitrogen isotope signature suggested a decrease in trophic level with increasing age of fish, while the PCB concentrations tended to decline with age for this population. Lake Hartwell and the Detroit River are also known to be contaminated systems. Lake Hartwell is a Superfund site owing to PCB releases from a capacitor manufacturer near Pickens, SC (Bzdusek, et al. 2006) while the Detroit River is designated as a Great Lakes Area of Concern with both PCBs and Hg listed as priority pollutants (Drouillard et al. 2006; Szalinska et al. 2006). Thus, diet shifts and heterogeneous contamination across diet concentrations are more likely to occur for fish from these systems. Contaminant concentrations tend to be patchy and spatially variable at more contaminated sites, so even small scale movements by fish within the site could profoundly affect their contaminant concentrations and our ability to model them (McLeod et al. 2015). Future study on contaminant levels in Bluegill food items across age classes would be necessary to improve the model inputs, particularly for Detroit River and Lake Hartwell and to further validate the model for these populations. Moreover, energy costs associated with reproduction also needs to be accounted for, which could further improve the accuracy of model outcome.

In summary, a combined toxicokinetic and bioenergetic model that accounts for population specific differences in growth was able to provide accurate prediction of age-specific Hg and PCB concentrations in Bluegill from several populations. The relatively poor performance of the model for some locations was attributed to changes in the feeding behavior of fish and associated change in prey contamination with such diet shifts. Overall, growth and baseline prey contamination inferred from YOY fish concentrations, accounted for 80% of the variation in contaminant bioaccumulation across populations. The notable exceptions were for the Detroit River and Lake Hartwell, two known contaminated sites likely to experience higher heterogeneity in spatial contamination compared to the other systems of study. This study also examined differences in proximate tissue content with age for lean dry protein and lipids in different Bluegill populations. Lean dry protein was normally a constant proportion of the whole body weight, whereas lipids exhibited higher seasonal and annual variation leading to discrepancies in the bioaccumulation trajectories and individual variation observed for Hg and PCBs. These results support a conclusion that age specific differences in lipid growth plays a role in explaining differences in PCB bioaccumulation rates among fish populations whereas more consistent growth of lean dry protein contributes to less variation in bioaccumulation slopes for Hg in fish populations between systems.

4.5 References

- Arnot, J. A.; Gobas, F. A. P. C. A food web bioaccumulation model for organic chemicals in aquatic ecosystems. *Environ. Toxicol. Chem.* 2004, 23, 2343-2355.
- Berg, O. K.; Bremset, G. Seasonal changes in the body composition of young riverine Atlantic salmon and brown trout. *J. Fish Biol.* 1998, 52(6), 1272-1288.

- Bloom, N. S. On the chemical form of mercury in edible fish and marine invertebrate tissue. *Can. J. Fish Aquat. Sci.* 1992, 49, 1010-1017.
- Escobar-Briones, E.; Alcocer, J. ; Cienfuegos, E.; Morales, P. Carbon stable isotopes ratios of pelagic and littoral communities in Alchichica crater-lake, Mexico. *Int. J. Salt Lake Res.* 1998. 7: 345-355.
- Burtnyk, M. D.; Paterson, G.; Drouillard, K. G.; Haffner, G. D. Steady and non-steady state kinetics describe polychlorinated biphenyl bioaccumulation in natural populations of Bluegill (*Lepomis macrochirus*) and cisco (*Coregonus artedi*). *Can. J. Fish. Aquat. Sci.* 2009, 66, 2189-2198.
- Bzdusek, P. A.; Christensen, E. R.; Lee, C. M.; Pakdeesusuk, U.; Freedman, D. L. PCB congeners and dechlorination in sediments of Lake Hartwell; South Carolina; determined from cores collected in 1987 and 1998. *Environ. Sci. Technol.* 2006, 40(1), 109-119.
- Chezik, K. A.; Lester, N. P.; Venturelli, P. A. Fish growth and degree-days I: selecting a base temperature for a within-population study. *Can. J. Fish. Aquat. Sci.* 2014, 71, 47-55.
- Daley, J. M.; Paterson, G.; Drouillard, K. G. Bioamplification as a bioaccumulation mechanism for persistent organic pollutants (POPs) in wildlife. *Rev. Environ. Contam. Toxicol.* 2014, 227, 107-155.
- Debruyne, A. M. H.; Gobas, F. A. P. C. The sorptive capacity of animal protein. *Environ. Toxicol. Chem.* 2007, 26, 1803-1808.
- Drouillard, K. G.; Paterson, G.; Haffner, G. D. A combined food web toxicokinetic and species bioenergetic model for predicting seasonal PCB elimination by yellow perch (*Perca flavescens*). *Environ. Sci. Technol.* 2009, 43(8), 2858-2864.
- Drouillard, K. G.; Tomczak, M.; Reitsma, S.; Haffner, G. D. A river-wide survey of polychlorinated biphenyls (PCBs), polycyclic aromatic hydrocarbons (PAHs), and selected organochlorine pesticide residues in sediments of the Detroit River—1999. *J. Great Lakes Res.* 2006, 32, 209-226.

- Gobas, F. A. P. C.; Wilcockson, J. B.; Russell, R. W.; Haffner, G. D. Mechanism of biomagnification in fish under laboratory and field conditions. *Environ. Sci. Technol.* 1999, 33, 133-141.
- Gobas, F. A. P. C.; Zraggen, M. N.; Zhang, X. Time response of the Lake Ontario ecosystem to virtual elimination of PCBs. *Environ. Sci. Technol.* 1995, 29, 2038-2046.
- Hall, B. D.; Bodaly, R. A.; Fudge, R. J. P.; Rudd, J. W. M. Rosenberg, D. M. Food as the dominant pathway of methylmercury uptake by fish. *Water, Air, and Soil Pollut.* 1997, 100, 13-24.
- Hanson, P. C.; Johnson, T. B.; Schindler, D. E.; Kitchell, J. F. "Fish Bioenergetics 3.0." University of Wisconsin Sea Grant Institute, Madison, Wisconsin.
- Holker, F.; Haertel, S. S. 2004. Application of a bioenergetics model to roach. *J. Appl. Ichthyol.* 1997, 20(6), 548-550.
- Kitchell, J. F.; Stewart, D. J.; Weininger, D. Applications of a bioenergetics model to yellow perch (*Perca flavescens*) and walleye (*Stizostedion vitreum vitreum*). *J. Fish. Res. Bd. Can.* 1977, 34(10), 1922-1935.
- Leaner, J. J.; Mason, R. P. Methylmercury uptake and distribution kinetics in sheepshead minnows, *Cyprinodon variegatus*; after exposure to CH₃Hg-spiked food. *Environ. Toxicol. Chem.* 2004, 23(9), 2138-2146.
- Li, J.; Drouillard, K. G.; Branfireun, B.; Haffner, G. D. Comparison of the toxicokinetics and bioaccumulation potential of mercury and polychlorinated biphenyls in goldfish (*Carassius auratus*). *Environ. Sci. Technol.* 2015, 49, 11019-11027.
- Liu, J.; Haffner, G. D.; Drouillard, K. G. The influence of diet on the assimilation efficiency of 47 polychlorinated biphenyl congeners in Japanese Koi (*Cyprinus carpio*). *Environ. Toxicol. Chem.* 2010, 29, 401-409.
- Mackay, D. Correlation of bioconcentration factors. *Environ. Sci. Technol.* 1982, 16(5), 274-278.

- Madenjian, C. P.; O'Connor, D. V.; Pothoven, S. A.; Schneeberger, P. J.; Rediske, R. R.; O'Keefe, J. P.; Bergstedt, R. A.; Argyle, R. L.; Brandt, S. B. Evaluation of a lake whitefish bioenergetics model. *Trans. Am. Fish. Soc.* 2006, 135(1), 61-75.
- Mason, R. P.; Reinfelder, J. R.; Morel, F. M. M. Bioaccumulation of mercury and methylmercury. *Water, Air, and Soil Pollut.* 1995, 80, 915-921.
- McCombie, A. M. Some relations between air temperatures and the surface water temperatures of lakes. *Limnol. Oceanogr.* 1959, 4(3), 252-258.
- McIntyre, J. K.; Beauchamp, D. A. Age and trophic position dominate bioaccumulation of mercury and organochlorines in the food web of Lake Washington. *Sci. Tot. Env.* 2007, 372, 571-584.
- McKim, J. M.; Schmieder, P. K.; Veith, G. D. Absorption dynamics of organic chemical transport across trout gills as related to octanol-water partition coefficient. *Toxicol. Appl. Pharmacol.* 1985, 77, 1-10.
- McLeod, A. M.; Paterson, G.; Drouillard, K. G.; Haffner, G. D. Ecological implications of steady state and nonsteady state bioaccumulation models. *Environ. Sci. Technol.* 2016, 50, 11103-11111.
- McLeod, A. M.; Arnot, J. A.; Borgå K.; Selck, H.; Kashian, D. R.; Krause, A.; Paterson, G.; Haffner, G. D.; Drouillard, K. G. Quantifying uncertainty in the trophic magnification factor related to spatial movements of organisms in a food web. *Integr. Environ. Assess. Manag.* 2015, 11(2), 306-18.
- Norstrom, R. J.; McKinnon, A. E.; DeFreitas, A. S. W. Bioenergetics-based model for pollutant accumulation by fish simulation of PCB and methylmercury residue levels in Ottawa River yellow perch (*Perca flavescens*). *J. Fish. Res. Bd. Can.* 1976, 33, 248-267.
- Overturf, K.; Barrows, F. T.; Hardy, R. W.; Brezas, A.; Dumas, A. Energy composition of diet affects muscle fiber recruitment; body composition; and growth trajectory in rainbow trout (*Oncorhynchus mykiss*). *Aquaculture.* 2016, 457, 1-14.

- Paterson, G.; Drouillard, K. G.; Haffner, G. D. An evaluation of stable nitrogen isotopes and polychlorinated biphenyls as bioenergetic tracers in aquatic systems. *Can. J. Fish. Aquat. Sci.* 2006, 63, 628-641.
- Paterson, G.; Drouillard, K. G.; Haffner, G. D. PCB elimination by yellow perch (*Perca flavescens*) during an annual temperature cycle. *Environ. Sci. Technol.* 2007, 41, 824-829.
- Paterson, G.; Drouillard, K. G.; Leadley, T. A.; Haffner, G. D. Long-term polychlorinated biphenyl elimination by three size classes of yellow perch (*Perca flavescens*). *Can. J. Fish. Aquat. Sci.* 2007, 64, 1222-1233.
- Post, D. M. Using stable isotopes to estimate trophic position: models, methods, and assumptions. *Ecology*. 2002. 83(3):703-718.
- Ricker, W.E. Growth rates and models. In *Fish physiology*. Edited by W.S. Hoar; D.J. Randall; J.R. Brett. Academic Press; New York. 1979.
- Roesijadi, G. Metallothioneins in metal regulation and toxicity in aquatic animals. *Aquat. Toxicol.* 1992, 22(2), 81-114.
- Scott, W. B.; Crossman, E. J. *Freshwater fishes of Canada*. Bull. Fish. Res. Board Can. No.184. 1973.
- Simoneau, M.; Lucotte, M.; Garceau, S.; Laliberte, D. Fish growth rates modulate mercury concentrations in walleye (*Sander vitreus*) from eastern Canadian lakes. *Environ. Res.* 2005, 98(1), 73-82.
- Szalinska, E.; Drouillard, K. G.; Fryer, B.; Haffner, G. D. Distribution of Heavy Metals in Sediments of the Detroit River. *J. Great Lakes Res.* 2006, 32, 442-454.
- Trudel, M.; Rasmussen, J. B. Bioenergetics and mercury dynamics in fish, a modelling perspective. *Can. J. Fish. Aquat. Sci.* 2006, 63, 1890-1902.
- Trudel, M.; Rasmussen, J. B. Modeling the elimination of mercury by fish. *Environ. Sci. Technol.* 1997, 31, 1716-1722.
- Trudel, M.; Rasmussen, J. B. Predicting mercury concentration in fish using mass balance models. *Ecol. Appl.* 2001, 11, 517-529.

Table 4.1 Summarized biological data, total mercury (THg) concentrations, sum PCB (Σ PCB) concentrations, $\delta^{13}\text{C}$ and $\delta^{15}\text{N}$ signatures for Bluegill collected from five sampling locations across North America. Values represent mean \pm 1 standard error with data minima and maxima included in parentheses.

Sampling Location (n)	Length (mm)	Mass (g)	THg		Σ PCB		$\delta^{15}\text{N}$ (‰)	$\delta^{13}\text{C}$ (‰)
			(ng g ⁻¹ wet wt)	(ng g ⁻¹ LDW ^a)	(ng g ⁻¹ wet wt)	(ng g ⁻¹ lipid)		
Apsey Lake (41)	7.5 \pm 0.4 (3.3 – 12.5)	9.6 \pm 1.1 (0.4 – 32.8)	38.6 \pm 1.9 (16.4 – 102.3)	171.6 \pm 8.5 (72.8 – 285.1)	4.2 \pm 0.6 (1.1 – 24.6)	103.8 \pm 18.6 (21.6– 765.6)	8.4 \pm 0.5 (7.3 – 9.2)	-20.3 \pm 1.1 (-22.5 – -18.4)
Sharbot Lake (47)	7.8 \pm 0.4 (3.6 – 15.5)	10.4 \pm 1.5 (0.6 – 57.2)	62.7 \pm 1.6 (34.7 – 90.8)	289.0 \pm 8.9 (153.9 – 422.0)	4.6 \pm 1.0 (ND ^b – 44.2)	88.6 \pm 17.3 (ND – 749.7)	9.3 \pm 0.5 (8.2 – 10.1)	-28.1 \pm 1.4 (-29.3 – -23.9)
Detroit River (54)	8.5 \pm 0.5 (2.6 – 18.3)	18.5 \pm 3.3 (0.2 – 130.9)	101.9 \pm 3.0 (61.0 \pm 153.9)	433.7 \pm 14.0 (246.4 – 680.0)	26.2 \pm 2.8 (4.4 – 104.3)	604.6 \pm 70.1 (95.7 – 2916)	10.7 \pm 0.9 (9.2 – 13.1)	-16.0 \pm 3.0 (-22.5 – -11.1)
Stonelick Lake (47)	8.2 \pm 0.6 (2.9 – 17.3)	17.9 \pm 3.3 (0.2 – 100.0)	41.8 \pm 3.2 (22.3 – 160.1)	188.6 \pm 14.2 (96.6 – 606.1)	7.2 \pm 1.3 (ND – 17.1)	206.1 \pm 41.7 (ND – 2012)	11.8 \pm 0.6 (10.5 – 12.9)	-25.8 \pm 0.7 (-27.1 – -24.5)
Lake Hartwell (62)	9.6 \pm 0.4 (4.6 – 15.8)	16.9 \pm 2.0 (1.4 – 68.0)	54.7 \pm 3.6 (14.3 – 150.8)	244.7 \pm 15.6 (66.9 – 635.8)	1411.7 \pm 100.3 (115.7 – 4020)	12362 \pm 2702 (5764 – 1.1 x 10 ⁵)	10.6 \pm 1.2 (8.5 – 12.1)	-25.9 \pm 1.5 (-29.5 – -22.5)

^a LDW indicates lean dry weight.

^b ND represents non-detect.

Table 4.2 Measured total mass (mean±SE), lipid to whole body weight ratio (mean±SE), and lean dry weight (LDW) to whole body weight ratio (mean±SE) for fish of each age class from each location.

Site	Age	Scenario 1	Scenario 2 (measured in fish)					
		All ages	YOY	1	2	3	4	5
Apsey Lake	Sample size	41	11	6	5	13	3	3
	Mass (g)	--	0.78±0.13	2.75±0.09	8.41±0.77	15.44±0.69	21.48±1.20	24.94±2.69
	Lipid (%)	3.28±0.19	4.18±0.22	3.87±0.51	3.08±0.59	2.98±0.29	2.20±0.69	1.48±0.25
	LDW (%)	22.51±0.33	21.51±0.21	22.73±0.67	23.93±1.73	22.13±0.44	24.17±2.22	23.32±0.51
Sharbot Lake	Sample size	47	10	15	6	10	4	2
	Mass (g)	--	0.92±0.06	5.62±0.42	11.05±0.39	19.07±1.31	45.15±2.51	56.40±0.80
	Lipid (%)	3.95±0.75	3.90±0.15	4.10±0.23	4.06±0.16	3.95±0.31	3.55±0.38	3.64±0.61
	LDW (%)	22.30±0.22	21.68±0.15	22.84±0.44	22.25±0.35	22.23±0.70	22.26±0.47	21.98±1.14
Detroit River	Sample size	54	9	11	25	5	3	1
	Mass (g)	--	1.34±0.15	3.86±0.32	18.48±1.11	39.66±2.54	85.10±2.67	130.9
	Lipid (%)	3.72±0.22	5.08±0.41	4.41±0.60	2.99±0.24	2.96±0.72	3.58±0.21	2.57
	LDW (%)	23.81±0.30	23.50±0.57	25.73±0.93	24.24±0.38	22.00±0.91	22.92±1.01	20.04
Stonelick Lake	Sample size	47	21	6	12	5	2	1
	Mass (g)	--	1.58±0.19	6.37±0.81	28.39±1.82	51.44±2.45	75.50±3.4	100
	Lipid (%)	3.40±0.15	3.22±0.13	3.24±0.27	3.38±0.33	4.63±0.85	3.78±0.0003	1.62
	LDW (%)	22.92±0.24	22.29±0.24	23.88±0.55	23.08±0.54	23.31±1.28	24.05±0.02	22.53
Lake Hartwell	Sample size	62	9	25	15	7	2	4
	Mass (g)	--	2.49±0.18	6.72±0.47	20.98±0.97	30.67±1.88	41.65±1.45	61.53±2.31
	Lipid (%)	1.78±0.14	2.27±0.39	1.92±0.23	1.17±0.19	2.00±0.40	1.20±0.80	2.06±0.65
	LDW (%)	22.47±0.21	21.88±0.55	22.58±0.30	22.10±0.53	23.03±0.53	24.10±0.74	22.72±0.73

Table 4.3 Linear regression between predicted and observed total Hg and PCB 180 concentrations under two growth scenarios.

Sampling site	Chemical	Growth scenario 1						Growth scenario 2					
		β (slope)			α (intercept)		R square	β (slope)			α (intercept)		R square
		Value	SE	p	Value	SE		Value	SE	p	Value	SE	
Apsey Lake	Hg	0.680	0.084	0.001	0.682	0.191	0.942	0.621	0.102	0.004	0.803	0.231	0.903
	PCB	0.542	0.174	0.035	0.230	0.103	0.709	0.696	0.204	0.027	0.167	0.121	0.745
Sharbot Lake	Hg	1.052	0.198	0.006	-0.098	0.49	0.876	1.068	0.203	0.006	-0.138	0.502	0.874
	PCB	0.264	0.178	0.214	0.594	0.146	0.353	0.274	0.181	0.205	0.589	0.148	0.364
Detroit River	Hg	0.331	0.534	0.569	1.861	1.419	0.088	1.041	0.505	0.108	-0.014	1.343	0.515
	PCB	0.085	0.059	0.220	1.022	0.11	0.345	0.12	0.057	0.104	0.979	0.107	0.525
Stonelick Lake	Hg	0.413	0.185	0.090	1.337	0.437	0.554	0.421	0.168	0.067	1.31	0.397	0.61
	PCB	0.218	0.176	0.282	0.813	0.186	0.279	0.508	0.152	0.029	0.525	0.162	0.735
Lake Hartwell	Hg	0.558	0.14	0.016	0.907	0.329	0.798	0.551	0.123	0.011	0.917	0.289	0.834
	PCB	-0.179	0.331	0.617	3.687	0.963	0.068	-0.076	0.35	0.839	3.388	1.018	0.012

Table 4.4 The fraction of Hg and PCB retained for each age class under the model simulation

Location	age	Scenario 1		Scenario 2	
		Hg retained %	PCB retained %	Hg retained %	PCB retained %
Apsey Lake	1	32.19	44.09	32.32	46.51
	2	30.65	41.12	30.55	39.52
	3	25.5	35.27	25.69	32.55
	4	19.28	27.78	19.38	20.04
	5	12.74	19.53	12.89	3.70
	All age	20.76	29.33	20.91	21.39
Sharbot Lake	1	35.02	49.23	34.96	50.06
	2	23.56	36.26	23.56	36.76
	3	20.7	31.81	20.73	31.62
	4	27.75	39.58	27.89	37.02
	5	18.97	30.41	19.06	28.33
	All age	23.37	35.16	23.45	33.63
Detroit River	1	26.15	39.65	25.96	42.37
	2	32.29	44.59	32.59	39.66
	3	26.74	38.52	27.22	33.45
	4	27.43	38.86	27.49	39.05
	5	23.17	34.02	23.85	25.65
	All age	25.95	37.28	26.42	32.73
Stonelick Lake	1	29.23	38.99	29.24	38.43
	2	31.4	41.96	31.4	42.01
	3	22.98	32.46	22.64	39.5
	4	17.73	25.65	17.61	27.95
	5	14.53	21.25	14.86	1.4
	All age	19.73	27.91	19.84	23.09
Lake Hartwell	1	24.6	23.95	24.73	24.33
	2	23.9	23.94	24.1	17.71
	3	14.53	14.1	14.45	17.89
	4	11.04	10.76	11	6.37
	5	12.86	12.72	12.83	16.4
	All age	15.02	14.78	14.99	14.96



Figure 4.1 Map of sampling location. Stars represent sampling sites.

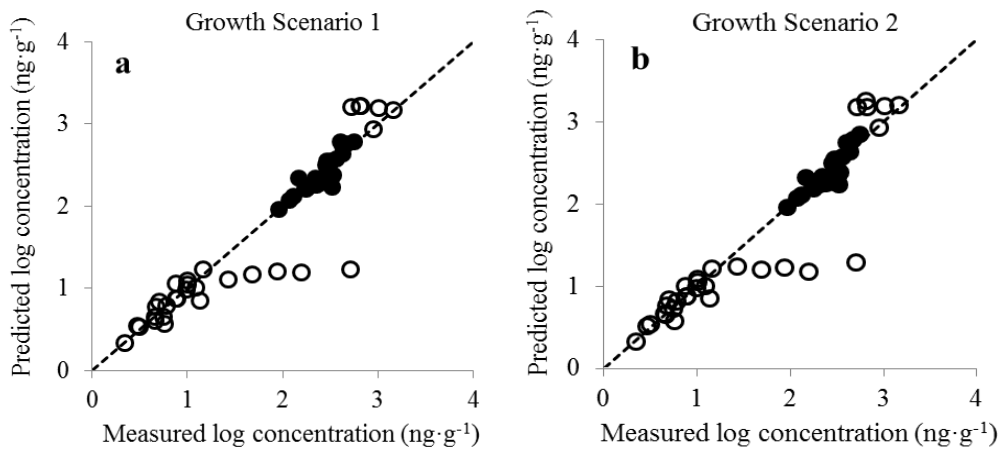
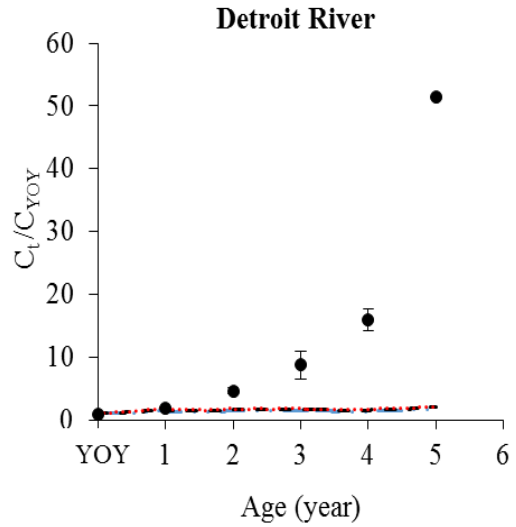
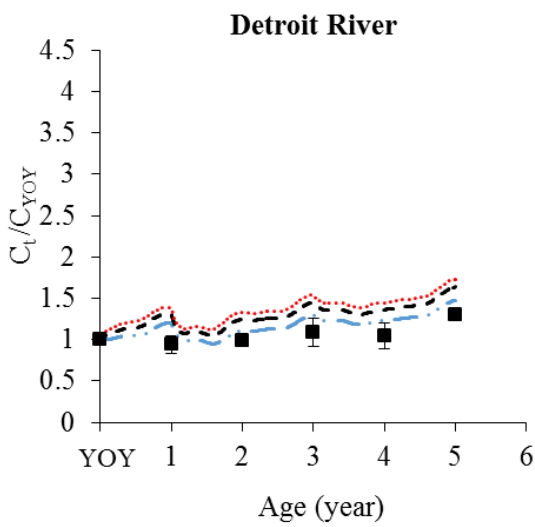
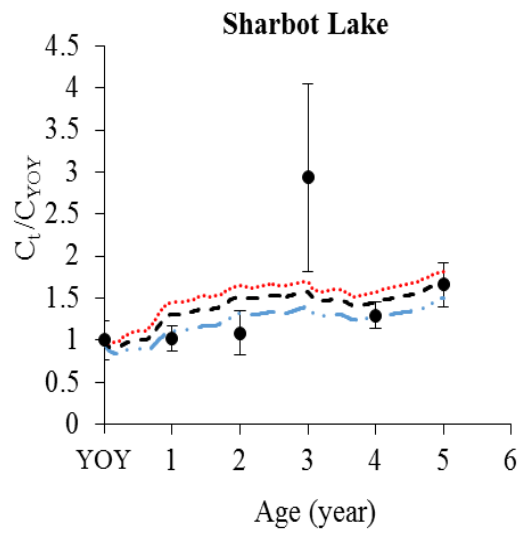
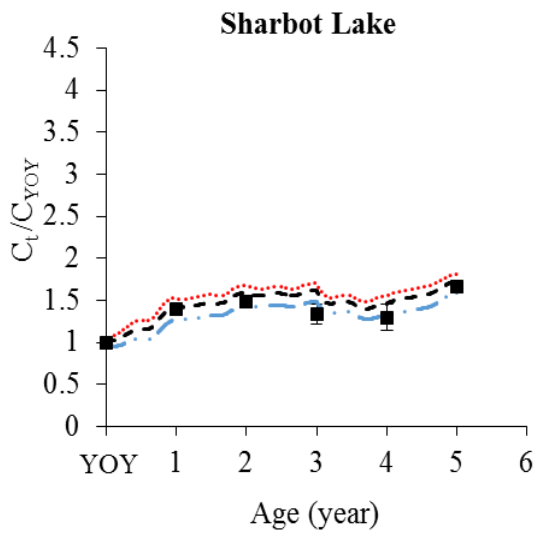
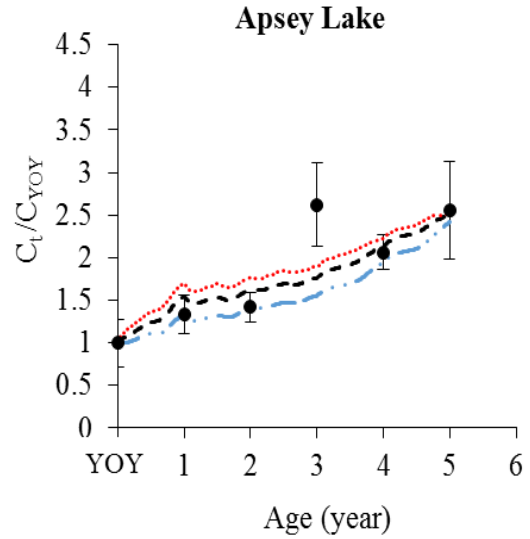
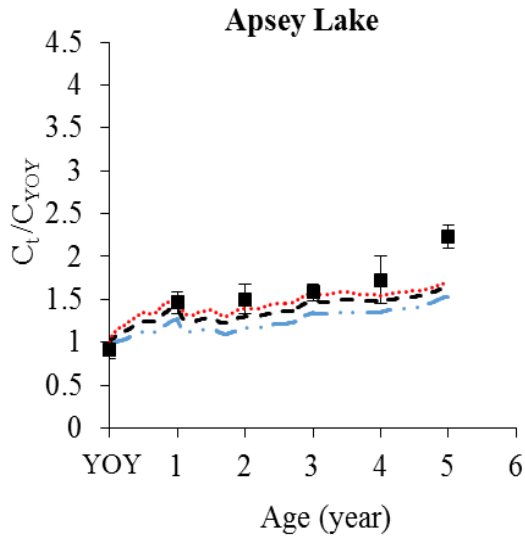


Figure 4.2 Relationships between predicted and observed total Hg and PCB 180 concentrations across lake populations and age classes under model assumptions of; (a) lipid and protein growth rates proportional to whole body growth (Scenario 1) and; (b) population specific lipid and protein growth rates (Scenario 2). In both panels, solid (●) and open (○) symbols represent Hg and PCB 180, respectively. Dashed lines represent the 1:1 regression fit. The outliers in (a) and (b) reflect PCB 180 concentrations of fish from the Detroit River.



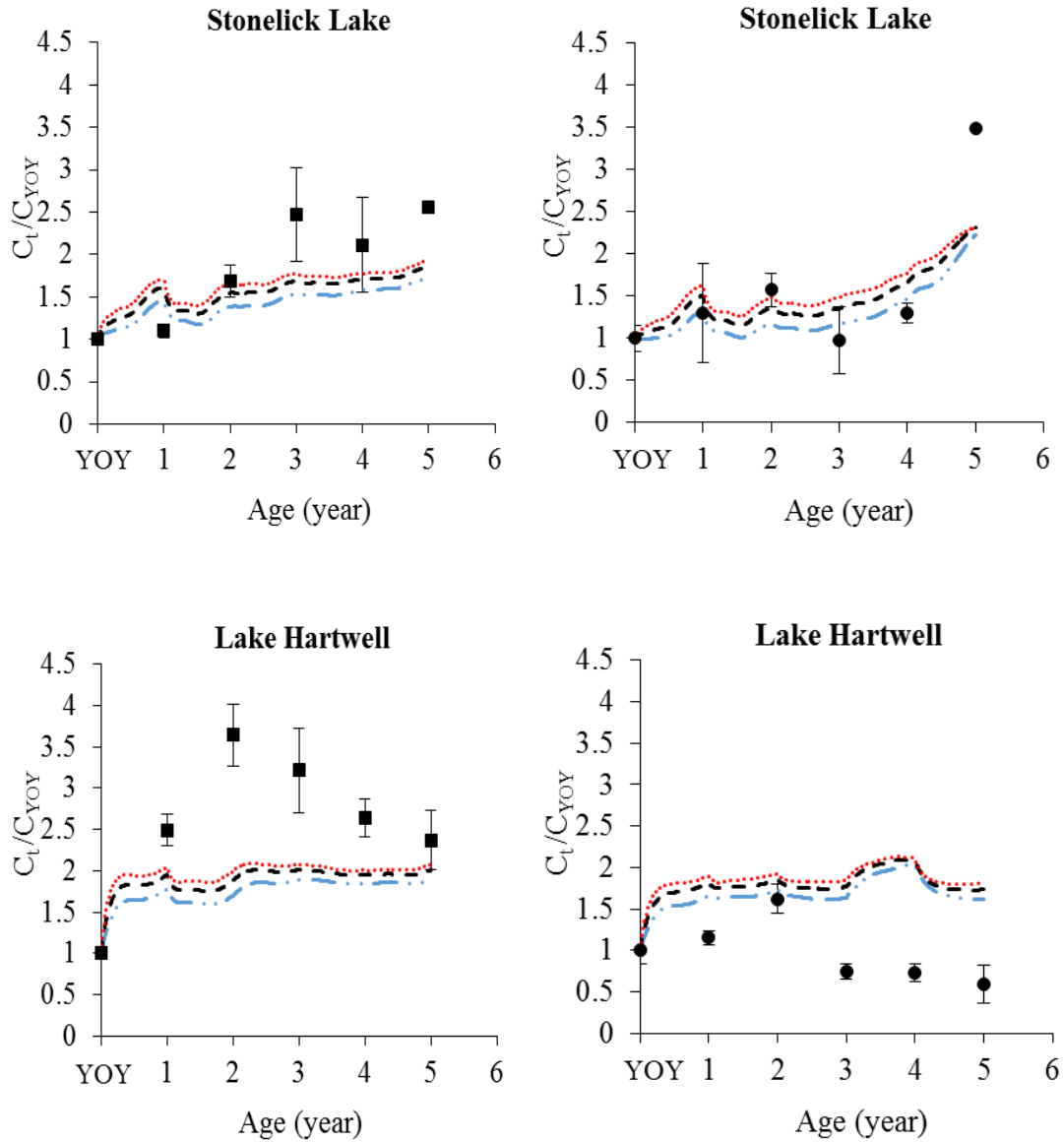


Figure 4.3 Relationship between relative chemical level (chemical concentration in fish [C_t] divided by chemical concentration in YOY [C_{YoY}]) and age for individual lake populations. Squares (■) represent THg and circles (●) represent PCB 180. Error bars used standard error; dashed lines (---) represent the modeled concentrations at activity levels = 1 (blue), 1.5 (black), and 2 (red), respectively

CHAPTER 5

Sensitivity Analysis on a Non-steady State Bioenergetics/kinetic Model

5.1 Introduction

A coupled bioenergetic-toxicokinetic model was developed by Drouillard et al. (2009). It showed overall good performance to estimate daily changes in PCB elimination rate and successfully described seasonal trends in PCB depuration by Yellow Perch (*Perca flavescens*). This model was modified to simulate Hg and PCBs bioaccumulation of Bighead carp (*Hypophthalmichthys nobilis*) and Silver carp (*Hypophthalmichthys molitrix*) from Three Gorge Reservoir (Chapter 3), as well as Bluegill (*Lepomis macrochirus*) from five river/lake systems (Chapter 4). Although the model was able to generate reasonable predictions, which generally fit with field collected data for many fish and locations, it was unclear which parameters were responsible for generating the most uncertainty in the model predictions. Understanding the parameters that primarily determine the model output (i.e. model sensitivity analysis) can be helpful for model developers and users to focus their efforts on improving the accuracy of key parameters, which could further improve the accuracy of the model predictions (MacLeod et al. 2002; Cariboni et al. 2007). Running models non-deterministically by allowing realistic error and random selection of model parameter values under sets of iterated simulations (e.g. Monte Carlo simulations) provides further information about model uncertainty, which can be used to help discriminate between different simulation scenarios and their accuracy for describing independent field validation data sets.

In order to evaluate the major variables affecting the bioenergetic-toxicokinetic model output, a formalized sensitivity analysis (Monte Carlo analysis) was applied for three

modeled species, which were Bighead carp, Silver carp and Bluegill. The model inputs, such as growth rate and stable isotope signature generated from field observations applied actual measured error in the sensitivity analysis. In contrast, toxicokinetic and bioenergetic parameters representative of variables collated from published sub-models assigned a uniform distribution with the same range of variability ($\pm 10\%$ of the value as upper and lower limits around the mean) in the sensitivity analysis. The results of the sensitivity analysis were compared between species with the goal of identifying common key parameters that dominated model sensitivity for the non-steady state bioenergetic/toxicokinetic bioaccumulation model. A second objective was to contrast the model sensitivity to age specific and tissue specific growth coefficients against changes in uptake rate due to ontogenetic diet shifts. Much of the literature on chemical biomagnification has focussed on the importance of prey trophic position on concentration in predicting fish bioaccumulation. However, growth and age specific growth have been understudied concepts with respect to their consideration in bioaccumulation models, particularly as it applies to non-steady state bioaccumulation dynamics in fish.

5.2 Methods

5.2.1 Temperature Profile

For the carp model, daily water temperature (T_d , °C) was simulated by a polynomial function that was fitted to the 2011 water temperature profile of Daning River (Zhao et al. 2015),

$$T_d = 0.00000001602 \cdot d^4 - 0.00001343 \cdot d^3 + 0.0033 \cdot d^2 - 0.1964 \cdot d + 15.209 \quad (5.1)$$

where d is the day of the year (Jan 1 to Dec 31 is day 1 to 365).

For Bluegill, it was estimated based on local air temperature of Lake Hartwell.

$$T_d = 0.0000000001965 \cdot d^4 - 0.000001088 \cdot d^3 - 0.000032 \cdot d^2 - 0.1547 \cdot d + 7.743 \quad (5.2)$$

To set up the sensitivity analysis, daily temperature (T_d) was calculated by multiplying initial temperature (T_0) by a factor (T_d/T_0) for each day. Then, T_0 was set as model input for sensitivity analysis, and assigned to a uniform distribution with $\pm 10\%$ variation, so that T_d also obtained a $\pm 10\%$ variation (Table 5.2).

5.2.2 Growth Model

Growth model of each species was established based on field measured lipid, lean dry protein (excluding moisture and lipid content (Li et al. 2015)), and whole body growth in Bighead Carp and Silver Carp that were collected from Daning River, Wushan, China, as well as Bluegills collected from Lake Hartwell. Annual growth of whole body weight ($\Delta W_{wb,y}$; g), lipid ($\Delta W_{lip,y}$; g), and lean dry protein ($\Delta W_{pro,y}$; g) for each age class was calculated as:

$$\Delta W_{wb,y} = \bar{W}_{wb,y+1} - \bar{W}_{wb,y} \quad (5.3)$$

$$\Delta W_{lip,y} = \bar{W}_{lip,y+1} - \bar{W}_{lip,y} \quad (5.4)$$

$$\Delta W_{pro,y} = \bar{W}_{pro,y+1} - \bar{W}_{pro,y} \quad (5.5)$$

where $\bar{W}_{wb,y}$ and $\bar{W}_{wb,y+1}$ are measured mean body weight (g) of fish of a given species for a given age class and the mean body weights (g) of fish from the same species for the next age class. For the sensitivity analysis, $\Delta W_{wb,y}$, $\Delta W_{lip,y}$, and $\Delta W_{pro,y}$ of each age class was set as a model input with a normal distribution. The standard deviation of $\Delta W_{wb,y}$ for each age class was calculated as the geometric mean of the measured standard deviation of $W_{wb,y}$ and $W_{wb,y+1}$ (Table 5.3). The standard deviations of $\Delta W_{lip,y}$ and $\Delta W_{pro,y}$ were obtained by the same procedure.

It was assumed that daily increment of whole body weight ($\Delta W_{wb,d}$; g), lipid ($\Delta W_{lip,d}$; g), and lean dry protein ($\Delta W_{pro,d}$; g) were dependent on water temperature (Berg and Bremset, 1998; Shoji et al, 2007), and they were estimated as follows:

$$\Delta W_{wb,d} = \Delta W_{wb,y} \left(\frac{T_d}{\sum_{d=1}^{365} T_d} \right) \quad (5.6)$$

$$\Delta W_{lip,d} = \Delta W_{lip,y} \left(\frac{T_d}{\sum_{d=1}^{365} T_d} \right) \quad (5.7)$$

$$\Delta W_{pro,d} = \Delta W_{pro,y} \left(\frac{T_d}{\sum_{d=1}^{365} T_d} \right) \quad (5.8)$$

5.2.3 Bioenergetic and Toxicokinetic Model

Bioenergetic models for Bighead Carp, Silver Carp, as well as Bluegill were developed according to Drouillard et al. (2009). Food consumption rates (Q_C ; g food g⁻¹ d⁻¹), gill ventilation volumes (Q_V ; mL g⁻¹ d⁻¹), and fecal production rates (Q_{EX} ; g feces g⁻¹ d⁻¹) are predicted as follows:

$$Q_C = \frac{(\Delta W_{lip,d} \cdot ED_{lip} + \Delta W_{pro,d} \cdot ED_{pro}) + R \cdot D_{O_2} + S + U}{E_C \cdot ED_{food}} \quad (5.9)$$

$$Q_V = \frac{R \cdot D_{O_2} + S + U}{D_{O_2} \cdot C_{O_2} \cdot E_{O_2} \cdot W} \quad (5.10)$$

$$Q_{EX} = Q_C \cdot (1 - (X_{L,D} \cdot E_L + X_{P,D} \cdot E_P)) \quad (5.11)$$

All parameters are defined in Table 5.1.

For Silver Carp and Bighead Carp, specific rate of respiration (R , g g⁻¹ d⁻¹) is calculated using Equation 1 of the Wisconsin bioenergetic model version 3.0 (Hanson et al. 1997), and described in Cooke and Hill (2010):

$$R = RA \cdot W_{wb,d}^{RB} \cdot e^{RQ \cdot T_d} \cdot ACT \quad (5.12)$$

For Bluegill, R is calculated using Equation 2 of Wisconsin bioenergetic model version 3.0 (Hanson et al. 1997):

$$R = RA \cdot W_{wb,d}^{RB} \cdot V^X \cdot e^{(X \cdot (1-V))} \cdot ACT \quad (5.13)$$

where

$$V = \frac{RTM - T}{RTM - RTO}$$

$$X = \frac{Z^2 \cdot (1 + (1 + 40/Y)^{0.5})^2}{400}$$

$$Z = LN(RQ) \cdot (RTM - RTO)$$

$$Y = LN(RQ) \cdot (RTM - RTO + 2)$$

For all three species, specific dynamic action (S , $\text{kJ g}^{-1} \text{d}^{-1}$) and energy lost to excretion (U , $\text{kJ g}^{-1} \text{d}^{-1}$) are derived from R (Eq. 5.12-5.13) and daily growth increments according to:

$$S = SDA \cdot (R \cdot D_{O_2} + |\Delta W_{lip,d} \cdot ED_{lip}| + |\Delta W_{pro,d} \cdot ED_{pro}|) \quad (5.14)$$

$$U = UA \cdot T_d^{UB} \cdot e^{UG} \cdot (R \cdot D_{O_2} + |\Delta W_{lip,d} \cdot ED_{lip}| + |\Delta W_{pro,d} \cdot ED_{pro}|) \quad (5.15)$$

Energy assimilation from food (E_C ; unitless), energy density of food (ED_{food} ; kJ g^{-1}) and oxygen concentration in water (C_{O_2} ; $\text{g O}_2 \text{ mL}^{-1}$) are estimated via Eqs.16-18, which were taken from Drouillard et al. (2009).

$$E_C = \frac{ED_{lip} \cdot X_{L,D} \cdot E_L + ED_{pro} \cdot X_{P,D} \cdot E_P}{ED_{Food}} \quad (5.16)$$

$$ED_{Food} = ED_{lip} \cdot X_{L,D} + ED_{pro} \cdot X_{P,D} \quad (5.17)$$

$$C_{O_2} = \frac{14.45 - 0.413 \cdot T_d + 5.56 \times 10^{-3} \cdot T_d^2}{1000000} \quad (5.18)$$

Methylmercury (MeHg) accounted for more than 95% of the total Hg in fish (Bloom, 1992), thus, Hg and MeHg were exchangeable in this study. Because food is the dominant Hg uptake route (Hall et al. 1997), aqueous uptake was not considered. The daily change in Hg concentration is calculated as:

$$\frac{dC_P}{dt} = \frac{C_{d,Hg,y} \cdot Q_C \cdot W_{wb,d} \cdot AE_{Hg}}{W_{pro,d}} - \left(k_{tot,Hg} + \frac{\Delta W_{pro,d}}{W_{pro,d}} \right) \cdot C_P \quad (5.19)$$

Dietary Hg concentration for YOY fish ($C_{d,Hg,YOY}$; ng g⁻¹) was estimated using Hg concentration of YOY ($C_{YOY,Hg}$; ng g⁻¹) from the corresponding species divided by a biomagnification factor (BMF). Using the trophic enrichment factor of 3.4‰ (Minagawa and Wada 1984), dietary Hg concentrations for a given age class ($C_{d,Hg,y}$; ng g⁻¹) is estimated based on $C_{d,Hg,YOY}$ and the increment of nitrogen stable isotope signature ($\Delta\delta^{15}N_y$; ‰):

$$C_{d,Hg,y} = \frac{C_{YOY,Hg}}{BMF} \cdot BMF^{\left(\frac{\Delta^{15}N_y}{3.4}\right)} \quad (5.20)$$

$\Delta\delta^{15}N_y$ of each age class is calculated as:

$$\Delta\delta^{15}N_y = \bar{\delta^{15}N_y} - \bar{\delta^{15}N_{YOY}} \quad (5.21)$$

For the sensitivity test, $C_{YOY,Hg}$ and $\Delta\delta^{15}N_y$ were included as model inputs and allowed to vary on a normal distribution. The measured mean and standard deviation of $C_{YOY,Hg}$ was applied. The standard deviation of $\Delta\delta^{15}N_y$ was calculated as the geometric mean of the measured standard deviation of $\delta^{15}N_y$ and $\delta^{15}N_{YOY}$ (Table 5.3).

$k_{tot,Hg}$ was scaled to the routine metabolic rate by a ratio ($r_{k_{tot}}$, unitless) derived from empirical data (Trudel and Rasmussen, 1997), and it is estimated according to:

$$k_{tot,Hg} = \left(\left| \Delta W_{lip,d} \cdot ED_{lip} \right| + \left| \Delta W_{pro,d} \cdot ED_{pro} \right| + R \cdot D_{O_2} + S + U \right) \cdot r_{k_{tot}} \quad (5.22)$$

For PCB, PCB 180 was chosen as a representative congener, and the daily change in PCB concentration is modeled by:

$$\frac{dC_L}{dt} = \frac{C_{d,PCB,y} \cdot Q_C \cdot W_{wb,d} \cdot AE_{PCB} + C_w \cdot W_{wb,d} \cdot Q_V \cdot E_w}{W_L} - (k_2 + k_{EX} + \frac{\Delta W_L}{W_L}) \cdot C_L \quad (5.23)$$

Similar to $C_{d,Hg,y}$, the same procedure was used to calibrate dietary PCB concentration ($C_{d,PCB,y}$, ng g⁻¹) for each species of each age class. PCB concentration of the water was assumed to be at thermodynamic equilibrium with PCB concentration of the young-of-year fish ($C_{YOY,PCB}$, ng g⁻¹lipid). Thus, C_w is calculated as:

$$C_w = \frac{C_{YOY}}{K_{OW}} \quad (5.24)$$

The gill elimination rate constant (k_2 ; d⁻¹) is calculated as:

$$k_2 = \frac{E_w \cdot Q_V}{K_{BW}} \quad (5.25)$$

The algorithms for estimating chemical exchange efficiency across the gills (E_w ; unitless) and biota/water partition coefficient (K_{BW} ; unitless) are as follows:

$$E_w = (1.85 + \frac{155}{K_{OW}})^{-1} \quad (5.26)$$

$$K_{BW} = X_{L,B} \cdot K_{OW} + 0.05 \cdot X_{P,B} \cdot K_{OW} \quad (5.27)$$

Fecal elimination rate constants (k_{EX} ; d⁻¹) are estimated by:

$$k_{EX} = \frac{E_{EX} \cdot Q_{EX}}{K_{B,EX}} \quad (5.28)$$

The biota/feces partition coefficient ($K_{B,EX}$; unitless) is:

$$K_{B,EX} = \frac{X_{L,B} + 0.05 \cdot X_{P,B}}{X_{L,EX} + 0.05 \cdot X_{P,EX}} \quad (5.29)$$

5.2.4 Data Analysis

Monte Carlo simulations were used for sensitivity testing. As shown in Table 5.2, toxicokinetic and bioenergetic parameters derived from published sub-models were assigned to a uniform distribution with the same range of variability ($\pm 10\%$ of the value as upper and lower limits around the mean) in the sensitivity analysis. Uniform distribution and $\pm 10\%$ error was applied because it is common practice in previous studies (Cooke and Hill, 2010). Table 5.3 presents the model inputs generated from field observations, such as chemical concentration in YOY fish, annual growth increment, and stable isotope signature. For these parameters, actual mean and standard deviation were applied in the sensitivity analysis. Hg and PCB 180 concentrations of a 6 year old Bighead Carp, a 4 year old Silver Carp, and a 5 year old Bluegill were each set as model outputs. The model was run for 10000 iterations, and sensitivity of each parameter was quantified using the proportion of contribution to total variance. Monte Carlo simulation was performed using Crystal Ball software. In the results, the contribution of $\Delta W_{lip,y}$, $\Delta W_{pro,y}$, $\Delta W_{wb,y}$, and $\Delta \delta^{15}N_y$ of all age classes were added up, and reported as ΔW_{lip} , ΔW_{pro} , ΔW_{wb} and $\Delta \delta^{15}N$, respectively. Notably, the Bluegill model was originally developed to simulate Hg and PCB bioaccumulation for fish from five different waterbodies. Because the Bluegill models for all five locations adopted the same bioenergetics parameters, only the results for Lake Hartwell were presented in this study.

5.3 Results

5.3.1 Sensitivity Analysis for Hg Models

Table 5.4 presents the results of sensitivity testing for Hg lean dry weight concentration of a 6 year old bighead carp, a 4 years old Silver Carp, and a 5 years old Bluegill. For Bighead Carp, $C_{YOY,Hg}$ accounted for the most variance (70.03%) in Hg concentration, followed by $\Delta\delta^{15}N$ and ΔW_{pro} with 14.28% and 9.13% contribution to the total variance, respectively. Hg concentration of Bighead Carp was negatively related to ΔW_{pro} , and positively related to the rest of the aforementioned parameters. Similar to Bighead Carp, Hg concentration of Silver Carp was most sensitive (74.5%) to $C_{YOY,Hg}$. In addition, the results showed that ΔW_{pro} and ΔW_{wb} were responsible for 8.62% and 7.05% of the total variance, respectively. Hg concentration of Silver Carp was negatively correlated to ΔW_{pro} , and positively correlated to $C_{YOY,Hg}$ and ΔW_{wb} . For Bluegill, Hg concentration was primarily sensitive (>5%) to $\Delta\delta^{15}N$, $C_{YOY,Hg}$, ΔW_{pro} , and ΔW_{wb} , which contributed to 35.32%, 21.21%, 19.99%, and 12.96% of the total variance, respectively. Increase in $\Delta\delta^{15}N$, $C_{YOY,Hg}$, and ΔW_{wb} resulted in an increase in Hg concentration of Bluegill, however, an increase in ΔW_{pro} resulted in a decrease.

5.3.2 Sensitivity Analysis for PCB Models

As shown in Table 5.5, the PCB 180 lipid-equivalent concentrations of all three species were most influenced (77.51%~80.22%) by $C_{YOY,PCB}$. For Bighead Carp, PCB concentration was also sensitive to ΔW_{lip} and $\Delta\delta^{15}N$, which were responsible for 10.32%, and 6.12% of the total variance. Both $C_{YOY,PCB}$ and $\delta^{15}N$ were positively related to PCB level in Bighead Carp, while ΔW_{lip} had a negative effect. For Silver Carp, the results showed that ΔW_{lip} and $\Delta\delta^{15}N$ accounted for 6.63% and 4.18% of the total variance. PCB concentration in Silver Carp was negatively related to ΔW_{lip} , and positively related to the rest of the aforementioned parameters. For Bluegill, PCB concentration was also

influenced by $\Delta\delta^{15}\text{N}$ and ΔW_{lip} , which contributed to 9.89%, and 4.27% of the total variance, respectively. Increases in $C_{\text{YOY, PCB}}$ and $\Delta\delta^{15}\text{N}$ resulted in increases in PCB concentration in Bluegill, while an increase in ΔW_{lip} resulted in a decrease.

5.4 Discussion

In this study, Hg concentrations for all three species were most influenced by Hg concentration in YOY, annual increment of nitrogen stable isotope, as well as annual increment of lean dry protein and whole body weight. However, the actual measured standard deviations were applied for these parameters, while the rest of the model inputs were assigned a marginal 10% error. Higher errors in these parameters could explain their relatively higher contribution to total variance compared with other model parameters. Consequently, comparison of the model sensitivity should only be made among parameters with real error, or among those with 10% error.

Among the parameters that applied measured error, the Hg concentration in YOY reflected the baseline input to the waterbody (i.e. source from the watershed and atmospheric deposition), which is one of the most important drivers for Hg bioaccumulation in fish (Chen et al. 2000). For instance, Hg levels in fish from contaminated areas (Harada, 1995) could be a thousand-fold higher compared to fish of a similar trophic level from pristine lakes (Perrot et al. 2012). Therefore, in this study, Hg concentration in YOY, reflective of Hg inputs to a given lake, was the most sensitive factor affecting Hg concentration in both carp species and the second most sensitive factor affecting Hg in Bluegill.

The annual increment of nitrogen stable isotope signature was a reflection of ontogenetic diet shifts of fish, which according to the model structure, causes a change in diet contamination level. Also, a positive relationship between nitrogen stable isotope value and fish contamination level has been widely reported (Zhang et al. 2012). Thus, the annual increment of nitrogen stable isotope was the most influential factor for Hg concentration in Bluegill, the second in Bighead Carp, and fourth in Silver Carp. The annual increment of lean dry protein and whole body weight represented the growth rate of lean dry protein and fish whole body weight, which govern variation in model output due to growth dilution. Previous studies found that growth dilution played an important role in Hg bioaccumulation in fish (Dang and Wang, 2012), which supports our observation that tissue growth and whole body growth contributed to a major portion of the total variance of the model outputs for the three modeled species. It is noteworthy that growth rate and stable isotope signature had comparable contributions to total variance in Hg concentration for all three species, which suggested that growth dilution should be treated at least as important as the feeding ecology for Hg modeling practice. More attention is especially required for the tissue growth rate, which is unique to the models developed in this study.

Among model inputs with 10% errors, the Hg concentrations of these species were also sensitive to assimilation efficiency of Hg, assimilation efficiency of protein, assimilation efficiency of lipid, prey biomagnification factor, activity levels, energy density of the diet, as well as elimination rate coefficient. Usually, low variabilities were expected for assimilation efficiency and elimination rate coefficient, as these have been consistent in previous studies (Buckman et al. 2004; Leaner and Mason, 2004; Wang and Wang, 2012;

Li et al. 2015). Consequently, the model outcome of the three species was mainly dependent on parameters with relatively higher variation among species and their environment, such as activity levels and energy density of the diet.

In this study, Hg concentration in all three species was not very sensitive to parameters related to specific dynamic action, excretion, and respiration. A close examination of the model simulation revealed that specific dynamic action and excretion only accounted for a relatively small fraction (<10%) of the total metabolic rate, which could explain the relatively low contribution to the total variance of the model output by these parameters. In addition, it has been reported that Hg uptake through respiration is negligible (Hall et al. 1997), thus, aqueous uptake by fish was not considered in this study. Therefore, it was expected that Hg concentration was not sensitive to model inputs associated to respiration.

The results of sensitivity analysis on PCB models showed that PCB levels of the three species were most influenced by PCB concentration in YOY, annual increment of nitrogen stable isotope, and annual increment of lipid. For all three species, PCB concentration in YOY accounted for more than 75% of the variance in PCB concentration, which confirmed the decisive role of baseline contamination to PCB bioaccumulation in fish. Similar to Hg, the lipid growth rate and nitrogen stable isotope had comparable influence on PCB concentration predictions in fish for all three species. The results further indicated the importance of the tissue growth rate to chemical bioaccumulation. Among other parameters, the PCB concentrations of these fish were sensitive to assimilation efficiency of PCB and lipid, biomagnification factor, energy density of the diet, as well as parameters associated with respiration. Additionally, PCB

concentration was not sensitive to parameters related to specific dynamic action and excretion. In general, these results were similar to the results for Hg models, except that PCB uptake through respiration was considered in the PCB model, thus, respiration had higher contribution to the total variance in the PCB model compared with the Hg model.

Overall, the results of both Hg and PCB models revealed comparable influences of tissue growth rate and feeding ecology to chemical bioaccumulation, suggesting more efforts are needed to incorporate population specific differences in tissue growth rate when modelling bioaccumulation of these contaminants. Due to different characteristics of different parameters, some model inputs naturally had higher variabilities than others. Future sensitivity analysis using realistic variation for each bioenergetic parameter would be necessary to further identify the key parameters and improve the accuracy of model prediction.

5.5 References

- Arnot, J. A.; Gobas, F. A. P. C. A food web bioaccumulation model for organic chemicals in aquatic ecosystems. *Environ. Toxicol. Chem.* 2004, 23, 2343-2355.
- Arts, M. T.; Robarts, R. D.; Evans, M. S. Energy reserve lipids of zooplanktonic crustaceans from an oligotrophic saline lake in relation to food resources and temperature. *Can. J. Fish. Aquat. Sci.* 1993, 50, 2404-2420.
- Bloom, N. S. On the chemical form of mercury in edible fish and marine invertebrate tissue. *Can. J. Fish Aquat. Sci.* 1992, 49, 1010-1017.
- Buckman, A. H.; Brown, S. B.; Hoekstra, P. F.; Solomon, K. R.; Fisk, A. T. Toxicokinetics of three polychlorinated biphenyl technical mixtures in rainbow trout (*Oncorhynchus mykiss*). *Environ. Toxicol. Chem.* 2004, 23, 1725-1736.

- Cariboni, J.; Gatelli, D.; Liska, R.; Saltelli, A. The role of sensitivity analysis in ecological modelling. *Ecol. Model.* 2007, 203, 167-182.
- Chen, C.Y.; Stemberger, R.S.; Klaue, B.; Blum, J. D.; Pickhardt, P.C.; Folt, C.L. Accumulation of heavy metals in food web components across a gradient of lakes. *Limnol. Oceanogr.* 2000, 45, 1525-1536.
- Cheng, Z.; Liang, P.; Shao, D.; Wu, S.; Nie, X.; Chen, K.; Wong, M. Mercury biomagnification in the aquaculture pond ecosystem in the pearl river delta. *Archives of Environ. Contam. Toxicol.* 2011, 61(3), 491-499.
- Cooke, S. L.; Hill, W. R. Can filter-feeding Asian carp invade the Laurentian Great Lakes? A bioenergetic modelling exercise. *Freshwater Biol.* 2010, 55, 2138-2152.
- Dang, F.; Wang, W. X. Why mercury concentration increases with fish size? Biokinetic explanation. *Environ. Pollut.* 2012, 163, 192-198.
- Dawson, A. S.; Grimm, A. S. Quantitative seasonal changes in the protein, lipid and energy content of the carcass, ovaries and liver of adult female plaice, *Pleuronectes platessa* L. *J. Fish Biol.* 1980, 16, 493-504.
- Drouillard, K. G.; Paterson, G.; Haffner, G. D. A combined food web toxicokinetic and species bioenergetic model for predicting seasonal PCB elimination by yellow perch (*Perca flavescens*). *Environ. Sci. Technol.* 2009, 43(8), 2858-2864.
- Graham, J. M., Graham, L. E.; Zulkifly, S. B.; Pflieger, B. F.; Hoover, S. W.; Yoshitani, J. Freshwater diatoms as a source of lipids for biofuels. *J. Ind. Microbiol. Biotechnol.* 2012, 39, 419-428.
- Hall, B. D.; Bodaly, R. A.; Fudge, R. J. P.; Rudd, J. W. M.; Rosenberg, D. M. Food as the dominant pathway of methylmercury uptake by fish. *Water, Air, and Soil Pollut.* 1997, 100, 13-24.
- Hanson, P. C.; Johnson, T. B.; Schindler, D. E.; Kitchell, J. F. *Fish Bioenergetics 3.0*. University of Wisconsin Sea Grant Institute, Madison, Wisconsin. 1997.
- Harada, M. Minamata Disease- Methylmercury poisoning in Japan caused by environmental pollution. *Crit. Rev. Toxicol.* 1995, 25 (1), 1-24.

- Hawker, D. W.; Connell, D. W. Octanol-water partition coefficients of polychlorinated biphenyl congeners. *Environ. Sci. Technol.* 1988, 22, 382-387.
- Leaner J. J.; Mason R. P. Methylmercury uptake and distribution kinetics in sheepshead minnows, *Cyprinodon variegatus*, after exposure to CH₃Hg-spiked food. *Environ. Toxicol. Chem.* 2004, 23(9), 2138-2146.
- Li, J.; Drouillard, K. G.; Branfireun, B.; Haffner, G. D. Comparison of the toxicokinetics and bioaccumulation potential of mercury and polychlorinated biphenyls in goldfish (*Carassius auratus*). *Environ. Sci. Technol.* 2015, 49, 11019-11027.
- Liu, J.; Haffner, G. D.; Drouillard, K. G. The influence of diet on the assimilation efficiency of 47 polychlorinated biphenyl congeners in Japanese Koi (*Cyprinus carpio*). *Environ. Toxicol. Chem.* 2010, 29, 401-409.
- MacLeod, M.; Fraser, A. J.; Mackay, D. Evaluating and expressing the propagation of uncertainty in chemical fate and bioaccumulation models. *Environ. Toxicol. Chem.* 2002, 21, 700-709.
- McKim, J. M.; Schmieder, P. K.; Veith, G. D. Absorption dynamics of organic chemical transport across trout gills as related to octanol-water partition coefficient. *Toxicol. Appl. Pharmacol.* 1985, 77, 1-10.
- Minagawa, M.; Wada, E. Stepwise enrichment of ¹⁵N along food chains: further evidence and the relation between $\delta^{15}\text{N}$ and animal age. *Geochim. Cosmochim. Acta*, 1984, 48, 1135-1140.
- Norstrom, R. J.; McKinnon, A. E.; DeFreitas, A. S. W. Bioenergetics-based model for pollutant accumulation by fish simulation of PCB and methylmercury residue levels in Ottawa River yellow perch (*Perca flavescens*). *J. Fish. Res. Bd. Can.* 1976, 33, 248-267.
- Perrot, V.; Pastukhov, M. V.; Epov, V. N.; Husted, S.; Donard, O.F.; Amouroux, D. Higher Mass-independent isotope fractionation of methylmercury in the pelagic food web of Lake Baikal (Russia). *Environ.Sci. Technol.* 2012, 46 (11), 5902-5911.
- Sakizadeh, M. ; Sari, A. E.; Abdoli, A.; Bahramifar, N.; Hashemi, S. H. Determination of polychlorinated biphenyls and total mercury in two fish species (*Esox lucius* and

- Carassius auratus) in Anzali Wetland, Iran. Environ Monit Assess. 2012, 184, 3231-3237.
- Schmidt-Nielsen, K. (Ed.) Animal Physiology: Adaptation and Environment (5th Edition). Cambridge University Press, New York , 1997.
- Trudel, M.; Rasmussen, J. B. Bioenergetics and mercury dynamics in fish: a modelling perspective. Can. J. Fish. Aquat. Sci. 2006, 63, 1890-1902.
- Trudel, M.; Rasmussen, J. B. Modeling the elimination of mercury by fish. Environ. Sci. Technol. 1997, 31, 1716-1722.
- Trudel, M.; Rasmussen, J. B. Predicting mercury concentration in fish using mass balance models. Ecol. Appl. 2001, 11, 517-529.
- Visha, A.; Gandhi, N.; Bhavsar, S. P.; Arhonditsis, G. B. A Bayesian assessment of the mercury and PCB temporal trends in lake trout (*Salvelinus namaycush*) and walleye (*Sander vitreus*) from lake Ontario, Ontario, Canada. Ecotoxicol. Environ. Saf. 2015, 117, 174-86.
- Wang, R.; Wang, W. X. Contrasting mercury accumulation patterns in tilapia (*Oreochromis niloticus*) and implication on somatic growth dilution. Aquat. Toxicol. 2012, 114-115, 23-30.
- Zhang, L.; Campbell, L.M.; Johnson, T.B. Seasonal variation in mercury and food web biomagnification in Lake Ontario, Canada. Environ. Pollut. 2012, 161, 178-184.
- Zhao, X.; Feng, C.; Wu, M. Sophisticated 3D modeling for eutrophication in Daning River Three Gorges Reservoir area. J. Yangtze Riv. Sci. Res. Inst. 2015, 32(06), 25-31.

Table 5.1 Description of bioenergetics and toxicokinetics parameters

Parameter	Description
ACT	Activity multiplier (unitless)
AE _{Hg}	Hg assimilation efficiency (unitless)
AE _{PCB}	PCB assimilation efficiency (unitless)
C _L	Lipid equivalent PCB concentration in the animal (ng g ⁻¹)
C _{O2}	Concentration of oxygen dissolved in water (g O ₂ mL ⁻¹)
C _P	Hg lean dry weight concentration in the animal (ng g ⁻¹)
C _w	PCB concentration in water (ng g ⁻¹)
C _{YOY,Hg}	Hg concentration in YOY fish (ng g ⁻¹)
C _{YOY,PCB}	PCB concentration in YOY fish (ng g ⁻¹)
D _{O2}	Oxycalorific coefficient for converting O ₂ respired to energy (kJ g ⁻¹ O ₂)
E _C	Energy assimilation efficiency from food (unitless)
ED _{Food}	Total energy density of food (kJ g ⁻¹)
ED _{lip}	Energy density of lipid (kJ g ⁻¹)
ED _{pro}	Energy density of protein (kJ g ⁻¹)
E _{EX}	PCB organism/fecal exchange efficiency (unitless)
E _L	Assimilation efficiencies of dietary lipid (unitless)
E _{O2}	Oxygen extraction efficiency across the gills (unitless)
E _P	Assimilation efficiencies of dietary protein (unitless)
E _w	Chemical exchange efficiency across the gills (unitless)
k ₂	Elimination rate constants for chemical depuration across the gills (d ⁻¹)
K _{B,EX}	Biota/feces partition coefficient (unitless)
K _{BW}	Biota/water partition coefficient (unitless)
k _{EX}	Elimination rate constants for chemical depuration across feces (d ⁻¹)
K _{OW}	Octanol/water partition coefficient of the chemical (unitless)
k _{tot,Hg}	Whole body Hg elimination rate coefficient (g g ⁻¹ d ⁻¹)
R	Specific rate of respiration (g g ⁻¹ d ⁻¹)
RA	Intercept of the allometric mass function (g g ⁻¹ d ⁻¹)
RB	Slope of the allometric mass function (unitless)
RQ	Approximates Q ₁₀ over relatively low water temperatures (°C ⁻¹)
RTO	Optimum temperature for respiration (°C)
RTM	Maximum water temperature (°C)

S	Specific dynamic action ($\text{kJ g}^{-1} \text{d}^{-1}$)
SDA	Proportion of assimilated energy lost to specific dynamic action (unitless)
U	Energy lost to excretion ($\text{kJ g}^{-1} \text{d}^{-1}$)
U _A	Intercept of the proportion of consumed energy excreted versus water temperature (unitless)
U _B	Coefficient of water temperature dependence of excretion (unitless)
U _G	Coefficient for feeding level dependence of excretion (unitless)
ΔW_L	Daily change of lipid equivalent weight (g)
W_L	Lipid equivalent weight of the animal (g)
$W_{wb,d}$	Fish body weight for a given day (g)
$X_{L,D}$	Mass fraction of lipid in the diet (unitless)
$X_{L,EX}$	Fraction of lipid in the feces (unitless)
$X_{P,D}$	Mass fraction of protein in the diet (unitless)
$X_{P,EX}$	Fraction of lean dry protein in the feces (unitless)

Table 5.2 Mean and distribution of model inputs based on literature or assumptions.

Parameter (unit)	Bighead Carp		Silver Carp		Bluegill	
	Mean	Uniform distribution	Mean	Uniform distribution	Mean	Uniform distribution
ACT (unitless)	1 ^a	0.9~1.1	1 ^a	0.9~1.1	1.5	1.35~1.65
AE _{Hg} (unitless)	87% ^b	78.3~95.7%	87% ^b	78.3~95.7%	90% ^c	81~99%
AE _{PCB} (unitless)	44% ^b	39.6~48.4%	44% ^b	39.6~48.4%	60% ^d	54~66%
BMF (unitless)	2 ^e	1.8~2.2	2 ^e	1.8~2.2	2 ^e	1.8~2.2
D _{O2} (kJ g ⁻¹ O ₂)	14.3 ^f	12.87~15.73	14.3 ^f	12.87~15.73	14.3 ^f	12.87~15.73
ED _{lip} (kJ g ⁻¹)	39.3 ^g	35.37~43.23	39.3 ^g	35.37~43.23	39.3 ^g	35.37~43.23
ED _{pro} (kJ g ⁻¹)	18.0 ^g	16.2~19.8	18.0 ^g	16.2~19.8	18.0 ^g	16.2~19.8
E _{EX} (unitless)	44% ^b	39.6~48.4%	44% ^b	39.6~48.4%	60% ^d	39.6~48.4%
E _L (unitless)	0.92 ^h	0.828~1.012	0.92 ^h	0.828~1.012	0.92 ^h	0.828~1.012
E _{O2} (unitless)	0.6 ⁱ	0.54~0.66	0.6 ⁱ	0.54~0.66	0.6 ⁱ	0.54~0.66
E _P (unitless)	0.6 ^h	0.54~0.66	0.6 ^h	0.54~0.66	0.6 ^h	0.54~0.66
RA (g g ⁻¹ d ⁻¹)	0.0053 ^a	0.00477~0.00583	0.0028 ^a	0.00252~0.00308	0.0154 ^j	0.01386~0.01694
RB (unitless)	-0.299 ^a	-0.3289 ~ -0.2691	-0.239 ^a	-0.2629 ~ -0.2151	-0.2 ^j	-0.22 ~ -0.18
r _{ktot} (unitless)	0.0659 ^k	0.05931~0.07249	0.0659 ^k	0.05931~0.07249	0.0659 ^k	0.05931~0.07249
RQ (°C ⁻¹)	0.048 ^a	0.0432~0.0528	0.076 ^a	0.0684~0.0836	2.1 ^j	1.89~2.31
RTO (°C)					36 ^j	32.4~39.6
RTM (°C)					40 ^j	36~44

SDA (unitless)	0.1 ^a	0.09~1.1	0.1 ^a	0.09~1.1	0.172 ^j	0.1548~0.1892
T ₀ (°C)	15	13.5~16.5	15	13.5~16.5	8	7.2~8.8
UA (unitless)	0.031 ^a	0.0279~0.0341	0.031 ^a	0.0279~0.0341	0.0253 ^j	0.02277~0.02783
UB (unitless)	0.58 ^a	0.522~0.638	0.58 ^a	0.522~0.638	0.58 ^j	0.522~0.638
UG (unitless)	-0.299 ^a	-0.3289 ~ -0.2691	-0.299 ^a	-0.3289 ~ -0.2691	-0.299 ^j	-0.3289 ~ -0.2691
X _{L,D} (unitless)	6% ^l	5.4~6.6%	2.50% ^m	2.25~2.75%	2.26% ⁿ	2.034~2.486%
X _{P,D} (unitless)	4% ^l	3.6~4.4%	7.50% ^m	6.75~8.25%	21.88% ⁿ	19.692~24.068

^aCooke and Hill, 2010

^bLi et al. 2015

^cLeaner and Mason 2004

^dLiu et al. 2010

^eCheng et al. 2011

^fNorstrom et al. 1976

^gDrouillard et al. 2009

^hArnot and Gobas, 2004

ⁱMcKim et al. 1985

^jHanson et al. 1997

^kChapter 2&3

^lArts et al. 1993

^mGraham et al. 2012

ⁿAssumed to be equal to that of YOY

Table 5.3 Mean and standard deviation (SD) of model inputs based on observed field data.

Parameter (unit)	Bighead Carp		Silver Carp		Bluegill	
	Mean	SD	Mean	SD	Mean	SD
$C_{YOY,Hg}$	8.83	5.70	2.60	1.02	--	--
$C_{YOY,PCB}$	0.0312	0.0306	0.0071	0.0024	881.84	441.30
$\Delta W_{lip,YOY}$ (g)	--	--	4.53	4.85	0.07	0.09
$\Delta W_{lip,1}$ (g)	8.72	7.04	13.68	22.06	0.12	0.18
$\Delta W_{lip,2}$ (g)	45.68	4.92	82.67	106.90	0.37	0.42
$\Delta W_{lip,3}$ (g)	70.60	126.90	543.56	104.70	-0.12	0.63
$\Delta W_{lip,4}$ (g)	142.71	311.16	--	--	0.77	1.04
$\Delta W_{lip,5}$ (g)	858.99	829.88	--	--	--	--
$\Delta W_{pro,YOY}$ (g)	--	--	20.87	23.27	0.97	0.60
$\Delta W_{pro,1}$ (g)	83.85	40.76	102.11	42.29	3.12	1.17
$\Delta W_{pro,2}$ (g)	360.06	31.62	142.75	90.30	2.43	1.53
$\Delta W_{pro,3}$ (g)	117.27	297.87	526.96	81.22	2.97	1.15
$\Delta W_{pro,4}$ (g)	498.02	520.01	--	--	3.94	1.96
$\Delta W_{pro,5}$ (g)	1142.80	452.78	--	--	--	--
$\Delta W_{wb,YOY}$ (g)	--	--	177.40	88.96	4.23	2.43
$\Delta W_{wb,1}$ (g)	404.87	182.03	488.43	164.53	14.26	4.43
$\Delta W_{wb,2}$ (g)	1609.53	141.43	757.80	399.22	9.69	6.22
$\Delta W_{wb,3}$ (g)	782.40	1269.96	2763.83	373.41	10.98	5.37
$\Delta W_{wb,4}$ (g)	1523.00	1354.74	--	--	19.88	5.06
$\Delta W_{wb,5}$ (g)	4825.00	909.67	--	--	--	--
$\Delta\delta^{15}N_{YOY}$ (‰)	--	--	0.51	0.65	-0.13	0.99
$\Delta\delta^{15}N_1$ (‰)	0.01	0.88	0.94	0.50	-1.11	1.10
$\Delta\delta^{15}N_2$ (‰)	1.59	0.74	1.02	0.44	-1.38	1.37
$\Delta\delta^{15}N_3$ (‰)	1.52	0.37	2.03	0.52	-1.89	0.70
$\Delta\delta^{15}N_4$ (‰)	-0.36	0.41	--	--	-1.99	1.40
$\Delta\delta^{15}N_5$ (‰)	1.23	1.65	--	--	--	--

Table 5.4 Sensitivity analysis on Hg lean dry weight concentration of an age 6 Bighead Carp, an age 4 Silver Carp, and an age 5 Bluegill. The parameters with the five greatest contributions to total variance are presented.

Bighead Carp		Silver Carp		Bluegill	
Parameters	Contribution	Parameters	Contribution	Parameters	Contribution
$C_{YOY, Hg}$	70.03% (+)	$C_{YOY, Hg}$	74.50% (+)	$\Delta\delta^{15}N$	35.32% (+)
$\Delta\delta^{15}N$	14.28% (+)	ΔW_{pro}	8.62% (-)	$C_{YOY, Hg}$	21.21% (+)
ΔW_{pro}	9.13% (-)	ΔW_{wb}	7.05% (+)	ΔW_{pro}	19.99% (-)
ΔW_{wb}	3.05% (+)	$\Delta\delta^{15}N$	4.18% (+)	ΔW_{wb}	12.96% (+)
ΔW_{lip}	1.14% (+)	AE_{Hg}	1.47% (+)	BMF	3.62% (-)

Table 5.5 Sensitivity analysis on PCB lipid-equivalent concentration of an age 6 Bighead Carp, an age 4 Silver Carp, and an age 5 Bluegill. The parameters with the five greatest contributions to total variance are presented.

Bighead Carp		Silver Carp		Bluegill	
Parameters	Contribution	Parameters	Contribution	Parameters	Contribution
$C_{YOY, PCB}$	80.22% (+)	$C_{YOY, PCB}$	77.51% (+)	$C_{YOY, PCB}$	79.81% (+)
ΔW_{lip}	10.32% (-)	ΔW_{lip}	6.63% (-)	$\Delta\delta^{15}N$	9.89% (+)
$\Delta\delta^{15}N$	6.12% (+)	$\Delta\delta^{15}N$	4.18% (+)	ΔW_{lip}	4.27% (-)
ΔW_{wb}	0.61% (+)	AE_{PCB}	2.09% (+)	E_L	2.02% (+)
AE_{PCB}	0.46% (+)	ΔW_{wb}	1.80% (+)	BMF	1.45% (-)

CHAPTER 6

General Discussion

6.1 Summary

The primary aim of this study was to improve our understanding of the mechanism of mercury (Hg) and polychlorinated biphenyls (PCBs) accumulation dynamics in fish and develop a universal bioaccumulation model. In Chapter 2, dietary assimilation efficiencies and elimination rate coefficients of Hg and PCB were simultaneously compared in a freshwater fish species, Goldfish (*Carassius auratus*). Dietary assimilation efficiencies (AE) were higher for Hg compared with that for all detectable PCB congeners. The Hg elimination coefficient (k_{tot}) was found equivalent to that observed for highly hydrophobic PCB congeners with a log K_{OW} equivalent of 7.2. It was concluded that Hg elimination was a first order process and Hg had a 118% higher biomagnification factor (BMF) in Goldfish than the highest BMF of PCB congeners.

Chapter 3 evaluated the effect of growth of different tissues on the bioaccumulation of Hg and PCBs in Silver Carp (*Hypophthalmichthys molitrix*) and Bighead Carp (*Hypophthalmichthys nobilis*) from the Three Gorges Reservoir (TGR), China. A non-steady state toxicokinetic model, combined with a Wisconsin bioenergetics model, was developed to simulate Hg and PCB concentration in these two fast growing carp species. In comparison to whole body elimination, growth dilution was a dominant process for Hg and PCB bioaccumulation. Furthermore, the tissue specific growth rate model had better goodness of fit to field data compared with the whole body growth rate model. Finally, the growth rate of lipid was higher than the growth rate of protein in both fish species. A

wider fluctuation in lipid versus protein growth rate led to higher variability in the PCB bioaccumulation rates compared to Hg.

Chapter 4 further evaluated the effect of tissue growth rate on Hg and PCB bioaccumulation in a common North American fish species, Bluegill (*Lepomis macrochirus*), which was collected from five different locations over a latitudinal gradient. A non-steady state combined toxicokinetic and bioenergetics model was applied to simulate Hg and PCB bioaccumulation in Bluegill. Similar to Chapter 3, model simulations indicated that growth dilution was a major component of contaminant bioaccumulation patterns in fish especially during early life stages and was predicted to be more important for highly hydrophobic PCBs compared to Hg. Moreover, simulations which considered tissue specific growth provided some improvement in model performance, particularly for PCBs. The highest growth rates were observed in the populations from the most Southern latitudes, and the growth rate of lipid was higher than the growth rate of protein in all populations.

Although the model developed from Chapters 3 and 4 was able to generate Hg and PCB bioaccumulation curves that generally fit with field collected data, it was unclear which input parameters were responsible for the most variance in the model outcome. In order to evaluate the relative importance of each model input, Chapter 5 conducted a formalized sensitivity analysis (Monte Carlo analysis) for the three species in Chapter 3 and 4 (Bighead Carp, Silver Carp and Bluegill). The analysis found that model outcome was most sensitive to the baseline input to the waterbody, and that tissue growth rate was as important as the feeding ecology of fish to explain Hg and PCB bioaccumulation in all three modeled species.

6.2 Discussion

This dissertation simultaneously measured dietary assimilation efficiencies and elimination rate coefficients of Hg and PCB within the same organism. Chapter 2 improved our understanding of key toxicokinetics parameters identified in Eq. 1.1, which in turn contributed to the model development and application in Chapters 3 and 4. It is usually assumed that chemical AE is constant and independent of diet type, as shown in previous studies where AE was typically above 90% for MeHg (Leaner and Mason, 2004; Wang and Wang, 2012) and under 60% for PCBs (Fisk et al, 1998; Liu et al. 2010). In Chapter 2, AE values of $98 \pm 12\%$ for MeHg and $40 \pm 9\%$ for PCBs supported the common interpretation of higher assimilation of MeHg relative to PCBs. Moreover, previous studies conventionally assumed Hg elimination was a first order process despite the lack of empirical data to support this assumption. No significant difference was found in k_{tot} among the three dosing groups of goldfish in Chapter 2, which confirmed the first order kinetics of Hg elimination. This also confirmed that, similar to PCB elimination, Hg elimination is independent of the chemical burden in fish. Therefore, k_{tot} of both Hg and PCB should only be regulated by metabolic rate and water temperature. Finally, BMFs for both Hg and PCB showed very high variation in previous studies, making it impossible to directly compare their bioaccumulation potential (Borgmann and Whittle, 1992; Fisk et al. 1998; Wang and Wong, 2003; Buckman et al. 2004). In Chapter 2, BMFs were 6.1 for MeHg, and ranged from 0.72 to 3.8 for PCBs in goldfish, indicating a 1.7 fold higher food web bioaccumulation potential of Hg compare to PCBs. The results are well supported by the fact that Hg is a much more common cause for global fish consumption advisories than PCBs.

While steady state models have been widely accepted and used for predicting chemical bioaccumulation (Norstrom et al. 1976; Trudel and Rasmussen, 2006), this dissertation adopted a non-steady state toxicokinetic/bioenergetics model. Historically, steady state models, which have the advantage of using relatively simple model inputs, have made great contribution in decision making processes (i.e. environmental guidelines for environmental protection and remediation management) (McLeod et al. 2016). However, it is unlikely to address temporal changes during the bioaccumulation processes through steady state models, since time is normally not considered in these types of models (Arnot and Gobas, 2004; Trudel and Rasmussen, 2006). Therefore, only the non-steady state model could allow us to incorporate age specific growth rate and further evaluate its effect on the Hg and PCBs bioaccumulation process. The results of Chapter 3 and 4 also indicated that the non-steady model was generally able to explain the differences in PCBs and Hg bioaccumulation trends in Bighead Carp, Silver Carp, and Bluegills.

In addition, Chapters 3 and 4 concluded that, for Bighead Carp, Silver Carp, and Bluegill, models using tissue specific growth rate can better account for deviations in bioaccumulation patterns of Hg and PCBs compared with those using whole body growth rate. In previous bioaccumulation studies, growth rates normally receive less attention compared with chemical elimination rates (Eichinger et al. 2010; Wang and Wang, 2012). As shown in Figure 6.1, the ratio of $k_{g,pro}/k_{tot,Hg}$ was generally less than 1 for all species and all age classes, except for 3 year old Bighead Carp. The $k_{g,pro}/k_{tot,Hg}$ ratios of Silver Carp and Bighead Carp were generally higher than that of Bluegill. In addition, the ratio of $k_{g,pro}/k_{tot,Hg}$ for carp was independent of age ($p>0.05$, linear regression), whereas Bluegill showed significant decrease in $k_{g,pro}/k_{tot,Hg}$ ratio with age ($p<0.05$, $R^2=0.46$). The

average $k_{g,pro}/k_{tot,Hg}$ across all age classes was 0.69 ± 0.25 and 0.59 ± 0.15 for Bighead Carp and Silver Carp, respectively. For Bluegill, the average $k_{g,pro}/k_{tot,Hg}$ was 0.40 ± 0.11 for 1-2 year old fish, decreased to 0.27 ± 0.10 for 3-4 year old fish, and dropped to 0.13 ± 0.05 for 5 year olds. For PCB 180, the $k_{g,lip}/k_{tot,PCB}$ ratio was normally above 1 for the two carp species. It approached 7 for 4 year old Silver Carp, and exceeded 7 for 6 year old Bighead Carp. The $k_{g,lip}/k_{tot,PCB}$ ratio started increasing in the two carp species when the fish reached 3 years old, showing a different growth trajectory and importance of growth dilution for lipids compared to protein. For Bluegill, the $k_{g,lip}/k_{tot,PCB}$ approached 1 for the younger age classes (1-2 year) in the Southern populations (i.e. Stonelick Lake and the Detroit River). Similar to $k_{g,pro}/k_{tot,Hg}$, the $k_{g,lip}/k_{tot,PCB}$ ratio of Bluegill generally decreased with age ($p < 0.05$, $R^2 = 0.40$). However, the $k_{g,lip}/k_{tot,PCB}$ was overall higher than the magnitude of $k_{g,pro}/k_{tot,Hg}$. This indicated that for the three species of fish examined, growth dilution was a more important process regulating the bioaccumulation of PCBs than Hg. Combining these observations with Chapter 2, there are two factors that contribute to an overall higher bioaccumulation potential of Hg relative to PCBs. The two factors include a higher AE of Hg relative to PCBs, which contributes to higher uptake flux of Hg, and a greater importance of growth dilution for PCBs compared to Hg, which reduces PCB concentrations.

Chapter 3 and 4 also observed higher variation in lipid growth compared with that of lean dry protein among these fish populations, as well as greater variation in PCB bioaccumulation slopes compared with Hg. These observations suggest that lipid and protein tissues, as the main storage compartments for PCBs and Hg, represented the capacities for PCBs and Hg accumulation within organisms (Mackay, 1982; Roesijadi,

1992; Stohs and Bagchi, 1995). In fish species, protein normally accounts for approximately 20% of the body weight, whereas lipid, which represents a much smaller fraction of body weight (Dumas et al. 2007; Overturf et al. 2016), has greater leeway to fluctuate relative to whole body weight trends (Daley et al. 2014). Lipids are also expected to undergo wider fluctuations across ages and on a seasonal basis compared to protein. For example, winter weight loss in fish is usually associated with a decrease in lipids but with little or no change in lean dry weight (Paterson et al. 2007). Since the elimination flux of PCBs depends on the lipid normalized concentration of PCBs in the organism (Paterson et al. 2007), high variation in lipid content contributes to high variation in elimination flux at seasonal scales and across age classes. In contrast, Hg elimination flux is more consistent through time, because protein compartment size is more consistent through time. This contributes to more consistent patterns in Hg bioaccumulation. For example, Hg concentration usually increases with fish size, whereas such patterns are less consistent for PCBs across fish populations (Dang and Wang, 2012; Dufour et al. 2001; Mcleod et al. 2014).

While previous studies conventionally used whole body growth rate in bioaccumulation models (Norstrom et al. 1976; Eichinger et al. 2010), this dissertation concluded that using tissue growth rate could improve the accuracy of model outcomes. Particularly, such improvement would become more evident when proximate tissue growth differs from whole body growth as was the case for lipids in the studied species.

In Chapter 4, to ensure different growth rates for each population, the Bluegill samples were collected over a latitudinal gradient to generate different thermal regimes. On the one hand, northern lakes have longer winters that could reduce the magnitude of k_{tot} ,

which in turn is expected to cause higher annual chemical retention in fish, and potentially higher bioaccumulation potential compared to southern lakes. On the other hand, fish from northern lakes also have lower growth rate, which facilitates higher chemical elimination during the summer and in turn reduces chemical retention. It is unclear whether the increase in chemical retention due to longer winter can be offset by the decrease in chemical retention in the summer due to slower growth. Further research to quantify the differences in chemical retention caused by changes in growth and elimination rate is required to provide a better understanding of this process.

Although models in Chapter 3 and 4 were generally able to explain the differences in Hg and PCB concentrations for the studied species, there was still considerable unexplained variation for PCB concentrations in Bluegill from Lake Hartwell (>90%), as well as Hg concentrations for Bighead and Silver Carp from TGR (>80%). The relatively poor performance of the model for these fish was attributed to feeding ecology and changes in diet that resulted in commensurate changes in prey contamination. To understand the model uncertainty caused by these parameters, Chapter 5 conducted a sensitivity analysis for the three modeled species in Chapter 3 and 4. Although Chapter 5 found that the factors regulating concentrations in YOY fish overwhelmed all other parameters in the model, it was noteworthy that parameters which represent age specific tissue growth rate were comparable with parameters which represent the ontogenetic diet shifts, indicating that growth is as important as ontogenetic diet shift for explaining age specific variation in chemical bioaccumulation. The results strongly supported the observations from Chapter 3 and 4. While early studies assumed bioaccumulation processes by fish was primarily regulated by chemical-physical properties (Mackay, 1982), a growing number

of studies demonstrated that biological and ecological factors also play important roles in this process (Madenjian et al. 1994; Paterson et al. 2007; Dang and Wang, 2012).

Furthermore, a detailed examination of the magnitude of growth dilution relative to whole body elimination conducted within the present chapter indicates that growth dilution is an overall more important process for PCB bioaccumulation compared to Hg bioaccumulation. Thus, differences in bioaccumulation potentials for Hg and PCBs can be related to differences in both the assimilation efficiency and contrasting effect of growth dilution across the two chemicals. Again, through a series of studies based on field observation and model validation, this dissertation strongly recommends that future models of Hg and PCB bioaccumulation incorporate tissue specific growth rates for more accurate predictions.

Overall, this dissertation was the first to directly compare chemical toxicokinetics between Hg and PCBs within the same organism, and concluded that Hg had a higher bioaccumulation potential in fish compared to PCBs. In addition, this study developed a non-steady state bioenergetics/kinetics model, which was able to explain the differences in bioaccumulation patterns of Hg and PCBs among fish populations with different growth rates. It was suggested that a non-steady state model was a better tool for accurately predicting changes in chemical concentration in a changing environment compared with a steady state model. This dissertation also provided the first evaluation of tissue specific growth to describe chemical toxicokinetics, and demonstrated that tissue specific growth could improve the accuracy of model predictions for populations where tissue growth differs from whole body growth. Lastly, this study further revealed the

importance of the growth rate, especially the tissue growth rate, for bioaccumulation of Hg and PCBs.

6.3 Future Studies

For toxicokinetic studies, using simultaneous chemical exposures in other fish species would be useful to verify if bioaccumulation potential of Hg exceeds that of PCB for other species. Additionally, since differences in prey concentrations were found to be important to explain species differences in contamination, it was believed that model studies would benefit from more realistic model inputs on contaminant levels in various fish food items across age classes. However, another factor not considered by the model developed in this dissertation was sex based differences in contaminant elimination.

Although both PCBs and Hg exhibited sex based differences in concentration (Madenjian et al. 2016), our study did not separate males from females to evaluate sex based differences in chemical concentrations nor did the model consider applying different values of k_{tot} for male and female fish for the two pollutant types. However, these modifications could be readily adopted within the model by separate model parameterization to individual sexes. Thus, future research to monitor both seasonal changes in proximate tissue content between ages and sexes as well as contaminant concentrations are necessary to substantiate daily and seasonal patterns in Hg and PCB bioaccumulation estimated by the model. Lastly, for future uncertainty analysis, using realistic variation for each bioenergetic parameter would be necessary to further identify the key parameters and improve the accuracy of the model prediction.

6.4 References

- Arnot, J. A.; Gobas, F. A. P. C. A food web bioaccumulation model for organic chemicals in aquatic ecosystems. *Environ. Toxicol. Chem.* 2004, 23, 2343-2355.
- Borgmann, U.; Whittle, B. M. Bioenergetics and PCB, DDE, and mercury dynamics in Lake Ontario lake trout (*Salvelinus namaycush*): a model based on surveillance data. *Can. J. Fish. Aquat. Sci.* 1992, 49, 1086-1896.
- Buckman, A. H.; Brown, S. B.; Hoekstra, P. F.; Solomon, K. R.; Fisk, A. T. Toxicokinetics of three polychlorinated biphenyl technical mixtures in rainbow trout (*Oncorhynchus mykiss*). *Environ. Toxicol. Chem.* 2004, 23, 1725-1736.
- Daley, J. M.; Paterson, G.; Drouillard, K.G. Mechanism for persistent organic pollutants (POPs) in wildlife. *Rev. Environ. Contam. Toxicol.* 2014. 227.
- Dang, F.; Wang, W. X. Why mercury concentration increases with fish size? Biokinetic explanation. *Environ. Pollut.* 2012, 163, 192-198.
- Dufour, E.; Gerdeaux, D.; Corvi, C.; Khim-Heang, S.; Mariotti, A. Assessment of the contaminant concentration variability among Lake Geneva arctic char using stable isotopic composition ($\delta N-15$ and $\delta C-13$). *Environ. Toxicol.* 2001, 16(2), 185-191.
- Dumas, C.F.M.; de Lange, J.; France, Bureau, D.P. Quantitative description of body composition and rates of nutrient deposition in rainbow trout (*Oncorhynchus mykiss*) *Aquaculture* 2007, 273, 165-181.
- Eichinger, M.; Loizeau, V.; Rounsarda, F.; Le Guellec, A. M.; Bacherb, C. Modelling growth and bioaccumulation of Polychlorinated biphenyls in common sole (*Solea solea*). *J. Sea Res.* 2010, 64 (3), 373-385.
- EPA-FDA. Eating fish: what pregnant women and parents should know. www.epa.gov/fishadvice. 2017.
- Fisk, A. T.; Norstrom, R. J.; Cymbalisty, C. D.; Muir, D. C. G. Dietary accumulation and depuration of hydrophobic organochlorines: bioaccumulation parameters and their

- relationship with the octanol/water partition coefficient. *Environ. Toxicol. Chem.* 1998, 17, 951-961.
- Leaner, J. J.; Mason, R. P. Methylmercury uptake and distribution kinetics in sheepshead minnows, *Cyprinodon variegatus*, after exposure to CH₃Hg-spiked food. *Environ. Toxicol. Chem.* 2004, 23(9), 2138-2146.
- Liu, J.; Haffner, G. D.; Drouillard, K. G. The influence of diet on the assimilation efficiency of 47 polychlorinated biphenyl congeners in Japanese Koi (*Cyprinus carpio*). *Environ. Toxicol. Chem.* 2010, 29, 401-409.
- Mackay, D. Correlation of bioconcentration factors. *Environ. Sci. Technol.* 1982, 16, 274-278.
- Madenjian, C. P.; Carpenter, S. R.; Rand, P. S. Why are the PCB concentrations of salmonine individuals from the same lake so highly variable. *Can. J. Fish. Aquat. Sci.* 1994, 51 (4), 800-807.
- Madenjian, C. P.; Rediske, R. R.; Krabbenhoft, D. P.; Stapanian, M. A.; Chernyak, S. M.; O'Keefe, J. P. Sex differences in contaminant concentrations of fish: a synthesis. *Biology of Sex Differences.* 2016.7: 42.
- McLeod, A. M.; Paterson, G.; Drouillard, K. G.; Haffner, G. D. Ecological factors contributing to variability of persistent organic pollutant bioaccumulation within forage fish communities of the Detroit River, Ontario, Canada. *Environ. Toxicol. Chem.* 2014, 33(8), 1825-1831.
- Norstrom, R. J.; McKinnon, A. E.; DeFreitas, A. S. W. Bioenergetics-based model for pollutant accumulation by fish simulation of PCB and methylmercury residue levels in Ottawa River yellow perch (*Perca flavescens*). *J. Fish. Res. Bd. Can.* 1976, 33, 248-267.
- Ministry of the Environment and Climate Change. Guide to eating Ontario fish. Queen's Printer for Ontario. 2015.
- Overturf, K.; Barrows, F. T.; Hardy, R. W.; Brezas, A.; Dumas, A. Energy composition of diet affects muscle fiber recruitment, body composition, and growth trajectory in rainbow trout (*Oncorhynchus mykiss*). *Aquaculture* 2016, 457, 1-14.

- Paterson, G.; Drouillard, K. G.; Haffner, G. D. PCB elimination by yellow perch (*Perca Flavescens*) during an annual temperature cycle. *Environ. Sci. Technol.* 2007, 41, 824-829;
- Paterson, G.; Drouillard, K. G.; Leadley, T. A.; Haffner, G. D. Long-term polychlorinated biphenyl elimination by three size classes of yellow perch (*Perca flavescens*). *Can. J. Fish. Aquat. Sci.* 2007, 64, 1222-1233.
- Roesijadi; G. Metallothioneins in metal regulation and toxicity in aquatic animals. *Aquat. Toxicol.* 1992, 22(2), 81-114.
- Ser, P.H.; Waranabe, C. Fish advisories in the USA and Japan: risk communication and public awareness of a common idea with different backgrounds. *Asia Pac. J. Clin. Nutr.* 2012, 21 (4), 487-494.
- Stohs, S. J.; Bagchi, D. Oxidative mechanisms in the toxicity of metal ions. *Free Rad. Biol. Med.* 1995, 18, 321-336.
- Wang, R.; Wang, W. X. Contrasting mercury accumulation patterns in tilapia (*Oreochromis niloticus*) and implication on somatic growth dilution. *Aquat. Toxicol.* 2012, 114-115, 23-30.
- Wang, W.; Wong, R. S. K. Bioaccumulation kinetics and exposure pathways of inorganic mercury and methylmercury in a marine fish, the sweetlips (*Plectorhinchus gibbosus*). *Mar. Ecol. Prog. Ser.* 2003, 261, 257-268.

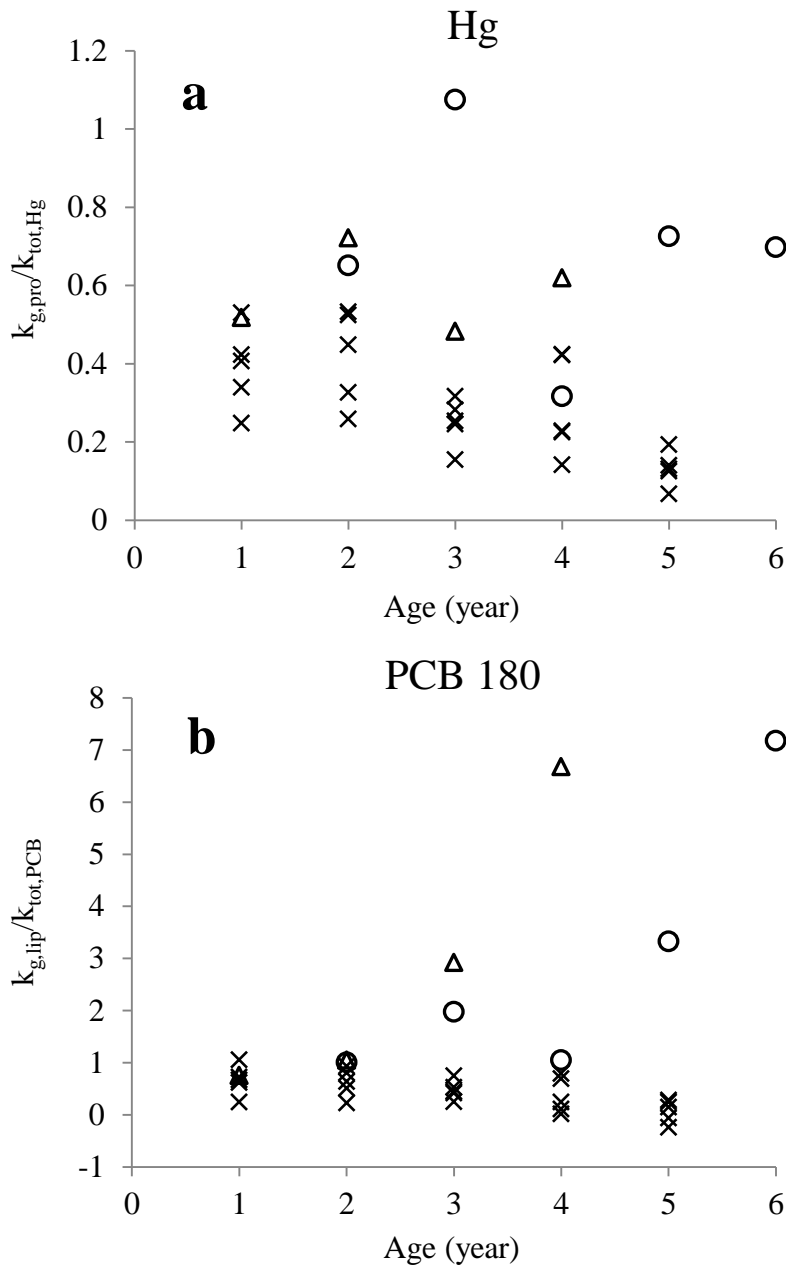


Figure 6.1 The mean protein growth rate ($k_{g,pro}$) to Hg elimination rate ($k_{tot,Hg}$) ratio (a) and the mean lipid growth rate ($k_{g,lip}$) to PCB elimination rate ($k_{tot,PCB}$) ratio (b) for each age class of Bighead Carp, Silver Carp as well as Bluegill from five locations. Circles (○) represent Bighead Carp, triangles (Δ) represent Silver Carp, and crosses (×) represent Bluegill.

APPENDICES

Appendix A

Copyright form for Chapter 2 manuscript:

11/24/2017

Rightslink® by Copyright Clearance Center



RightsLink®

Home

Create Account

Help



Title: Comparison of the Toxicokinetics and Bioaccumulation Potential of Mercury and Polychlorinated Biphenyls in Goldfish (*Carassius auratus*)

Author: Jiajia Li, Ken G. Drouillard, Brian Branfireun, et al

Publication: Environmental Science & Technology

Publisher: American Chemical Society

Date: Sep 1, 2015

Copyright © 2015, American Chemical Society

LOGIN
If you're a [copyright.com](#) user, you can login to RightsLink using your [copyright.com](#) credentials. Already a RightsLink user or want to [learn more?](#)

PERMISSION/LICENSE IS GRANTED FOR YOUR ORDER AT NO CHARGE

This type of permission/license, instead of the standard Terms & Conditions, is sent to you because no fee is being charged for your order. Please note the following:

- Permission is granted for your request in both print and electronic formats, and translations.
- If figures and/or tables were requested, they may be adapted or used in part.
- Please print this page for your records and send a copy of it to your publisher/graduate school.
- Appropriate credit for the requested material should be given as follows: "Reprinted (adapted) with permission from (COMPLETE REFERENCE CITATION). Copyright (YEAR) American Chemical Society." Insert appropriate information in place of the capitalized words.
- One-time permission is granted only for the use specified in your request. No additional uses are granted (such as derivative works or other editions). For any other uses, please submit a new request.

BACK

CLOSE WINDOW

Copyright © 2017 Copyright Clearance Center, Inc. All Rights Reserved. [Privacy statement](#). [Terms and Conditions](#).
Comments? We would like to hear from you. E-mail us at customercare@copyright.com

VITA AUCTORIS

NAME: Jijia Li
PLACE OF BIRTH: Mianyang, China

YEAR OF BIRTH: 1986

EDUCATION: Mianyang Nanshan High School, Mianyang, China, 2004

Southwest University, B.Sc., Chongqing, China, 2008

Southwest University, M.Sc., Chongqing, China, 2011